

# Polaritonic response theory for exact and approximate wave functions

Matteo Castagnola,<sup>1</sup> Rosario Roberto Riso,<sup>1</sup> Alberto Barlini,<sup>2</sup> Enrico Ronca,<sup>3, a)</sup> and Henrik Koch<sup>1, 2, b)</sup>

<sup>1)</sup>*Department of Chemistry, Norwegian University of Science and Technology, 7491 Trondheim, Norway*

<sup>2)</sup>*Scuola Normale Superiore, Piazza dei Cavalieri 7, 56126 Pisa, Italy*

<sup>3)</sup>*Dipartimento di Chimica, Biologia e Biotecnologie, Università degli Studi di Perugia, Via Elce di Sotto, 8, 06123, Perugia, Italy*

*Polaritonic chemistry* is an interdisciplinary emerging field that presents several challenges and opportunities in chemistry, physics and engineering. A systematic review of polaritonic response theory is presented, following a chemical perspective based on molecular response theory. We provide the reader with a general strategy for developing response theory for *ab initio* cavity quantum electrodynamics (QED) methods and critically emphasize details that still need clarification and require cooperation between the physical and chemistry communities. We show that several well-established results can be applied to strong coupling light-matter systems, leading to novel perspectives on the computation of matter and photonic properties. The application of the Pauli-Fierz Hamiltonian to polaritons is discussed, focusing on the effects of describing operators in different mathematical representations. We thoroughly examine the most common approximations employed in *ab initio* QED, such as the dipole approximation. We introduce the polaritonic response equations for recently developed *ab initio* QED Hartree-Fock and QED coupled cluster methods. The discussion focuses on the similarities and differences from standard quantum chemistry methods, providing practical equations for computing the polaritonic properties.

## 1. INTRODUCTION

Hybrid light-matter states, referred to as *polaritons*, were described in the 1950s from the interaction of optical modes and lattice excitons in crystals.<sup>1–3</sup> In 1963, Jaynes and Cummings described with a phenomenological quantum picture the formation of polaritons from the interaction of photons and atomic states.<sup>4</sup> Their predictions were later confirmed experimentally for Rydberg atoms in a quantum microcavity.<sup>5,6</sup> The use of quantum optical devices to confine the fields, such as Fabry-Pérot cavities or metal nanostructures,<sup>7–12</sup> increase the coupling between matter and light, and polaritons have been observed since the 1970s for inorganic semiconductors<sup>13,14</sup> and from the 1990s for organic molecules in optical cavities.<sup>15,16</sup> Polaritonics has recently attracted the interest of chemists since the pioneering work of Ebbesen and coworkers, who showed that the formation of polaritons can influence photochemical<sup>17</sup> and ground state reactivity.<sup>18–20</sup> Several experiments have now shown that electromagnetic confinement leads to essential modifications of processes such as chemical reactions,<sup>17–22</sup> singlet fission,<sup>23–25</sup> intersystem crossing,<sup>26–28</sup> crystallization and assembly,<sup>29,30</sup> as well as optical properties like absorption, scattering and emission,<sup>31–46</sup> although the reproducibility of the chemical reactivity modifications is not always straightforward.<sup>47</sup> Crucial experimental aspects are still to be clarified, and cooperation between experimentalists and theoreticians can be of great assistance in unravelling the conditions and the consequences of vibrational and electronic strong coupling. Since both the photon and the molecular degrees of freedom are important in such systems, their theoretical modelling is a challenging interdisciplinary task.<sup>48–55</sup> Following well-established electronic structure

theory, several *ab initio* quantum electrodynamics (QED) approaches have been developed recently. These include QED density functional theory (QEDFT),<sup>56</sup> reduced density matrix approaches for matter-photon systems,<sup>57,58</sup> polaritonic coupled cluster,<sup>59</sup> QED Hartree-Fock (QED-HF),<sup>60,61</sup> QED coupled cluster (QED-CC),<sup>60,61</sup> QED full configuration interaction (QED-FCI),<sup>60,61</sup> polarized Fock states approach (PFSs),<sup>62</sup> polaritonic unitary coupled cluster (QED-UCC),<sup>63</sup> strong coupling (SC)-QED-HF,<sup>64</sup> QED Møller-Plesset perturbation theory of second-order (QED-MP2),<sup>65</sup> and second-order QED algebraic diagrammatic construction scheme for the polarization propagator (QED-ADC(2)).<sup>65</sup> In addition, several approaches have been investigated combining phenomenological models from the quantum optics community with computational chemistry.<sup>2,4,52,66–83</sup>

The response theory formalism is a very successful and well-known framework employed in quantum chemistry to calculate approximate ground and excited state properties.<sup>84–93</sup> While several of these results are still valid for QED systems, essential and subtle differences arise due to the explicit modelling of the photon field, highlighting additional challenges and opportunities. Although some response schemes for QED methods have been proposed,<sup>94–101</sup> a systematic discussion of polaritonic response theory and its connections to molecular response theory is still not available.

This paper aims to fill this gap by proposing a systematic discussion of wave function based methods for computing polaritonic properties. We will review several results from molecular response theory that can be applied to polaritonic wave functions and critically discuss the limitations and future challenges such methods have to tackle. In section (2), we briefly introduce the most common optical devices employed to achieve strong coupling. In section (3), we present the Pauli-Fierz Hamiltonian and focus on how this framework is used to model the strong coupling regime. We review the most

<sup>a)</sup>Electronic mail: enrico.ronca@unipg.it

<sup>b)</sup>Electronic mail: henrik.koch@ntnu.no

common approximations for *ab initio* QED in section (4). In section (5), we discuss polaritonic response theory for exact states, focusing on similarities and differences with molecular response theory, and provide several examples of polaritonic response properties. The derived equations are equivalent to QED-FCI response theory. In section (6), we discuss how to develop response theory for approximate models and derive linear and quadratic response equations for QED-HF and QED-CC. Finally, section (7) recaps the main results described in this paper and contains some concluding remarks and future perspectives.

## 2. OPTICAL CAVITIES

This section provides a brief introduction to quantum optical devices. The discussion, although far from being exhaustive, aims at reviewing the most common experimental setups employed in polaritonic chemistry and provides the reader with phenomenological basics of light-matter strong coupling.

The use of quantum optical devices provides a non-invasive way to engineer a material's properties by exploiting the confinement of the electromagnetic field. The geometry and the material of the device define the resonator eigenmodes. In a real cavity, the confinement is always defective and depends specifically on the frequency of the field and the cavity material. The so-called  $Q$ -factor measures the quality of a cavity<sup>102</sup>

$$Q(\omega_0) = \omega_0 \frac{\text{energy stored}}{\text{power loss}}, \quad (1)$$

where  $\omega_0$  is the resonance frequency of the device. This equation implies that the electric field will exhibit an exponential decay

$$E(t) = E_0 e^{-i\omega_0 t} e^{-\frac{\omega_0}{2Q} t}, \quad (2)$$

such that the energy spectrum will show a Lorentzian lineshape

$$|E(\omega)|^2 \propto \frac{1}{(\omega - \omega_0)^2 + (\omega_0/2Q)^2}. \quad (3)$$

From Eq. (3), we have a more practical definition of the  $Q$ -factor as the ratio between the frequency of the hosted field mode  $\omega_0$  and the full width at half maximum (FWHM)  $\Delta\omega$  of the cavity spectrum

$$Q(\omega_0) = \frac{\omega_0}{\Delta\omega}. \quad (4)$$

The coupling  $\lambda$  between matter and the confined cavity modes is proportional to the inverse square root of the effective confinement volume  $V_{eff}$

$$\lambda \propto \frac{1}{\sqrt{V_{eff}}}. \quad (5)$$

The efficiency of a device in enhancing the interaction between light and matter can then be measured by the  $Q/V_{eff}$  ratio. Strong coupling conditions are obtained once the coupling strength exceeds the material and cavity losses (i.e. the coherent energy exchange rate between the electromagnetic field and the molecule exceeds the dissipation processes). Decoherence interactions with the environment are suppressed, and hybrid states between the cavity and the molecular eigenstates naturally describe the system. In this regime, the molecular properties are therefore affected even in the absence of an external photon pumping of the device.

The most straightforward optical device to confine light is a Fabry-Pérot cavity, composed of two planar parallel metal plates kept at a fixed distance.<sup>103–108</sup> These resonators are often produced by sputtering gold or silver on a substrate (often  $SiO_2$ ,  $BaF_2$  or  $ZnSe$ ), and direct contact with the sample is prevented by using a thin polymer film. The sample is then coated by this multilayer structure or injected into the hollow cavity. The cavity eigenmodes are linearly-polarized standing waves whose wavelength  $\lambda_n$  depends on the distance  $L$  between the mirrors

$$\lambda_n = \frac{2L}{n} \quad n = 1, 2, \dots \quad (6)$$

The spatial distribution of the optical mode can be observed by changing the position of a thin sample slab inside the cavity. The strong coupling features of this system are a function of the slab position, which gives us the field strength distribution.<sup>46,109</sup> Changing the form of the plates, e.g. using curved mirrors similar to lenses, can lead to modifications of the field shape and possibly an increase in the coupling constant.<sup>110–116</sup> The coupling strength  $\lambda$  in Fabry-Pérot cavities is limited by the diffraction limit, which restrains the field confinement. Devices which bound the fields on a scale smaller than the diffraction limit are called *subwavelength* cavities and can facilitate ultrastrong coupling. To this end, using nanostructured metamaterials in a suitable geometric arrangement can allow efficient confinement and overcome the diffraction limit, leading to efficient subwavelength cavities. In Fig. (1a), we show an example of a subwavelength "dogbone" metamaterial resonator, which can confine light on a scale of about one-tenth of the mode wavelength.<sup>117–122</sup> Metallic nanostructures can be used to confine electromagnetic fields through surface plasmon resonances, allowing for remarkably low-volume confinement. It is also possible to employ non-metallic plasmonic structures, such as graphene.<sup>123–128</sup> Coupling two or more plasmonic nanoparticles can lead to extreme field localization in hot spots between them, as schematically shown in Fig. (1b) for two nano prisms on a silicon substrate.<sup>129–133</sup> However, these systems can be very lossy, i.e. they have a low  $Q$ -factor, which effectively limits their use for strong coupling. Alternatively, dielectric materials can also be used to confine the electromagnetic field. In Fig. (1c), we show a cavity obtained by two distributed Bragg reflectors (DBRs) composed of several alternate dielectric slabs. By carefully choosing the number of slabs and their material, DBRs can achieve low-volume confinement

and high  $Q$ -factors.<sup>134–138</sup> Transparent high-reflection index dielectrics in curved or polygonal shapes can confine electromagnetic waves by total internal reflection. The optical modes of such resonators, called whispering-gallery modes (WGMs), can achieve extreme field localization and quality factors.<sup>139–146</sup>

The devices described so far cannot, in general, host any chiral eigenmodes. The helicity of a circularly polarized wave changes sign when reflected by a mirror surface, creating a mode with zero global helicity. In recent years, different helicity-preserving optical devices (chiral cavities) have been proposed based on the introduction of a chiral element in the resonator.<sup>115,147–161</sup> In Fig. (1d), we show a chiral Fabry-Pérot cavity formed by the insertion of a 2D chiral polymer slab.<sup>147</sup> The 2D chirality is achieved by applying torsional shear stress, and chiral eigenmodes are sustained in the device by a circular conversion dichroism mechanism.<sup>147</sup> Other chiral optical resonators have been proposed using chiral metasurfaces<sup>115,149–151</sup> and chiral plasmonics.<sup>157–161</sup>

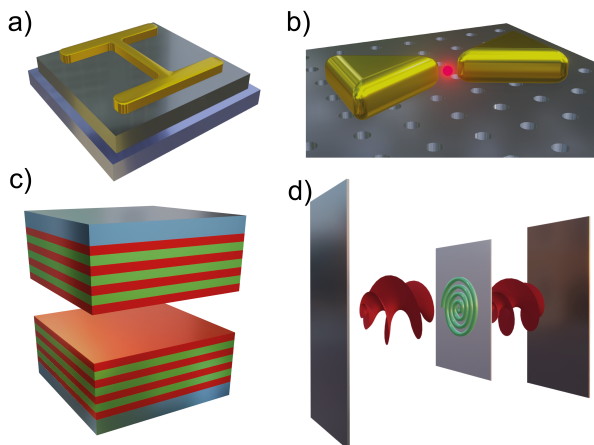


FIG. 1. (a) Metallic nanostructures can be used to confine electromagnetic fields through surface plasmon resonances. A "dog-bone" metamaterial can be employed as a subwavelength resonator, confining the electromagnetic field on a scale of a tenth of the mode wavelength.<sup>119</sup> Subwavelength optical devices can overcome the diffraction limit by employing suitable geometries and metamaterials, facilitating the fulfilment of strong coupling conditions.<sup>117–122</sup> (b) Two metal nanoparticles are coupled on a crystal substrate, increasing the electric field's intensity in a hotspot between them.<sup>129–133</sup> Metal nanoparticles can be used to achieve very low-volume confinement due to surface plasmon resonances, although dissipation processes are often significant. (c) Distributed Bragg reflectors (DBRs) are composed of alternate slabs of dielectric materials. Carefully choosing the number of slabs and their material, it is possible to achieve efficient confinement of the electromagnetic fields between two DBRs.<sup>134–138</sup> (d) A 2D chiral polymer film, obtained by torsional shear stress, inserted inside a Fabry-Pérot resonator endows the system with chiral eigenmodes.<sup>147</sup>

### 3. PAULI-FIERZ HAMILTONIAN

The starting point of molecular modelling is the nonrelativistic molecular Hamiltonian

$$H = \sum_M \frac{1}{2m_M} \mathbf{p}_M^2 + \sum_i \frac{1}{2} \mathbf{p}_i^2 + \frac{1}{2} \sum_{i \neq j} \frac{1}{|\mathbf{r}_i - \mathbf{r}_j|} - \sum_{i,M} \frac{Z_M}{|\mathbf{r}_i - \mathbf{R}_M|} + \frac{1}{2} \sum_{M \neq N} \frac{Z_M Z_N}{|\mathbf{R}_M - \mathbf{R}_N|}. \quad (7)$$

In Eq. (7), the capital indices  $M$  and  $N$  refer to nuclei of mass and charge  $m_M$  and  $Z_N$ ,  $i$  and  $j$  to electrons with mass  $m = 1$  and charge  $q = -1$ . The electronic and nuclear positions are labelled  $\mathbf{r}$  and  $\mathbf{R}$  respectively, and  $\mathbf{p}$  is the linear momentum of the particles. The first line of Eq. (7) contains the non-relativistic kinetic energy operators for nuclei and electrons, while the second line describes the Coulomb interaction.

Although it is often assumed that the Hamiltonian in Eq. (7) is sufficient to model a molecular system, this is not the case. This is apparent if we realise that the excited states of the system have an infinite lifetime, i.e. they do not radiate. In Eq. (7), we disregard the electromagnetic degrees of freedom, retaining only the electrostatic interaction between particles while neglecting retardation effects. The motion of electric charges generates radiation fields which in turn influence the particles' motion: this back-reaction mechanism is the origin of spontaneous decay. The inclusion of the electromagnetic degrees of freedom is also fundamental when optical devices are employed to modify the photon environment. It is then necessary to go beyond the Coulomb interaction terms and resort to Maxwell's electrodynamics to describe self-consistently the interaction between light and matter.<sup>102,162–164</sup> The particle motion is determined by the Lorenz force  $\mathbf{F}_L$

$$\mathbf{F}_L = m\mathbf{a} = q \left( \mathbf{E}(\mathbf{r}, t) + \frac{\mathbf{v}}{c} \times \mathbf{B}(\mathbf{r}, t) \right), \quad (8)$$

where  $c$  is the speed of light,  $\mathbf{v}$  and  $\mathbf{a}$  are the velocity and the acceleration of the particle,  $q$  is the charge and  $m$  is the mass. The electric  $\mathbf{E}$  and magnetic  $\mathbf{B}$  fields are determined by Maxwell's equations, here expressed in cgs units

$$\begin{cases} \nabla \cdot \mathbf{E} = 4\pi\rho(\mathbf{r}, t) \\ \nabla \cdot \mathbf{B} = 0 \\ \nabla \times \mathbf{E} = -\frac{1}{c} \frac{\partial \mathbf{B}}{\partial t} \\ \nabla \times \mathbf{B} = \frac{4\pi}{c} \mathbf{j}(\mathbf{r}, t) + \frac{1}{c} \frac{\partial \mathbf{E}}{\partial t} \end{cases}, \quad (9)$$

where  $\mathbf{r}$  is a vector defining a point in space,  $\rho(\mathbf{r}, t)$  is the charge density and  $\mathbf{j}(\mathbf{r}, t)$  is the current density. The fields are naturally described using *potentials*  $(\phi, \mathbf{A})$ , such that

$$\mathbf{B} = \nabla \times \mathbf{A} \quad (10)$$

$$\mathbf{E} = -\nabla\phi - \frac{1}{c} \frac{\partial \mathbf{A}}{\partial t}. \quad (11)$$

We notice that, unlike the fields  $\mathbf{B}$  and  $\mathbf{E}$ , the vector potential  $\mathbf{A}$  and the scalar potential  $\phi$  are not measurable quantities and must, therefore, only be seen as mathematical tools. In Eqs. (10) and (11), the potentials are identified only through their derivatives. This implies that the same fields, i.e. the same system, can be modelled using different potentials. The transformation

$$\mathbf{A} \rightarrow \mathbf{A} + \nabla \chi \quad (12)$$

$$\phi \rightarrow \phi - \frac{1}{c} \frac{\partial \chi}{\partial t}, \quad (13)$$

known as *gauge transformation*, leads to unchanged electromagnetic fields for any well-behaved scalar function  $\chi(\mathbf{r}, t)$ . This gauge freedom can be exploited to simplify the equations. We will make use of the so-called *Coulomb gauge*

$$\nabla \cdot \mathbf{A} = 0 \quad (14)$$

which allows us to account for the Coulomb interactions

among the particles explicitly. The scalar potential is, in this gauge, determined by the Poisson equation as in the electrostatic case

$$\nabla^2 \phi = -4\pi\rho, \quad (15)$$

while the vector potential is obtained from the following equation:

$$\nabla^2 \mathbf{A} - \frac{1}{c^2} \frac{\partial^2 \mathbf{A}}{\partial t^2} = -\frac{4\pi}{c} \mathbf{j}^\perp, \quad (16)$$

where  $\mathbf{j}^\perp$  is the solenoidal (divergence-free) part of the density current.

The Hamiltonian for the field-particle system is described in terms of the position of the particles, the vector potential and their conjugate momenta. The self-consistent interaction between molecules and light is described by the Pauli-Fierz Hamiltonian, for which Hamilton's equations can be shown to be equivalent to Eqs. (8) and (9)<sup>162,163</sup>

$$\begin{aligned} H_{PF} = & \sum_M \frac{1}{2m_M} \left( \mathbf{p}_M - \frac{Z_M}{c} \mathbf{A}(\mathbf{R}_M) \right)^2 + \sum_i \frac{1}{2} \left( \mathbf{p}_i + \frac{1}{c} \mathbf{A}(\mathbf{r}_i) \right)^2 \\ & + \frac{1}{2} \sum_{i \neq j} \frac{1}{|\mathbf{r}_i - \mathbf{r}_j|} - \sum_{i,M} \frac{Z_M}{|\mathbf{r}_i - \mathbf{R}_M|} + \frac{1}{2} \sum_{M \neq N} \frac{Z_M Z_N}{|\mathbf{R}_N - \mathbf{R}_M|} \\ & + \frac{1}{2} \int \left[ \mathbf{E}_\perp(\mathbf{r})^2 + \mathbf{B}(\mathbf{r})^2 \right] d\mathbf{r}. \end{aligned} \quad (17)$$

In the first line of Eq. (17), we have the vector potential  $\mathbf{A}$  computed at the positions of nuclei and electrons, and the second line describes the Coulomb interactions between the particles. The explicit separation of Coulomb interactions provided by the Coulomb gauge allows for the separation of Hamiltonian in Eq. (7), providing a natural chemical description of the system. The last line accounts for the electromagnetic field energy. Expanding the first terms, we obtain an interaction term between the particle Hamiltonian in Eq. (7) and the radiation fields mediated by the vector potential  $\mathbf{A}$

$$H_{int} = - \sum_x \frac{q_x}{2m_x c} (\mathbf{p}_x \cdot \mathbf{A}(\mathbf{r}_x) + \mathbf{A}(\mathbf{r}_x) \cdot \mathbf{p}_x) + \sum_x \frac{q_x^2}{2m_x c^2} \mathbf{A}^2(\mathbf{r}_x), \quad (18)$$

where  $x$  runs on both electrons and nuclei. Following the QED prescription, the vector potential in Eq. (17) is promoted to an operator

$$\mathbf{A} \longrightarrow \hat{\mathbf{A}} = \sum_{\mathbf{k}, \tau} \frac{c\lambda}{\sqrt{2\omega_{\mathbf{k}}}} \left( \epsilon_{\mathbf{k}\tau} e^{i\mathbf{k}\cdot\mathbf{r}} b_{\mathbf{k}\tau} + \epsilon_{\mathbf{k}\tau}^* e^{-i\mathbf{k}\cdot\mathbf{r}} b_{\mathbf{k}\tau}^\dagger \right), \quad (19)$$

where  $b_{\mathbf{k}\tau}^\dagger$  and  $b_{\mathbf{k}\tau}$  respectively create and annihilate a photon with wave vector  $\mathbf{k}$  and frequency  $\omega_{\mathbf{k}} = \frac{|\mathbf{k}|}{c}$ . The field polarization  $\epsilon_{\mathbf{k}\tau}$  with  $\tau = 1, 2$  spans the 2D plane perpendicular to

$\mathbf{k}$ . If we take the polarization  $\epsilon_{\mathbf{k}\tau}$  to be real, the fields are described by a superposition of linearly polarized plane waves. In an equivalent way, we can take the complex orthogonal unit vectors

$$\epsilon_{\mathbf{k}\pm} = \frac{1}{\sqrt{2}} (\epsilon_{\mathbf{k}1} \pm i\epsilon_{\mathbf{k}2}) \quad (20)$$

which describe left and right circularly polarized waves.

### Remarks

There are now some subtle points to mention. Choosing the Coulomb gauge, the vector potential only has (two) transverse components  $\mathbf{A} = \mathbf{A}_\perp$ . At the same time, the longitudinal component of the electric field (Coulomb field) is described by the scalar potential. In this gauge, the equations are not manifestly covariant. However, this does not imply a loss of relativistic invariance since the electromagnetic field prediction agrees with special relativity. In fact, the retardation of the interaction between particles is obtained by a cancellation of the instantaneous interactions from the Coulomb term and the transverse field. For a different gauge, the Coulomb interactions would also be mediated by the longitudinal component

of the vector potential.<sup>162,163</sup>

The canonical momentum  $\mathbf{p}_i$ , contrary to the standard quantum mechanical formulation, is not the linear momentum of the particle but here has a field-dependent component<sup>162,163</sup>

$$\mathbf{p}_i = m_i \mathbf{v}_i + \frac{q_i}{c} \mathbf{A}(\mathbf{r}_i). \quad (21)$$

This means that, although in Eq. (17) we can identify the original particle Hamiltonian in Eq. (7), the physical meaning of these two operators is different.

The Pauli-Fierz Hamiltonian is self-adjoint and bounded from below<sup>165,166</sup> such that a stable ground state exists. However, the original excited states of the particle Hamiltonian Eq. (7) become metastable (i.e. with a finite lifetime) because of their coupling to the continuous photonic spectrum.<sup>167-170</sup>

In Eq. (17), we have disregarded the nuclear and electronic spin, which could be introduced in Eq. (17) with the addition of the following contribution

$$H_{spin} = \frac{1}{2} \sum_i \boldsymbol{\sigma}_i \cdot \mathbf{B}(\mathbf{r}_i) - \sum_N \gamma_N \mathbf{I}_N \cdot \mathbf{B}(\mathbf{R}_N), \quad (22)$$

where the first term of Eq. (22) accounts for the interaction of the electronic spin, described by the Pauli matrices  $\boldsymbol{\sigma}_i$ , with the (internal) magnetic field  $\mathbf{B}$ , while the second term describes the energy associated with the nuclear spin  $\mathbf{I}_N$  with magnetogyric ratio  $\gamma_N$ .

Finally, in Eq. (17) particles can in principle interact with infinitely high-frequency modes. However, the description of the kinetic energy is nonrelativistic. When the field frequency is comparable with the rest energy of the particles  $\omega \sim mc^2$ , relativistic effects (e.g. creation of electron-positron pairs) not included in Eq. 17 become relevant.<sup>162</sup> It is then necessary to introduce a cutoff as the field's momentum  $\mathbf{k}$  increases (ultraviolet cutoff). Moreover, the masses in Eq. (17) are not the *physical masses* usually employed in quantum mechanics, which include the contribution of the electromagnetic energy created by the particle, but they are their *bare masses*.<sup>163</sup>

#### 4. APPROXIMATIONS FOR AB INITIO POLARITONIC CHEMISTRY

While the Hamiltonian in Eq. (17) allows for a consistent treatment of light and matter, approximations are needed to perform computational studies. The problem of the continuum of photonic modes could be overcome by employing a fine discretization of the spectrum. Moreover, different approaches can be developed depending on the treatment of the photonic degrees of freedom. In the Cavity Born-Oppenheimer approach (CBO),<sup>171-173</sup> the photon coordinates  $q_\alpha$  are embedded in the nuclear wave function  $\chi(\mathbf{R}, \mathbf{q}, t)$  and separated from the electronic degrees of freedom, described by an electronic wave function  $\phi(\mathbf{r}; \mathbf{R}, \mathbf{q})$ . The complete wave function can then be expanded as

$$\Psi(\mathbf{r}, \mathbf{R}, \mathbf{q}, t) = \sum_k \phi_k(\mathbf{r}; \mathbf{R}, \mathbf{q}) \chi_k(\mathbf{R}, \mathbf{q}, t). \quad (23)$$

In a polaritonic approach, the electronic and photon coordinates are treated on the same footing and described by a polaritonic wave function which depends parametrically on the nuclear coordinates only<sup>56,60,81,82,174-176</sup>

$$\Psi(\mathbf{r}, \mathbf{R}, \mathbf{q}, t) = \sum_k \phi_k(\mathbf{r}, \mathbf{q}; \mathbf{R}) \chi_k(\mathbf{R}, t). \quad (24)$$

While these Born-Huang expansions are in principle equivalent, approximations will lead to different results. In the simplest case, we take into account only a single term of these expansions as in standard electronic Born-Oppenheimer approximation. In the discussion of exact response theory in Section (5) we do not refer to any explicit form of the Hamiltonian. In Section (6), we focus on the polaritonic approach and describe the QED-CC and QED-HF response theory. The interaction between the nuclear motion and the electromagnetic degrees of freedom can lead to novel non-adiabatic coupling terms that could, in some situations, jeopardize the validity of the BO approximation.<sup>28,51,81,177-179</sup> Nevertheless, we will not explore such effects, and we will work in a fixed-nuclei framework. Although these approximations already reduce the complexity of the problem, further simplifications are needed to deal with the electromagnetic environment and treat the molecule and its interaction with the fields with chemical accuracy.

#### 4.1. Cavity QED

The Hamiltonian in Eq. (17) allows for simultaneous treatment of light and matter, where we could, in principle, include any optical device that contributes to a modification of the electromagnetic environment. Nevertheless, the molecular complexity and the presence of the optical apparatus make the problem impractical from a computational point of view.

The explicit modelling of the photonic device is avoided by defining an effective change in the structure of the electromagnetic modes. To this end, we impose boundary conditions on the fields (e.g. vanish on the surface of the optical device) to model the electromagnetic confinement induced by the cavity. The vector potential is expanded in terms of a complete orthonormal set of suitable electromagnetic normal mode functions  $\{\mathbf{S}_\alpha(\mathbf{r})\}$ .<sup>102,180</sup> For a rectangular parallelepiped with perfectly conducting walls of sides  $L_x$ ,  $L_y$  and  $L_z$ , the transverse mode functions are standing waves<sup>180</sup>

$$\begin{aligned} S_x(\mathbf{r}) &= \sqrt{\frac{8}{V_c}} \cos(k_x x) \sin(k_y y) \sin(k_z z) \\ S_y(\mathbf{r}) &= \sqrt{\frac{8}{V_c}} \sin(k_x x) \cos(k_y y) \sin(k_z z) \\ S_z(\mathbf{r}) &= \sqrt{\frac{8}{V_c}} \sin(k_x x) \sin(k_y y) \cos(k_z z), \end{aligned}$$

where  $V_c = L_x \times L_y \times L_z$  is the total volume of the paral-

lelepiped and  $\mathbf{k}$  is the wave vector which is now quantized:

$$k_i = n \frac{\pi}{L_i} \quad n = 1, 2, \dots \quad (25)$$

In the absence of external charges, if we assume that the walls of the parallelepiped are grounded, the scalar potential vanishes identically  $\phi = 0$ . The quantization is then performed by promoting the expansion coefficients to quantum operators, and the radiation Hamiltonian for the free fields inside the perfect optical device is discretized in terms of the cavity eigenmodes

$$H_{rad} = \sum_{\alpha} \omega_{\alpha} b_{\alpha}^{\dagger} b_{\alpha}, \quad (26)$$

where  $b_{\alpha}^{\dagger}$  is the creation operator for the  $\alpha$ -mode of frequency

$\omega_{\alpha}$ .

In the presence of molecules, which can be considered as a source of electromagnetic fields, we must also ensure that the scalar potential in Eq. (15) is consistent with the boundary conditions. We can enforce them by adding an auxiliary scalar field  $F$  to the particles' Coulomb potential. This potential can be thought of as a potential generated by *image charges*<sup>102,180</sup> placed outside the volume of quantization (i.e. outside the volume of interest of the system). This potential can be expressed in terms of a response kernel  $\Theta(\mathbf{s}; \mathbf{r})$  and the real charge distribution  $\rho$  inside the cavity<sup>102,180</sup>

$$F(\mathbf{r}) = \int_{\bar{V}} d^3s \frac{\int_{V_c} d^3r' \rho(\mathbf{r}') \Theta(\mathbf{s}; \mathbf{r}')}{|\mathbf{r} - \mathbf{s}|} \quad (27)$$

where  $\mathbf{s}$  is a point outside the cavity volume. The Hamiltonian describing the molecular system then reads<sup>180</sup>

$$\begin{aligned} H_c = & \sum_i \frac{1}{2} \mathbf{p}_i^2 + \frac{1}{2} \sum_{i \neq j} \frac{1}{|\mathbf{r}_i - \mathbf{r}_j|} - \sum_{i,M} \frac{Z_M}{|\mathbf{r}_i - \mathbf{R}_M|} + \frac{1}{2} \sum_{M \neq N} \frac{Z_M Z_N}{|\mathbf{R}_M - \mathbf{R}_N|} \\ & + \sum_i \frac{1}{2c} (\mathbf{p}_i \cdot \mathbf{A}(\mathbf{r}_i) + \mathbf{A}(\mathbf{r}_i) \cdot \mathbf{p}_i) + \sum_i \frac{1}{2c^2} \mathbf{A}^2(\mathbf{r}_i) \\ & + \sum_{\alpha} \omega_{\alpha} b_{\alpha}^{\dagger} b_{\alpha} + \frac{1}{2} \sum_M Z_M F(\mathbf{R}_M) - \frac{1}{2} \sum_i F(\mathbf{r}_i). \end{aligned} \quad (28)$$

As seen from (27), the last two terms introduced by  $F$  correspond to a modified Coulomb interaction kernel due to the boundary conditions, i.e. they lead to a modified longitudinal interaction among the particles. The factor 1/2 appears because it describes an interaction with an *image* charge distribution.<sup>102</sup> While some authors suggest that this contribution is the major difference from free space,<sup>181–183</sup> the discussion of these terms for *ab initio* QED is often neglected. Nevertheless, we will see that they can be handled in a more practical way by a suitable unitary transformation.<sup>72,180</sup>

### Remarks

The Hamiltonian in Eq. (28) now acts on a Hilbert space  $\mathcal{V}$  which is the direct product of the full-CI Fock space for the electrons  $\mathcal{V}_{FCI}$  and the photon space spanned by the cavity eigenmodes  $\mathcal{V}_C$

$$\mathcal{V} = \mathcal{V}_{FCI} \otimes \mathcal{V}_C. \quad (29)$$

However, each cavity setup corresponds to specific boundary requirements, leading to different quantum fields: different boundary conditions could substantially modify both the shape of the eigenmodes  $\mathcal{S}_{\alpha}(\mathbf{r})$  and the Coulomb kernel  $\Theta(\mathbf{s}; \mathbf{r})$ .

The photonic space  $\mathcal{V}_C$  is usually truncated, considering only a

few eigenmodes relevant to the system. Therefore, the excited states of the Hamiltonian in Eq. (28) are again true eigenstates with an infinite lifetime. Notice that, in the limit of an infinitely large cavity, if we retain a considerable number of modes we obtain again a fine energy discretization of the photon bath that recovers the decay channels.<sup>48</sup>

The masses of the particles in (28) are dependent on the electromagnetic mode structure and, in general, are different from their physical and free-space bare masses.<sup>163,184</sup> However, in QED *ab initio* calculations, the physical masses are usually employed, implicitly considering the interaction energy with the continuum photon bath<sup>48</sup>. The effects of the modification of the masses on chemical and physical properties from an *ab initio* perspective, to the best of our knowledge, is still to explore.

Finally, because of the states of the optical device  $\mathcal{V}_C$ , the system's symmetries now differ from the bare molecule ones due to the cavity's modified eigenmodes and potential in Eq. (27). This leads to modifications of selection rules and other symmetry-related properties.

## 4.2. Dipole approximation

The dipole approximation is commonly employed in *ab initio* polaritonic chemistry. It assumes that the (relevant) elec-

tromagnetic modes have a wavelength much larger than the characteristic lengths of the molecules. The complete shape of the modes  $\mathbf{S}_\alpha(\mathbf{r})$  is therefore irrelevant, and we only need to evaluate the fields at a point internal to the molecular struc-

ture. In Eq. (17), we then set  $\mathbf{A}(\mathbf{r}) \rightarrow \mathbf{A}(0)$ , and obtain the Pauli-Fierz Hamiltonian  $H_{PF}^v$  in dipole approximation and velocity representation

$$\begin{aligned} H_{PF}^v &= \sum_i \frac{1}{2} \mathbf{p}_i^2 + \frac{1}{2} \sum_{i \neq j} \frac{1}{|\mathbf{r}_i - \mathbf{r}_j|} - \sum_{i,M} \frac{Z_M}{|\mathbf{r}_i - \mathbf{R}_M|} + \frac{1}{2} \sum_{M \neq N} \frac{Z_M Z_N}{|\mathbf{R}_N - \mathbf{R}_M|} \\ &+ \sum_i \frac{1}{2c} (\mathbf{p}_i \cdot \mathbf{A}(0) + \mathbf{A}(0) \cdot \mathbf{p}_i) + \sum_i \frac{1}{2c^2} \mathbf{A}^2(0) \\ &+ \sum_\alpha \omega_\alpha b_\alpha^\dagger b_\alpha + \frac{1}{2} \sum_M Z_M \tilde{F}(\mathbf{R}_M) - \frac{1}{2} \sum_i \tilde{F}(\mathbf{r}_i), \end{aligned} \quad (30)$$

where we applied the BO approximation. The dipole approximation allows for the modelling of the photons only by adequately tuning the frequency  $\omega_\alpha$  and the coupling strength  $\lambda_\alpha$  for the cavity modes.<sup>48</sup> The problem is eventually reduced to a single effective cavity mode. Assuming to work with real field polarization vectors, the final Hamiltonian for our system is

$$\begin{aligned} H &= \sum_{pq} h_{pq} E_{pq} + \frac{1}{2} \sum_{pqrs} g_{pqrs} e_{pqrs} + h_{nuc} \\ &+ \sqrt{\frac{\omega_\alpha}{2}} (\boldsymbol{\lambda}_\alpha \cdot \mathbf{d}) (b_\alpha^\dagger + b_\alpha) + \frac{1}{2} (\boldsymbol{\lambda}_\alpha \cdot \mathbf{d})^2 \\ &+ \omega_\alpha b_\alpha^\dagger b_\alpha + \frac{1}{2} \sum_M Z_M \tilde{F}(\mathbf{R}_M) - \frac{1}{2} \sum_i \tilde{F}(\mathbf{r}_i), \end{aligned} \quad (31)$$

where  $\boldsymbol{\lambda}_\alpha = \lambda_\alpha \boldsymbol{\epsilon}_\alpha$  is the light-matter coupling vector of the  $\alpha$  electromagnetic mode, and we used standard second quantization notation for the electronic Hamiltonian.<sup>185</sup> This formulation is suitable for nonchiral cavities, while for helicity-preserving devices, we necessarily need to work with complex polarization vectors (see Eqs (19) and (20)). The Hamiltonian in Eq. (31) can be recast in a more convenient form, called length representation  $H_{PF}^l$ , by employing a unitary transformation  $U$  such that

$$U \mathbf{p} U^\dagger = \mathbf{p} - \frac{1}{c} \mathbf{A}(0), \quad (32)$$

which will allow us to write the interaction between the molecule and the fields in a manifestly dipolar fashion. The transformation is

$$U = \exp \left[ i \sum_i \mathbf{r}_i \cdot \frac{1}{c} \mathbf{A}(0) \right] = \exp \left[ -i \mathbf{d} \cdot \frac{1}{c} \mathbf{A}(0) \right] \quad (33)$$

where  $\mathbf{d}$  is the electronic dipole operator. By using Eq. (33) and a transformation which changes the phases of the creation/annihilation operators<sup>162,186–188</sup>

$$V = \exp \left[ -i \frac{\pi}{2} \sum_\alpha b_\alpha^\dagger b_\alpha \right], \quad (34)$$

we finally obtain

$$\begin{aligned} H_{PF}^l &= V U H_{PF}^v U^\dagger V^\dagger \\ &= \sum_i \frac{1}{2} \mathbf{p}_i^2 + \frac{1}{2} \sum_{i \neq j} \frac{1}{|\mathbf{r}_i - \mathbf{r}_j|} - \sum_{i,M} \frac{Z_M}{|\mathbf{r}_i - \mathbf{R}_M|} + \frac{1}{2} \sum_{M \neq N} \frac{Z_M Z_N}{|\mathbf{R}_N - \mathbf{R}_M|} \\ &+ \sum_\alpha \sqrt{\frac{\omega_\alpha}{2}} (\boldsymbol{\lambda}_\alpha \cdot \mathbf{d}) (b_\alpha^\dagger + b_\alpha) + \frac{1}{2} \sum_\alpha (\boldsymbol{\lambda}_\alpha \cdot \mathbf{d})^2 \\ &+ \sum_\alpha \omega_\alpha b_\alpha^\dagger b_\alpha \end{aligned} \quad (35)$$

The bilinear light-matter interaction term of this Hamiltonian can be interpreted as the interaction of the molecular dipole with the displacement field.<sup>162</sup> The quadratic term is called dipole self-energy and ensures the Hamiltonian leads to well-defined states and properties.<sup>186</sup> Moreover, transformation Eq. (33) cancels the image charge contribution from  $\tilde{F}$  so that no reference to the image charges appears in Eq. (35).<sup>72,163,180</sup> Notice that these Hamiltonians are also often referred to as length or velocity *gauge*, although in a QED framework this can be misleading, and the term *form* or *representation* is more appropriate. The hierarchy of approximations that are employed to study quantum light-matter systems is pictorially summarized in Fig. 2.

### Remarks

There are several advantages to employing the Pauli-Fierz Hamiltonian in the length representation. Contrary to the velocity representation Eq. (30), Eq. (35) has a light-matter interaction term linear in the field with no reference to the image charge distribution.

The transformation in Eq. (33) implies that the momentum operator  $\mathbf{p}$  now represents the kinetic momentum of particles

$$\mathbf{p} = m\mathbf{v}, \quad (36)$$

so that the first line of Eq. (35) truly represents the Coulomb and kinetic energy of the matter subsystem only.

The operator  $b^\dagger$  is no longer a purely photonic operator since

$U$  in Eq. (33) mixes electromagnetic and matter degrees of freedom. The original photon creation operator in the length representation after the transformoin is<sup>162,186,188</sup>

$$VU b_{\alpha}^{\dagger} U^{\dagger} V^{\dagger} = -i b_{\alpha}^{\dagger} - i \frac{1}{\sqrt{2\omega_{\alpha}}} (\boldsymbol{\lambda}_{\alpha} \cdot \mathbf{d}). \quad (37)$$

These operators are now connected to the auxiliary fields of the macroscopic Maxwell's equations, where we can recognize the transverse polarization<sup>162,186</sup>

$$\mathbf{P}_{\perp} = \frac{1}{4\pi} \sum_{\alpha} (\boldsymbol{\lambda}_{\alpha} \cdot \mathbf{d}) \boldsymbol{\lambda}_{\alpha}. \quad (38)$$

The separation into "matter" and "photon" degrees of freedom is, therefore, blurred in this representation.<sup>162</sup>

### 4.3. Beyond the dipole approximation

*Ab initio* QED calculations often rely upon the dipole approximation, which provides a good compromise between accuracy and affordability. Nevertheless, achieving a better description of the light-matter interaction is an essential challenge for polaritonic systems, and a few attempts in this direction have already been reported.<sup>189–191</sup> To go beyond the dipole approximation, we could replace the vector potential  $\mathbf{A}(\mathbf{r})$  with its first-order expansion around the molecular origin. For a sinusoidal field, this reduces to an expansion in terms of the wavevector  $\mathbf{k}$

$$e^{i\mathbf{k} \cdot \mathbf{r}} \approx 1 + i\mathbf{k} \cdot \mathbf{r} + \dots \quad (39)$$

This expansion is often employed in the semiclassical description of the fields to model, for instance, X-ray absorption leading to the well-known electric quadrupole and magnetic dipole interaction terms.<sup>192–194</sup> The corresponding QED Hamiltonian can then be obtained in the velocity representation by the following substitution in Hamiltonian Eq. (28)

$$\mathbf{A}(\mathbf{r}) \rightarrow \mathbf{A}(0) + \mathbf{r} \cdot \left. \frac{\partial \mathbf{A}}{\partial \mathbf{r}} \right|_{\mathbf{r}=0} + \dots \quad (40)$$

The multipolar Hamiltonian can be obtained similarly to the length representation of the dipole Hamiltonian, applying the Power-Zienau-Woolley (PZW) transformation with the multipolar expansion of the vector potential,<sup>163</sup> i.e. the transformation of Eq. (33) with the vector potential of Eq. (40). This transformation also leads to electric (dipole and quadrupole) and magnetic self-energy terms, which guarantee the boundedness of the Hamiltonian.<sup>163,186,190</sup> Overcoming the dipole approximation is particularly relevant when the molecules interact with chiral fields, which leads to novel phenomena such as cavity-induced circular dichroism or cavity enantiomeric discrimination.<sup>64,190</sup> The description of magnetic interactions is then essential. However, the multipolar expansion of the interaction beyond the electric dipole presents some difficulties, already in the semiclassical approximation,<sup>192–195</sup> as the interaction terms are now origin dependent. The dipole op-

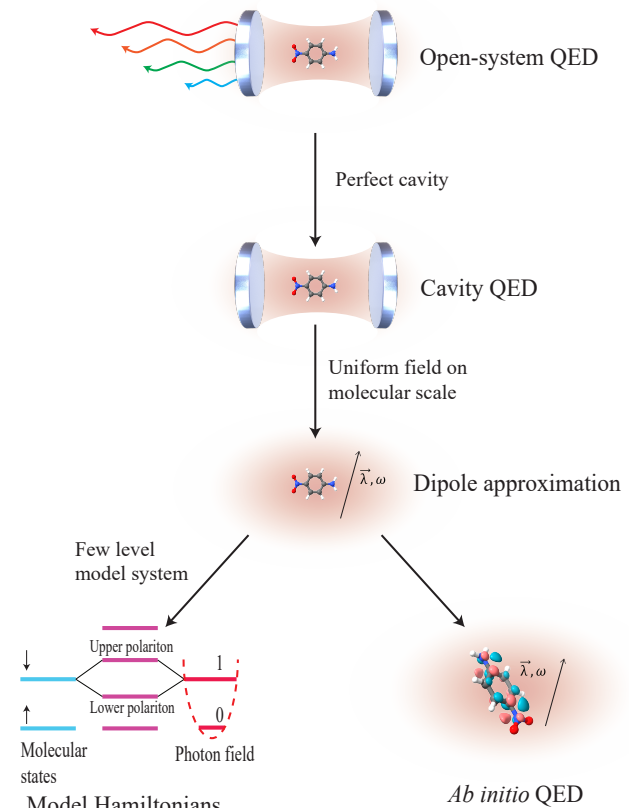


FIG. 2. Graphic summary of the hierarchy of approximations for computational polaritonic chemistry. The starting point is the open system described by the nonrelativistic Pauli-Fierz Hamiltonian, which includes the molecular system and the optical device immersed in the photon continuum. As a first approximation, the device is assumed to be perfect, and cavity QED formalism with a limited number of effective photon states is employed. Then, in the dipole approximation, the field is assumed to be uniform over the molecular scale. The exact shape of the photon states is irrelevant, and the system is described through an effective coupling. At the *ab initio* level, the polaritonic problem is approximated with a suitable parametrization.<sup>56,58–65</sup> Alternatively, there are phenomenological models where the molecular complexity is usually reduced to a few selected reference states, as, for instance, in the Jaynes-Cummings model.<sup>4</sup>

erator also depends on the choice of the origin for charged systems, but this can be shown to be equivalent to a gauge transformation on Hamiltonian Eq. (31). Manifest origin invariance can then be recovered by a suitable coherent state transformation, even for a finite electronic basis set (see Eqs. (201) and (202)).<sup>60,61,64</sup> At the same time, to the best of our knowledge, a similar solution has yet to be developed for higher-order Hamiltonians, and therefore using such an expansion could lead to unphysical results. This issue could be solved by retaining the complete shape of the field  $\mathcal{S}_{\alpha}(\mathbf{r})$  instead of relying upon a multipolar expansion. This is considered computationally and theoretically challenging also because of the dependence of the field shape on the



boundary conditions. Nevertheless, some progress has been made for a sinusoidal field in the semiclassical and QED frameworks.<sup>189,194,196–198</sup> Alternatively, effective reformulations of the QED problem in terms of reduced quantities, such as in QEDFT, can convey a different perspective for higher-order approximations.<sup>56,187,199–201</sup>

## 5. EXACT POLARITONIC RESPONSE THEORY

In this section, we highlight the similarities and differences with standard molecular response theory following the derivation of Jørgensen and Olsen,<sup>84</sup> with particular emphasis on the quantities that describe the cross-talk between light and matter.

From the exact solution of the time-dependent Schrödinger equation

$$i \frac{d}{dt} |\Psi\rangle = H |\Psi\rangle \quad (41)$$

we derive, for an operator  $\Omega$ , the Ehrenfest theorem<sup>202</sup>

$$\frac{d}{dt} \langle \Psi | \Omega | \Psi \rangle = -i \langle \Psi | [\Omega, H] | \Psi \rangle + \langle \Psi | \frac{\partial \Omega}{\partial t} | \Psi \rangle, \quad (42)$$

where  $H$  is here a polaritonic Hamiltonian and  $|\Psi\rangle$  are polaritonic states of entangled light-matter character. The operator  $\Omega$  can then be an electronic, photonic or mixed electron-photon operator. The exact eigenstates of the Hamiltonian are defined by the eigenvalue equation

$$H |n\rangle = E_n |n\rangle \quad n = 0, 1, 2, \dots, \quad (43)$$

and are assumed to form a complete basis for the radiation-

matter Hilbert space  $\mathcal{V}$ . We further assume that at the initial time the system is in its ground polaritonic state  $|0\rangle$ . We then apply the following perturbation operator

$$V^t = e^{\eta t} \sum_n \left( V^{\omega_n} e^{-i\omega_n t} + (V^{\omega_n})^\dagger e^{i\omega_n t} \right) \quad (44)$$

where  $\eta$  is a positive infinitesimal that ensures the perturbation to vanish for  $t \rightarrow -\infty$ . The time evolution of the initial ground state is then determined by the time-dependent Hamiltonian

$$H + V^t \quad (45)$$

and can be modelled by a unitary transformation

$$|\tilde{0}\rangle = \exp[iP'(t)] |0\rangle, \quad (46)$$

where we used a tilde to indicate the time-evolved state and  $P'(t)$  is a Hermitian operator:

$$P'(t) = \sum_{n>0} (P'_n |n\rangle \langle 0| + P_n'^* |0\rangle \langle n|) + (P'_0 + P_0'^*) |0\rangle \langle 0|. \quad (47)$$

The ground state phase evolution can be explicitly factorized<sup>85</sup>

$$|\tilde{0}\rangle = e^{i\phi(t)} \exp\left(i \sum_{n>0} (P_n |n\rangle \langle 0| + P_n^* |0\rangle \langle n|)\right) |0\rangle, \quad (48)$$

and if the operator  $\Omega$  in Eq. (42) does not involve time differentiation, it can be disregarded. We will then make use of the phase-isolated wave function

$$|\bar{0}\rangle = \exp\left(i \sum_{n>0} (P_n |n\rangle \langle 0| + P_n^* |0\rangle \langle n|)\right) |0\rangle \quad (49)$$

and perform an expansion of the state transfer coefficients in orders of the perturbation

$$P_n = P_n^{(0)} + P_n^{(1)} + P_n^{(2)} + P_n^{(3)} + \dots \quad (50)$$

which leads to the perturbative expansion of the phase-isolated state

$$|\bar{0}\rangle^{(0)} = |0\rangle \quad (51)$$

$$|\bar{0}\rangle^{(1)} = i \sum_{n>0} |n\rangle P_n^{(1)} \quad (52)$$

$$|\bar{0}\rangle^{(2)} = -\frac{1}{2} |0\rangle \sum_{j>0} P_j^{(1)} P_j^{*(1)} + i \sum_{n>0} |n\rangle P_n^{(2)} \quad (53)$$

$$|\bar{0}\rangle^{(3)} = -\frac{1}{2} |0\rangle \sum_{j>0} (P_j^{(2)} P_j^{*(1)} + P_j^{(1)} P_j^{*(2)}) + i \sum_{n>0} |n\rangle (P_n^{(3)} - \frac{1}{6} P_n^{(1)} \sum_{j>0} P_j^{(1)} P_j^{*(1)}). \quad (54)$$

By defining  $P_{-n} \equiv P_n^*$  and by using in Eq. (42) the state transfer operators  $\Omega \in \{|0\rangle \langle n| ; |n\rangle \langle 0|\}$ , we obtain the following

hierarchy of differential equations, for positive and negative indices<sup>84</sup>

$$i \operatorname{sgn}(k) \dot{P}_k^{(1)} - \omega_k P_k^{(1)} = -iV_k^t \quad (55)$$

$$i \operatorname{sgn}(k) \dot{P}_k^{(2)} - \omega_k P_k^{(2)} = \sum_n V_{k-n}^t P_n^{(1)} \quad (56)$$

$$i \operatorname{sgn}(k) \dot{D}_k^{(3)} - \omega_k D_k^{(3)} = \sum_n \left[ V_{k-n}^t P_n^{(2)} + i\theta(kn) V_n^t P_{-n}^{(1)} P_k^{(1)} \right] + iV_k^t \sum_{n>0} P_{-n}^{(1)} P_n^{(1)}, \quad (57)$$

where  $\theta(x)$  is the Heaviside step function, while  $\omega_k$ ,  $D_k^{(n)}$  and  $V_n^t$  are defined as

$$\omega_k = \omega_{-k} = E_k - E_0 \quad (58)$$

$$D_k^{(3)} = P_k^{(3)} - \frac{2}{3} P_n^{(1)} \sum_{j>0} P_j^{(1)} P_{-j} \quad (59)$$

$$V_k^t = \begin{pmatrix} \langle k|V^t|0\rangle \\ -\langle 0|V^t|-k\rangle \end{pmatrix}; \begin{pmatrix} k > 0 \\ k < 0 \end{pmatrix} \quad (60)$$

$$V_{kn}^t = \begin{pmatrix} 0 & \langle k|V^t|-n\rangle - \delta_{k,-n} \langle 0|V^t|0\rangle \\ \langle n|V^t|-k\rangle - \delta_{-k,n} \langle 0|V^t|0\rangle & 0 \end{pmatrix}; \begin{pmatrix} k, n > 0 & k > 0, n < 0 \\ k < 0, n > 0 & k, n < 0 \end{pmatrix} \quad (61)$$

Notice that the solutions for lower-order coefficients are necessary for higher-order equations. We can solve these equations, which all have the structure

$$i \operatorname{sgn}(k) \frac{df(t)}{dt} - \omega_k f(t) = g(t) \quad (62)$$

with the general solution

$$f(t) = -i \operatorname{sgn}(k) e^{-i\omega_k \operatorname{sgn}(k)t} \int_{-\infty}^t d\tau e^{i\omega_k \operatorname{sgn}(k)\tau} g(\tau), \quad (63)$$

which fulfils the vanishing initial conditions for the coefficients. Expressing the change of the time development average value of an observable  $A$  from its zero-order mean value in orders of the perturbation we obtain

$$\begin{aligned} \delta \langle A \rangle (t) &= A_{V^t}(t) - A_{V^t}(0) = \langle \tilde{0}|A|\tilde{0}\rangle - \langle 0|A|0\rangle = \\ &= \sum_n e^{-i\omega_n t + \eta t} \langle \langle A; V^{\omega_n} \rangle \rangle_{\omega_n + i\eta} \\ &+ \frac{1}{2} \sum_{mn} e^{-i\omega_n t - i\omega_m t + 2\eta t} \langle \langle A; V^{\omega_n}, V^{\omega_m} \rangle \rangle_{\omega_n + i\eta, \omega_m + i\eta} + \\ &+ \frac{1}{6} \sum_{lmn} e^{-i\omega_l t - i\omega_m t - i\omega_n t + 3\eta t} \langle \langle A; V^{\omega_l}, V^{\omega_m}, V^{\omega_n} \rangle \rangle_{\omega_l + i\eta, \omega_m + i\eta, \omega_n + i\eta} + \dots \end{aligned} \quad (64)$$

We then define the linear, quadratic and cubic response functions, respectively

$$\langle \langle A; V^{\omega_n} \rangle \rangle_{\omega_n} \quad (65)$$

$$\langle \langle A; V^{\omega_n}, V^{\omega_m} \rangle \rangle_{\omega_n, \omega_m} \quad (66)$$

$$\langle \langle A; V^{\omega_l}, V^{\omega_m}, V^{\omega_n} \rangle \rangle_{\omega_l, \omega_m, \omega_n}. \quad (67)$$

These functions express the linear, quadratic and cubic time-variation of an observable  $A$  as resulting from a perturbation in the frequency domain

$$\delta \langle A \rangle^{(1)}(\omega_1) = \langle \langle A; V^{\omega_1} \rangle \rangle_{\omega_1} \quad (68)$$

$$\delta \langle A \rangle^{(2)}(\omega_1, \omega_2) = \frac{1}{2} \langle \langle A; V^{\omega_1}, V^{\omega_2} \rangle \rangle_{\omega_1, \omega_2} \quad (69)$$

$$\delta \langle A \rangle^{(3)}(\omega_1, \omega_2, \omega_3) = \frac{1}{6} \langle \langle A; V^{\omega_1}, V^{\omega_2}, V^{\omega_3} \rangle \rangle_{\omega_1, \omega_2, \omega_3}, \quad (70)$$

and can therefore be interpreted as molecular (hyper)polarizabilities. For instance, for an electric dipole perturbation

$$V^\omega = -\mathbf{d} \cdot \mathbf{E}(\omega), \quad (71)$$

the first order variation of the molecular dipole reads

$$\delta \langle \mathbf{d} \rangle^{(1)}(\omega) = -\langle \langle \mathbf{d}; \mathbf{d} \rangle \rangle_\omega \cdot \mathbf{E}(\omega) \quad (72)$$

and the linear dipole-dipole response function  $\langle \langle \mathbf{d}; \mathbf{d} \rangle \rangle_\omega$  can then be interpreted as the (negative) time-dependent molecular polarizability at frequency  $\omega$ . Using the perturbation expansions of the coefficients and the state wave function Eqs. (50) and (51)-(54), we obtain

$$\begin{aligned} \langle A \rangle_{V^\omega} &= \langle 0|A|0 \rangle \\ &+ \langle 0^{(1)}|A|0 \rangle + \langle 0|A|0^{(1)} \rangle \\ &+ \langle 0^{(1)}|A|0^{(1)} \rangle + \langle 0|A|0^{(2)} \rangle + \langle 0^{(2)}|A|0 \rangle \\ &+ \langle 0^{(3)}|A|0 \rangle + \langle 0|A|0^{(3)} \rangle + \langle 0^{(1)}|A|0^{(2)} \rangle + \langle 0^{(2)}|A|0^{(1)} \rangle + \dots \\ &= \langle 0|A|0 \rangle \\ &-i \sum_n A_{-n} P_n^{(1)} \\ &-i \sum_n A_{-n} P_n^{(2)} + \sum_{n,j>0} P_{-j}^{(1)} A_{j-n} P_n^{(1)} \\ &-i \sum_n A_{-n} D_n^{(3)} + \sum_{n,k>0} P_{-k}^{(2)} A_{k-n} P_n^{(1)} + \sum_{n,k>0} P_{-k}^{(1)} A_{k-n} P_n^{(2)} + \dots \end{aligned} \quad (73)$$

By comparing Eqs. (64) and (73), using Eq. (63) for the state transfer parameters, we finally obtain the explicit expressions for the linear, quadratic and cubic response functions in terms of the eigenstates of the Hamiltonian<sup>84</sup>

$$\langle \langle A; V^\omega \rangle \rangle_\omega = -\sum_k \frac{\text{sgn}(k) A_{-k} V_k^\omega}{\omega - \text{sgn}(k) \omega_k} \quad (74)$$

$$\langle \langle A; V^{\omega_1}, V^{\omega_2} \rangle \rangle_{\omega_1, \omega_2} = \hat{P}(\omega_1, \omega_2) \left[ -\sum_{k,n} \frac{A_{-k} V_{k-n}^{\omega_1} V_n^{\omega_2}}{(\omega_1 + \omega_2 - \text{sgn}(k) \omega_k)(\omega_2 - \text{sgn}(n) \omega_n)} + \sum_{k,n>0} \frac{V_{-k}^{\omega_1} A_{k-n} V_n^{\omega_2}}{(\omega_1 + \omega_k)(\omega_2 - \omega_n)} \right] \quad (75)$$

$$\begin{aligned} \langle \langle A; V^{\omega_1}, V^{\omega_2}, V^{\omega_3} \rangle \rangle_{\omega_1, \omega_2, \omega_3} &= \hat{P}(\omega_1, \omega_2, \omega_3) \left\{ \sum_k \frac{A_{-k} \text{sgn}(k)}{\omega_1 + \omega_2 + \omega_3 - \text{sgn}(k) \omega_k} \times \left[ \sum_n \frac{\theta(kn) V_n^{\omega_1} V_{-n}^{\omega_2} V_k^{\omega_3}}{(\omega_2 + \text{sgn}(n) \omega_n)(\omega_3 - \text{sgn}(k) \omega_k)} \right. \right. \\ &- \sum_{n,m} \frac{V_{k-n}^{\omega_1} V_{n-m}^{\omega_2} V_m^{\omega_3}}{(\omega_2 + \omega_3 - \text{sgn}(n) \omega_n)(\omega_3 - \text{sgn}(m) \omega_m)} + \left. \sum_{n>0} \frac{V_k^{\omega_1} V_n^{\omega_2} V_{-n}^{\omega_3}}{(\omega_2 - \text{sgn}(n) \omega_n)(\omega_3 + \text{sgn}(n) \omega_n)} \right] \\ &- \sum_{m,n,k>0} \left( \frac{V_{-km}^{\omega_1} V_{-m}^{\omega_2} V_n^{\omega_3} A_{k-n}}{(\omega_1 + \omega_2 + \omega_k)(\omega_2 + \omega_m)(\omega_3 - \omega_n)} - \frac{V_{-k}^{\omega_1} V_{n-m}^{\omega_2} V_m^{\omega_3} A_{k-n}}{(\omega_2 + \omega_3 - \omega_n)(\omega_1 + \omega_k)(\omega_3 - \omega_m)} \right) \left. \right\} \end{aligned} \quad (76)$$

where  $\hat{P}(\omega_1, \omega_2)$  and  $\hat{P}(\omega_1, \omega_2, \omega_3)$  sum all the permutations of the frequencies

$$\hat{P}(\omega_1, \omega_2) f(\omega_1, \omega_2) = f(\omega_1, \omega_2) + f(\omega_2, \omega_1) \quad (77)$$

$$\begin{aligned} \hat{P}(\omega_1, \omega_2, \omega_3) f(\omega_1, \omega_2, \omega_3) &= f(\omega_1, \omega_2, \omega_3) + f(\omega_1, \omega_3, \omega_2) \\ &+ f(\omega_2, \omega_1, \omega_3) + f(\omega_2, \omega_3, \omega_1) \\ &+ f(\omega_3, \omega_1, \omega_2) + f(\omega_3, \omega_2, \omega_1), \end{aligned} \quad (78)$$

and we set the switching parameter  $\eta$  to zero.

These equations are identical to the expressions obtained in molecular response theory,<sup>84-93</sup> since they only rely on the Schrödinger equation. However, the explicit treatment

of internal electromagnetic fields as dynamical variables in our system leads to novel perspectives. First of all, we must remember that the eigenstates of the system are mixed matter-

photon states, so they belong to a larger Hilbert space than the usual molecular one. The properties of these field-dressed states will therefore differ from the bare-molecule ones, leading, for instance, to different excitation energies and transition moments. Moreover, additional possibilities for probing the properties of the system arise since the external perturbation  $V^t$  can now act on both matter and photon degrees of freedom. Furthermore, considering the internal electromagnetic fields allows us to explore additional observables connected to the radiation fields and their interactions with matter.

The linear response function Eq. (74) describes the first-order variation of an observable  $A$  and it is connected to the linear polarizabilities of the system. Its poles occur at the polaritonic excitation energies, and the corresponding residues are connected to the transition moments between the ground and

the excited states

$$\lim_{\omega \rightarrow \omega_n} (\omega - \omega_n) \langle \langle A; B \rangle \rangle_{\omega} = \langle 0|A|n \rangle \langle n|B|0 \rangle \quad (79)$$

$$\equiv A_{0n}B_{n0}$$

$$\lim_{\omega \rightarrow -\omega_n} (\omega + \omega_n) \langle \langle A; B \rangle \rangle_{\omega} = -\langle 0|B|n \rangle \langle n|A|0 \rangle \quad (80)$$

$$\equiv -B_{0n}A_{n0}.$$

The quadratic response function Eq. (75) is connected to the first hyperpolarizabilities of the system since it describes the second-order response to an external perturbation. Its residues are connected to the transition moments and matrices between the excited states. These can be obtained once the transition moments between ground and excited states have been computed

$$\lim_{\omega_2 \rightarrow \omega_m} (\omega_2 - \omega_m) \langle \langle A; B, C \rangle \rangle_{\omega_1, \omega_2} = \sum_{k>0} \left[ \frac{\langle 0|A|k \rangle (\langle k|B|m \rangle - \delta_{mk} \langle 0|B|0 \rangle)}{(\omega_1 + \omega_m - \omega_k)} - \frac{\langle 0|B|k \rangle (\langle k|A|m \rangle - \delta_{mk} \langle 0|A|0 \rangle)}{\omega_1 + \omega_k} \right] \langle m|C|0 \rangle \quad (81)$$

$$\lim_{\omega_1 \rightarrow -\omega_q} (\omega_1 + \omega_q) \lim_{\omega_2 \rightarrow \omega_m} (\omega_2 - \omega_m) \langle \langle A; B, C \rangle \rangle_{\omega_1, \omega_2} = -\langle 0|B|q \rangle (\langle q|A|m \rangle - \delta_{mq} \langle 0|A|0 \rangle) \langle m|C|0 \rangle. \quad (82)$$

These expressions also give us access to excited state properties such as the dipole moment. Finally, the cubic response function describes the third-order variations of an observable as a consequence of an external perturbation, and it is therefore connected to the second hyperpolarizabilities of the system.

The response functions exhibit the following symmetry relations:

$$\begin{aligned} \langle \langle A; B \rangle \rangle_{\omega} &= \langle \langle B; A \rangle \rangle_{-\omega} \\ &= \langle \langle A; B \rangle \rangle_{-\omega}^* \end{aligned} \quad (83)$$

$$\begin{aligned} \langle \langle A; B, C \rangle \rangle_{\omega_1, \omega_2} &= \langle \langle A; C, B \rangle \rangle_{\omega_2, \omega_1} \\ &= \langle \langle C; A, B \rangle \rangle_{-\omega_1 - \omega_2, \omega_1} \\ &= \langle \langle A; B, C \rangle \rangle_{-\omega_1, -\omega_2}^* \end{aligned} \quad (84)$$

$$\begin{aligned} \langle \langle A; B, C, D \rangle \rangle_{\omega_1, \omega_2, \omega_3} &= \langle \langle A; C, B, D \rangle \rangle_{\omega_2, \omega_1, \omega_3} \\ &= \langle \langle D; A, B, C \rangle \rangle_{-\omega_1 - \omega_2 - \omega_3, \omega_1, \omega_2} \\ &= \langle \langle A; B, C, D \rangle \rangle_{-\omega_1, -\omega_2, -\omega_3}^*, \end{aligned} \quad (85)$$

for Hermitian operators  $A, B, C$ , and  $D$ .

### Time-independent limit

The static response theory can be obtained from the previous derivation by setting the external frequencies  $\omega$  and the

switching parameter  $\eta$  to zero. Since the perturbation is now time-independent, it is possible to relate the static polaritonic properties to the derivatives of the Hamiltonian eigenvalues. The perturbation  $V$  acting on the system is time-independent and supposed to be smooth and small, and it is usually expressed as an external field  $\mathbf{F}$  acting on a molecular multipole  $\mathbf{x}$

$$V = -\mathbf{x} \cdot \mathbf{F}. \quad (86)$$

The perturbed Hamiltonian then reads

$$H = H_0 + V = H_0 - \mathbf{x} \cdot \mathbf{F}. \quad (87)$$

The Hamiltonian in Eq. (87) is endowed with well-defined eigenstates and eigenvalues, whose small changes compared to the unperturbed eigenvalues and eigenfunctions are commonly studied via the Rayleigh-Schrödinger (RS) perturbation theory.<sup>203</sup> From the eigenfunctions  $|n\rangle$  of the unperturbed Hamiltonian  $H_0$  (see Eq. (43)), the ground-state eigenfunction  $|\tilde{0}\rangle$  and the eigenvalue  $\tilde{E}$  of the perturbed operator are expressed as a power series:

$$|\tilde{0}\rangle = |0\rangle + |\tilde{0}^{(1)}\rangle + \dots \quad (88)$$

$$\tilde{E} = E_0 + E^{(1)} + E^{(2)} + \dots \quad (89)$$

The first- and second-order corrections to the energy read:

$$E^{(1)} = \langle 0|V|0 \rangle \quad (90)$$

$$E^{(2)} = \sum_{k=1}^{\infty} \frac{\langle 0|V|k \rangle \langle k|V|0 \rangle}{E_0 - E_k} = \frac{1}{2} \langle \langle V; V \rangle \rangle_{\omega=0}. \quad (91)$$

Eq. (90) is the well-known Hellmann-Feynman theorem<sup>204,205</sup> and only requires the knowledge of the unperturbed wave function, while Eq. (91) also includes a sum-over-states contribution from each excited state  $|k\rangle$  with energy  $E_k$ . The derivatives of the energy with respect to the external fields provide us with the ground state molecular properties. From Eqs. (86) and (90), we then identify the derivative of the energy with respect to the field  $\mathbf{F}$  as the ground state mean multipole value

$$-\left.\frac{d\tilde{E}}{d\mathbf{F}}\right|_{\mathbf{F}=0} = \langle 0|\mathbf{x}|0\rangle \quad (92)$$

From Eq. (91), the second derivative of the energy is then interpreted as the multipole polarizability to the field  $\mathbf{F}$ , and from Eq. (74) we identify the linear response function for  $\omega = 0$

$$\left.\frac{d^2\tilde{E}}{d^2\mathbf{F}}\right|_{\mathbf{F}=0} = 2 \sum_{k=1}^{\infty} \frac{\langle 0|\mathbf{x}|k\rangle \langle k|\mathbf{x}|0\rangle}{E_0 - E_k} = \langle\langle \mathbf{x}; \mathbf{x} \rangle\rangle_{\omega=0}. \quad (93)$$

The second derivatives of the energy are then connected to the molecular polarizabilities. Higher-order derivatives relate hyperpolarizabilities and nonlinear response functions. Notice that these expressions are the same as standard molecular static response theory, and they also hold for exact polaritonic states since they are based only on the Schrödinger equation.

### 5.1. On the rotational average of computed molecular properties

In this section, we discuss the problem of the orientational average of the computed polarizabilities, which is straightforwardly accomplished in standard molecular response theory to connect the single-molecule calculation to the macroscopic sample response. Since we are now considering states that belong to the extended light-matter Hilbert space in Eq. (29), we have to consider the molecule and the electromagnetic environment, which are defined by the optical device. In general, this introduces anisotropy in the system. The cavity field can also break the molecular symmetry, possibly allowing for otherwise symmetry-forbidden transitions. This anisotropy-symmetry breaking introduces further complications in the computation of molecular properties.

The bare molecular states are independent of the spatial orientation of the molecule. The energy is invariant for rigid-body rotations of the system, while the charge density rotates following the molecular structure, and so do properties such as molecular polarizabilities. However, the strong coupling between molecular and cavity states depends on the projection of the molecular dipole operator onto the cavity field, as can be seen in the electron-photon interaction term in Hamiltonian Eq. (31). This also means that there is a non-trivial energy dependence on the relative molecular orientation in the cav-

ity field. Excited states will be particularly affected by this

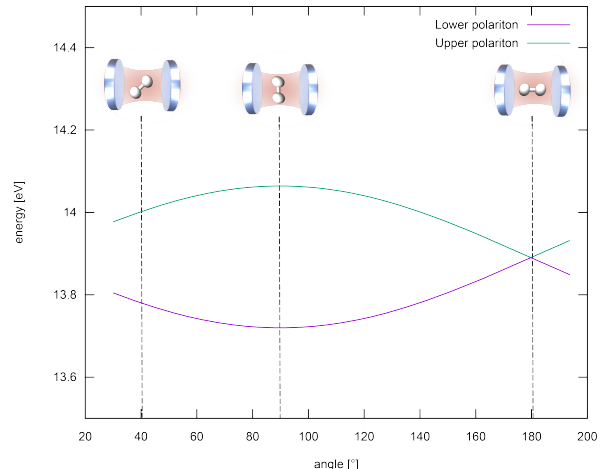


FIG. 3. Potential energy surfaces for a hydrogen molecule's upper and lower polaritons resonantly coupled with a quantum cavity, as a function of the molecular orientation. The energies are computed by using the time-dependent quantum electrodynamic Hartree-Fock method with a cc-pVDZ basis set and coupling constant set to  $\lambda = 0.01$  a.u. (see section (6)). When the molecule's transition dipole moment is aligned with the cavity field ( $90^\circ$ ), the Rabi splitting is maximal, while it decreases to zero when the transition moment is perpendicular to the field's polarization ( $180^\circ$ ).

orientation dependence. A bare electronic excitation with a transition moment orthogonal to the cavity field will have a negligible direct coupling with the photonic states. On the other hand, if the transition dipole moment is aligned with the field polarization, there will be mixing, giving rise to intense polaritonic excitations of hybrid light-matter character. This is illustrated in Fig. (3), where we plot the upper and lower polaritonic energies of a hydrogen molecule as a function of the angle between the transition dipole moment and the cavity field. These considerations on the molecular orientation pose some issues for the computation of molecular properties, as the direction of the cavity field is fixed in space by the experimental setup. In contrast, inside the cavity, the molecules are usually randomly or quasi-randomly oriented. Following a chemical approach, we could compute the sample's properties using the frequency-dependent polarizability Eq. (74), which must be averaged over the different molecular orientations<sup>193,206</sup>. The molecular orientation will be defined by a general set of parameters  $\Omega$ . For instance, it can be uniquely defined by the three Euler's angles  $(\phi, \theta, \chi)$ . Notice that a different set of parameter can be convenient depending on the setup. For instance, for a Fabry-Pérot resonator with two degenerate modes with wavevector  $\mathbf{k}$  and perpendicular polarizations, a rotation of the molecule along  $\mathbf{k}$  does not change the Hamiltonian. Then it is sufficient to use only two parameters instead of the three Euler's angles. If we consider the Boltzmann weight of each different orientation, we have

$$\overline{\langle\langle A ; B \rangle\rangle}_{\omega} = \int_{\Omega} e^{-\frac{E_0(\Omega)}{k_B T}} \sum_k \left( \frac{A_{0k}(\Omega) B_{k0}(\Omega)}{\omega - \omega_k(\Omega)} - \frac{B_{0k}(\Omega) A_{k0}(\Omega)}{\omega + \omega_k(\Omega)} \right) d\Omega \Big/ \int_{\Omega} e^{-\frac{E_0(\Omega)}{k_B T}} d\Omega, \quad (94)$$

where  $\overline{\langle\langle A ; B \rangle\rangle}_{\omega}$  is the averaged response function,  $E_0(\Omega)$  is the ground state energy of the polaritonic system as a function of the molecular orientation,  $k_B$  is the Boltzmann constant, and  $T$  is the temperature. Even if we disregard the Boltzmann weight and perform an isotropic average, the result does not simply lead to an isotropic polarization tensor. The excitation energies in the denominator depend on the orientation, as well as the numerator. The polarization will be generally anisotropic because of the introduction of the optical device.

As a concrete example, we can consider the computation of absorption spectra. The linear absorption spectrum is connected to the dipole-dipole polarizability, where  $A$  and  $B$  in Eq. (74) are components of the dipole operator  $d_i$ <sup>84,85,206</sup>

$$\langle\langle d_i ; d_j \rangle\rangle_{\omega} = \sum_{k>0} \left( \frac{\langle 0 | d_i | k \rangle \langle k | d_j | 0 \rangle}{\omega - \omega_k} - \frac{\langle 0 | d_j | k \rangle \langle k | d_i | 0 \rangle}{\omega + \omega_k} \right).$$

Neglecting the dependence of the polaritons on the molecular orientation, we obtain the usual expression for absorption by randomly oriented molecules in terms of the oscillator strength

$$f_{k0} = \frac{2}{3} \omega_k \sum_{i=x,y,z} |\langle 0 | d_i | k \rangle|^2. \quad (95)$$

This corresponds to fixing the relative molecule-field orientation. A fictitious peak-broadening is often applied to the computed spectrum  $S(\omega)$ , e.g. a Lorentzian lineshape with bandwidth broadening parameter  $\Delta$

$$\Gamma(\omega, \omega_k) = \frac{1}{\pi} \frac{\Delta}{(\omega - \omega_k)^2 + \Delta^2} \quad (96)$$

as reported in Refs.<sup>94,95</sup> so that the computed spectrum is

$$S(\omega) = \sum_k f_{k0} \Gamma(\omega, \omega_k). \quad (97)$$

However, different orientations could play an important role in determining the properties of the sample, and the choice of a fixed relative orientation does not give the full picture. For instance, if we are interested in a specific transition, we could suppose the field polarization to be parallel to the transition dipole moment. However, this could lead to biased results as certain effects could be enhanced while others suppressed.

The study of orientational disorder in *ab initio* polaritonic chemistry is still to be addressed. A possible approach would be to perform molecular dynamics simulations that sample the different orientations of the molecule inside the cavity and perform an average of the spectra obtained for each snapshot. This corresponds to an incoherent superposition of the spectra of an ensemble. The appearance of collective effects can introduce further complications in the computation of molecular properties. If we could perform an *ab initio* simulation including a sufficiently large number of molecules randomly or quasi-randomly oriented, the corresponding computed properties would include both collective and orientational effects. Alternatively, collective effects can initially be addressed with a simplified model, such as the Tavis-Cummings (TC) model,<sup>67,68</sup> which considers an ensemble of identical two-level non-interacting systems. Moreover, it disregards the dipole self-energy, the molecular dipoles and the so-called counter-rotating terms of the Hamiltonian. The Rabi splitting is then predicted to scale with the square root of the number of molecules and, therefore, it is sufficient to employ a smaller coupling strength compared to single-molecule calculations. The generalization of the TC model to an energy-broadened set of two-level molecules<sup>207</sup> predicts a Rabi splitting dependent on the *quadratic average* of the coupling strengths and on the energy broadening. The predicted spectrum would be very different from the one obtained by an average of single-molecule absorption spectra.

The interplay between single-molecule and collective effects will need a careful comparison between simplified models<sup>2,4,67,68</sup> and more accurate simulations, and recently some methods to study polaritonic chemistry in an impurity-like approach by an effective embedding have been proposed.<sup>200,201,208–211</sup> We believe both these effects are important. However, which one dominates will likely depend on the experimental conditions. Both should be carefully considered when accurately modelling polaritonic properties, and further studies in this direction are needed.

## 5.2. Equivalent expressions for polaritonic properties

In this section, we derive equations of motion for polaritonic response functions. Inserting the expansion Eq. (64) into Ehrenfest theorem Eq. (42), we obtain a set of equations as in standard molecular response theory<sup>84</sup>

$$\omega_1 \langle \langle A; V^{\omega_1} \rangle \rangle_{\omega_1} = \langle \langle [A, H]; V^{\omega_1} \rangle \rangle_{\omega_1} + \langle 0 | [A, V^{\omega_1}] | 0 \rangle \quad (98)$$

$$(\omega_1 + \omega_2) \langle \langle A; V^{\omega_1}, V^{\omega_2} \rangle \rangle_{\omega_1, \omega_2} = \langle \langle [A, H]; V^{\omega_1}, V^{\omega_2} \rangle \rangle_{\omega_1, \omega_2} + \hat{P}(\omega_1, \omega_2) \langle \langle [A, V^{\omega_1}]; V^{\omega_2} \rangle \rangle_{\omega_2} \quad (99)$$

Considering Eq. (98) and the position-momentum operator identity

$$\mathbf{p} = -i[\mathbf{r}, H^l] \quad (100)$$

which holds for the dipole Hamiltonian in the length representation Eq. (35), we obtain the relation

$$\omega \langle \langle \mathbf{r}; \mathbf{r} \rangle \rangle_{\omega} = i \langle \langle \mathbf{p}; \mathbf{r} \rangle \rangle_{\omega}, \quad (101)$$

which states that the frequency-dependent dipole polarizability can be evaluated regarding the position or the conjugate momentum. This ensures the equivalence of expressions in the dipole and velocity form of transition dipole moments

$$\omega_n \langle 0 | \mathbf{r} | n \rangle = i \langle 0 | \mathbf{p} | n \rangle, \quad (102)$$

where  $|n\rangle$  is an excited state and  $\omega_n$  is the excitation energy. We note that for the velocity representation, in Eq. (30), the analogous relation is

$$\mathbf{p} + \frac{1}{c} \mathbf{A}(\mathbf{r}) = -i[\mathbf{r}, H^v], \quad (103)$$

which states, exactly as Eq. (102), an equivalence between the transition dipole moment and the transition *kinetic* momentum of the electrons. Indeed, Eqs. (100) and (103) are connected by the transformation in Eq. (33). We recall that in second quantization, Eqs. (100) and (103) are fulfilled only in the limit of a complete basis set.<sup>185</sup>

An example of a relation introduced by the electromagnetic degrees of freedom is provided by the commutation relation between the Hamiltonian and the annihilation operators in the length form

$$[b_{\alpha}, H^l] = \lambda_{\alpha} \sqrt{\frac{\omega_{\alpha}}{2}} (\mathbf{d} \cdot \boldsymbol{\epsilon}_{\alpha}) + \omega_{\alpha} b_{\alpha}, \quad (104)$$

which through Eq. (98) leads to

$$\begin{aligned} \omega \langle \langle b_{\alpha}; B \rangle \rangle_{\omega} &= \langle \langle \lambda_{\alpha} \sqrt{\frac{\omega_{\alpha}}{2}} \mathbf{d} \cdot \boldsymbol{\epsilon}_{\alpha} + \omega_{\alpha} b_{\alpha}; B \rangle \rangle_{\omega} \\ &+ \langle 0 | [b_{\alpha}, B] | 0 \rangle \end{aligned} \quad (105)$$

for any operator  $B$ . We obtain from the residues of Eq. (105) the relation

$$(\omega_n - \omega_{\alpha}) \langle 0 | b_{\alpha} | n \rangle = \lambda_{\alpha} \sqrt{\frac{\omega_{\alpha}}{2}} \langle 0 | \mathbf{d} \cdot \boldsymbol{\epsilon}_{\alpha} | n \rangle \quad (106)$$

which allows the computation of photonic transition moments

in terms of matter transition moments. This reflects the entanglement between electronic and photonic degrees of freedom. The analogous relation for the creation operators is

$$(\omega_n + \omega_{\alpha}) \langle 0 | b_{\alpha}^{\dagger} | n \rangle = -\lambda_{\alpha} \sqrt{\frac{\omega_{\alpha}}{2}} \langle 0 | \mathbf{d} \cdot \boldsymbol{\epsilon}_{\alpha} | n \rangle. \quad (107)$$

Moreover, from the relation

$$[b_{\alpha} + b_{\alpha}^{\dagger}, H^l] = \omega_{\alpha} (b_{\alpha} - b_{\alpha}^{\dagger}) \quad (108)$$

we obtain

$$\omega_n \langle 0 | b_{\alpha} + b_{\alpha}^{\dagger} | n \rangle = \omega_{\alpha} \langle 0 | b_{\alpha} - b_{\alpha}^{\dagger} | n \rangle \quad (109)$$

$$= \lambda_{\alpha} \sqrt{\frac{\omega_{\alpha}}{2}} \langle 0 | \mathbf{d} \cdot \boldsymbol{\epsilon}_{\alpha} | n \rangle \frac{2\omega_n \omega_{\alpha}}{\omega_n^2 - \omega_{\alpha}^2} \quad (110)$$

If we introduce the conjugate field displacement  $q_{\alpha}$  and momentum  $p_{\alpha}$  coordinates

$$p_{\alpha} = i \sqrt{\frac{\omega_{\alpha}}{2}} (b_{\alpha}^{\dagger} - b_{\alpha}) \quad (111)$$

$$q_{\alpha} = \frac{1}{\sqrt{2\omega_{\alpha}}} (b_{\alpha}^{\dagger} + b_{\alpha}), \quad (112)$$

we can write Eq. (109) as

$$\omega_n \langle 0 | q_{\alpha} | n \rangle = i \langle 0 | p_{\alpha} | n \rangle \quad (113)$$

which is the equivalent relation of Eq. (102) for the photonic conjugate momenta. Similarly, by employing the Hamiltonian in the velocity form in Eq. (30) or through the transformation in Eq. (33), we obtain equivalent relations in the velocity representation. Notice that relation Eq. (109) also holds for the dipole Hamiltonian in the velocity form, but the physical meaning of the operators (111) and (112) is changed since they refer to a different representation. This will be discussed extensively in the following sections.

Analogous relations can be obtained from the higher-order equations of motion in Eqs. (99), for instance for the transition dipole moments among excited states we have

$$\begin{aligned} -i(\omega_m - \omega_n) (\langle n | r_i | m \rangle - \delta_{mn} \langle 0 | r_i | 0 \rangle) &= \\ \langle n | p_i | m \rangle - \delta_{mn} \langle 0 | p_i | 0 \rangle. \end{aligned} \quad (114)$$

Notice that relations similar to Eq. (114) also hold for the photonic conjugate momenta:

$$\begin{aligned} -i(\omega_m - \omega_n) (\langle n | q_{\alpha} | m \rangle - \delta_{mn} \langle 0 | q_{\alpha} | 0 \rangle) &= \\ \langle n | p_{\alpha} | m \rangle - \delta_{mn} \langle 0 | p_{\alpha} | 0 \rangle. \end{aligned} \quad (115)$$

### 5.3. Response functions in cavity QED

This section provides a discussion of response functions in cavity QED. Although far from exhaustive, we provide the reader with several examples of matter-photon and photon-photon response functions. We focus on the peculiarities introduced by the photon dressing, and we explicitly discuss the result of using different mathematical representations of the Hamiltonian.

The perturbation is described by a single frequency component of Eq. (44)

$$V^t = \left( V^\omega e^{-i\omega t} + V^{-\omega} e^{i\omega t} \right) e^{\eta t}, \quad (116)$$

where this also includes the case of static perturbations by imposing  $\omega = \eta = 0$ .

#### 5.3.1. External electromagnetic fields

Spectroscopic techniques probe the system by means of an external electromagnetic field, whose electric and magnetic components are coupled to the motion of particles. The external probe is treated as classical (non-quantized) fields, described by its own vector  $\mathbf{A}_e(\mathbf{r}, t)$  and scalar  $\phi_e(\mathbf{r}, t)$  potentials. It is not necessary to describe the internal and external fields through the same gauge. The Hamiltonian of the system in the Coulomb gauge and Born-Oppenheimer approximation reads<sup>162</sup>

$$H = \sum_i \frac{1}{2} \left( \mathbf{p}_i - \frac{1}{c} \mathbf{A}(\mathbf{r}_i) - \frac{1}{c} \mathbf{A}_e(\mathbf{r}_i) \right)^2 + V_{coul} - \sum_i \phi_e(\mathbf{r}_i) + \sum_\alpha \omega_\alpha b_\alpha^\dagger b_\alpha, \quad (117)$$

where  $\alpha$  labels the photon modes and  $i$  refers to electrons. Expanding the first term, we get the polaritonic Hamiltonian in Eq. (17) and the interaction term  $V^t$  with the external fields:

$$V^t = \frac{1}{c^2} \sum_i \mathbf{A}(\mathbf{r}_i) \cdot \mathbf{A}_e(\mathbf{r}_i) + \frac{1}{2c^2} \sum_i \mathbf{A}_e^2(\mathbf{r}_i) - \sum_i \frac{1}{2c} (\mathbf{A}_e(\mathbf{r}_i) \cdot \mathbf{p}_i + \mathbf{p}_i \cdot \mathbf{A}_e(\mathbf{r}_i)) - \sum_i \phi_e(\mathbf{r}_i). \quad (118)$$

While the last three terms of Eq. (118) are also found in molecular response theory in the semi-classical approximation,<sup>192,194,195,206</sup> the first term is a purely QED contribution. This term cancels the field contribution from the  $\mathbf{p}$  terms and ensures the coupling is only to the matter subsystem. When we perform the dipole approximation for the cavity fields and apply the transformation in Eq. (33), we obtain the length Hamiltonian  $H^l$ . The first term in Eq. (118) is cancelled, leaving only the familiar interaction terms. By a suitable expansion of the external potential, the interaction

term is obtained in a multipolar fashion as for the standard semiclassical theory<sup>192–194,206</sup>

$$H_{mult} = -\mathbf{d} \cdot \mathbf{E}_e - \mathbf{m} \cdot \mathbf{B}_e - \frac{1}{6} \Theta_{\alpha\beta} \partial_\alpha (E_e)_\beta - \frac{1}{2} (B_e)_\alpha (B_e)_\beta \chi_{\alpha\beta} + \dots \quad (119)$$

where we defined respectively the electric dipole  $\mathbf{d}$ , magnetic dipole  $\mathbf{m}$ , electric quadrupole  $\Theta_{\alpha\beta}$  and magnetic susceptibility  $\chi_{\alpha\beta}$  operators (in atomic units):

$$\mathbf{d} = \sum_M Z_M \mathbf{R}_M - \sum_i \mathbf{r}_i \quad (120)$$

$$\Theta_{\alpha\beta} = \sum_i (3r_{i\alpha} r_{i\beta} - \delta_{\alpha\beta} r_i^2) \quad (121)$$

$$\mathbf{m} = \sum_i \frac{1}{2c} \mathbf{l}_i = \sum_i \frac{1}{2c} \mathbf{r}_i \times \mathbf{p}_i \quad (122)$$

$$\chi_{\alpha\beta} = \sum_i \frac{1}{4c^2} (r_{i\alpha} r_{i\beta} - \delta_{\alpha\beta} r_i^2). \quad (123)$$

Note that since we employ the dipole approximation in the length form, these multipolar operators refer exclusively to the matter subsystem and have the same physical meaning as in standard response theory. On the contrary, in the velocity form the operators

$$\mathbf{m} = \sum_i \frac{1}{2c} \mathbf{l}_i = \sum_i \frac{1}{2c} \mathbf{r}_i \times \mathbf{p}_i \quad (124)$$

has a mixed matter-photon character because of the field component in the conjugate momentum  $\mathbf{p}$  (see Eq. (21)).

If we only retain the dipole interaction term in (119), the external electric field  $\mathbf{E}_e(0)$  computed at the molecular position is a constant that can be factorized out of the response functions. The dipole-dipole response function  $\langle\langle d_i ; d_j \rangle\rangle_\omega$  can then be interpreted as the negative molecular polarizability at frequency  $\omega$

$$\langle\langle d_i ; d_j \rangle\rangle_\omega = \sum_{k>0} \left( \frac{\langle 0 | d_i | k \rangle \langle k | d_j | 0 \rangle}{\omega - \omega_k} - \frac{\langle 0 | d_j | k \rangle \langle k | d_i | 0 \rangle}{\omega + \omega_k} \right) \quad (125)$$

where  $i$  and  $j$  refer to cartesian components of the dipole operator  $\mathbf{d}$  and  $k$  labels excited polaritonic states. This function describes the first-order time evolution of the molecular dipole moment subject to an external electric field:

$$\delta \langle \mathbf{d} \rangle^{(1)}(t) = - \int d\omega e^{-i\omega t + \eta t} \sum_{j=x,y,z} \langle\langle \mathbf{d}; d_j \rangle\rangle_{\omega+i\eta} E_j(\omega). \quad (126)$$

$$V^t = -\mathbf{d} \cdot \mathbf{E}(t) = -\mathbf{d} \cdot \left( e^{\eta t} \int d\omega e^{-i\omega t} \mathbf{E}(\omega) \right) \quad (127)$$

The poles occur when the frequency  $\omega$  matches the energy difference between the ground and excited states, and the cor-



responding residues

$$\lim_{\omega \rightarrow \omega_k} (\omega - \omega_k) \langle \langle d_i ; d_j \rangle \rangle_\omega = \langle 0 | d_i | k \rangle \langle k | d_j | 0 \rangle \quad (128)$$

$$\lim_{\omega \rightarrow -\omega_k} (\omega + \omega_k) \langle \langle d_i ; d_j \rangle \rangle_\omega = - \langle 0 | d_j | k \rangle \langle k | d_i | 0 \rangle \quad (129)$$

provide information on the transition dipole moments between the ground and the excited states. While these expressions are the same as in standard molecular response theory,<sup>84</sup> the states involved are here polaritonic and the predicted properties will consequently be modified.

If we replace one of the electric dipole operators with the magnetic dipole  $\mathbf{m}$  we obtain the electric dipole-magnetic dipole response function

$$\langle \langle d_i ; m_j \rangle \rangle_\omega = \sum_{k>0} \left( \frac{\langle 0 | d_i | k \rangle \langle k | m_j | 0 \rangle}{\omega - \omega_k} - \frac{\langle 0 | m_j | k \rangle \langle k | d_i | 0 \rangle}{\omega + \omega_k} \right), \quad (130)$$

which describes the electric dipole response when a magnetic field is applied

$$\delta \langle \mathbf{d} \rangle^{(1)}(t) = - \int d\omega e^{-i\omega t + \eta t} \sum_{j=x,y,z} \langle \langle \mathbf{d} ; m_j \rangle \rangle_{\omega+i\eta} B_j(\omega) \quad (131)$$

$$V^t = -\mathbf{m} \cdot \mathbf{B}(t) = -\mathbf{m} \cdot \left( e^{\eta t} \int d\omega e^{-i\omega t} \mathbf{B}(\omega) \right). \quad (132)$$

From the residues of the frequency-dependent electric dipole-magnetic dipole polarizability in Eq. (130), we obtain the rotational strength of optically active molecules

$$\lim_{\omega \rightarrow \omega_k} (\omega - \omega_k) \langle \langle d_i ; m_j \rangle \rangle_\omega = \langle 0 | d_i | k \rangle \langle k | m_j | 0 \rangle \quad (133)$$

$$\lim_{\omega \rightarrow -\omega_k} (\omega + \omega_k) \langle \langle d_i ; m_j \rangle \rangle_\omega = - \langle 0 | m_j | k \rangle \langle k | d_i | 0 \rangle. \quad (134)$$

As previously discussed, the operator  $\mathbf{m}$  can only in the length representation be interpreted as the molecular magnetic dipole operator, while it has a different physical meaning in the velocity Hamiltonian. Notice that in polaritonic systems, the optical activity can appear both from molecular and field chirality. As discussed in Sec. (2), several groups have recently developed chiral cavities,<sup>115,147-161</sup> which can host only one-handedness of light polarization within themselves. This opens up the possibility of engineering chiral properties through the chirality of the photon field,<sup>36,37,147,212-214</sup> which is transferred to molecular states via light-matter strong coupling. For instance, we expect it to induce chirality in a non-optically active molecule, similar to induced circular dichroism (ICD) when achiral molecules are placed in a chiral solvent.<sup>215-218</sup> On the other hand, chiral molecules interacting with a chiral field should give rise to "polaritonic diastereoisomers", possibly leading to novel approaches to chiral discrimination.

As the states of the system here belong to the radiation-

matter Hilbert space in Eq. (29), we can study how the perturbation of the matter subsystem leads to modifications of the photonic properties. If we focus on the perturbation in Eq. (127), in the velocity representation, the response function

$$\langle \langle b_\alpha^\dagger b_\alpha ; d_j \rangle \rangle_\omega = \sum_{k>0} \left( \frac{\langle 0 | b_\alpha^\dagger b_\alpha | k \rangle \langle k | d_j | 0 \rangle}{\omega - \omega_k} - \frac{\langle 0 | d_j | k \rangle \langle k | b_\alpha^\dagger b_\alpha | 0 \rangle}{\omega + \omega_k} \right) \quad (135)$$

describes the time evolution of the photon number in the  $\alpha$ -mode

$$\delta \langle b_\alpha^\dagger b_\alpha \rangle^{(1)} = - \int d\omega e^{-i\omega t + \eta t} \sum_j \langle \langle b_\alpha^\dagger b_\alpha ; d_j \rangle \rangle_{\omega+i\eta} E_j(\omega). \quad (136)$$

The residues computed at the polaritonic excitations

$$\lim_{\omega \rightarrow \omega_k} (\omega - \omega_k) \langle \langle b_\alpha^\dagger b_\alpha ; d_j \rangle \rangle_\omega = \langle 0 | b_\alpha^\dagger b_\alpha | k \rangle \langle k | d_j | 0 \rangle \quad (137)$$

$$\lim_{\omega \rightarrow -\omega_k} (\omega + \omega_k) \langle \langle b_\alpha^\dagger b_\alpha ; d_j \rangle \rangle_\omega = - \langle 0 | d_j | k \rangle \langle k | b_\alpha^\dagger b_\alpha | 0 \rangle \quad (138)$$

are now connected to dipole and photon number transition moments between the ground and the excited state. Note that to correctly model the coupling to an external field in the velocity representation, we should also include the first interaction term in Eq. (118). In the length form, the electric field mode creation (annihilation) operators are described by Eq. (37). The response function equivalent to Eq. (135) is then given by

$$\langle \langle (-ib_\alpha^\dagger - i\sqrt{\frac{\omega_\alpha}{2}} \boldsymbol{\lambda}_\alpha \cdot \mathbf{d})(ib_\alpha + i\sqrt{\frac{\omega_\alpha}{2}} \boldsymbol{\lambda}_\alpha \cdot \mathbf{d}) ; d_j \rangle \rangle_\omega. \quad (139)$$

The response function Eq. (135) represents the variation of the number of *displacement field* modes, in agreement with the transformation in Eq. (33).

In an analogous way, we can consider the time evolution of the field displacement coordinates Eqs. (111) and (112). Their time development is obtained by means of the response functions

$$\langle \langle q_\alpha ; d_j \rangle \rangle_\omega = \sum_{k>0} \left( \frac{\langle 0 | q_\alpha | k \rangle \langle k | d_j | 0 \rangle}{\omega - \omega_k} - \frac{\langle 0 | d_j | k \rangle \langle k | q_\alpha | 0 \rangle}{\omega + \omega_k} \right) \quad (140)$$

$$\langle \langle p_\alpha ; d_j \rangle \rangle_\omega = \sum_{k>0} \left( \frac{\langle 0 | p_\alpha | k \rangle \langle k | d_j | 0 \rangle}{\omega - \omega_k} - \frac{\langle 0 | d_j | k \rangle \langle k | p_\alpha | 0 \rangle}{\omega + \omega_k} \right), \quad (141)$$

with residues

$$\lim_{\omega \rightarrow \omega_k} (\omega - \omega_k) \langle\langle q_\alpha ; d_j \rangle\rangle_\omega = \langle 0 | q_\alpha | k \rangle \langle k | d_j | 0 \rangle \quad (142)$$

$$\lim_{\omega \rightarrow -\omega_k} (\omega + \omega_k) \langle\langle q_\alpha ; d_j \rangle\rangle_\omega = -\langle 0 | d_j | k \rangle \langle k | q_\alpha | 0 \rangle \quad (143)$$

$$\lim_{\omega \rightarrow \omega_k} (\omega - \omega_k) \langle\langle p_\alpha ; d_j \rangle\rangle_\omega = \langle 0 | p_\alpha | k \rangle \langle k | d_j | 0 \rangle \quad (144)$$

$$\lim_{\omega \rightarrow -\omega_k} (\omega + \omega_k) \langle\langle p_\alpha ; d_j \rangle\rangle_\omega = -\langle 0 | d_j | k \rangle \langle k | p_\alpha | 0 \rangle \quad (145)$$

that provide information on the transition dipole and photon moments.

### 5.3.2. Photonic environment perturbation

Classical charge currents  $\mathbf{J}_e(\mathbf{r}, t)$  are a source of electromagnetic fields, which means that they can directly perturb the cavity photon field. The interaction term for the Pauli-Fierz Hamiltonian in Eq. (17) coupled to a classical external current reads<sup>162</sup>

$$H_{J_e} = -\frac{1}{c} \int d^3r \mathbf{J}_e(\mathbf{r}, t) \cdot \mathbf{A}(\mathbf{r}). \quad (146)$$

Following Refs.<sup>56,94,187</sup>, resolving the external currents into modes which act directly on the  $\alpha$  mode of the cavity, in the dipole approximation and the length form, the interaction Hamiltonian can be written as

$$H_{J_e} = \sum_\alpha \frac{j_\alpha(t)}{2\omega_\alpha} p_\alpha = \sum_\alpha p_\alpha \frac{1}{2\omega_\alpha} \int d\omega \tilde{j}_\alpha(\omega) e^{-i\omega t} \quad (147)$$

where  $p_\alpha$  is the photon conjugate momentum of mode  $\alpha$ , and  $j_\alpha$  is connected to the  $\alpha$ -mode of the time-derivative of the external current  $\mathbf{J}_e$ .<sup>56,94,187</sup> The interaction Hamiltonian Eq. (147) generates mode excitations into the system. Due to the coupling of light and matter, this perturbation provides an indirect way to probe the matter and photon-matter correlation properties.

In the length form, the photonic response function

$$\langle\langle b_\alpha^\dagger b_\alpha ; p_\alpha \rangle\rangle_\omega = \sum_{k>0} \left( \frac{\langle 0 | b_\alpha^\dagger b_\alpha | k \rangle \langle k | p_\alpha | 0 \rangle}{\omega - \omega_k} - \frac{\langle 0 | p_\alpha | k \rangle \langle k | b_\alpha^\dagger b_\alpha | 0 \rangle}{\omega + \omega_k} \right) \quad (148)$$

describes the time evolution of the displacement field photon number. Interestingly, the more general response function

$$\langle\langle b_\beta^\dagger b_\beta ; p_\alpha \rangle\rangle_\omega = \sum_{k>0} \left( \frac{\langle 0 | b_\beta^\dagger b_\beta | k \rangle \langle k | p_\alpha | 0 \rangle}{\omega - \omega_k} - \frac{\langle 0 | p_\alpha | k \rangle \langle k | b_\beta^\dagger b_\beta | 0 \rangle}{\omega + \omega_k} \right), \quad (149)$$

which describes the time evolution of the  $\beta$ -photon number

when the system is coupled to the current  $j_\alpha(t)$

$$\langle\langle b_\beta^\dagger b_\beta \rangle\rangle^{(1)}(t) = \int d\omega e^{-i\omega t + \eta t} \langle\langle b_\beta^\dagger b_\beta, p_\alpha \rangle\rangle_{\omega+i\eta} \frac{\tilde{j}_\alpha(\omega)}{2\omega_\alpha} \quad (151)$$

is different from zero even when  $\alpha \neq \beta$ . This happens because of the coupling to matter degrees of freedom, which provide an indirect interaction between different photon modes. This result opens up the possibility of photon transfer between modes with different frequencies or polarization. In the limit of zero coupling, the response function Eq. (151) would differ from zero only when  $\alpha = \beta$ , as photons do not directly interact. Analogously, the response function

$$\langle\langle p_\alpha ; p_\beta \rangle\rangle_\omega = \sum_{k>0} \left( \frac{\langle 0 | p_\alpha | k \rangle \langle k | p_\beta | 0 \rangle}{\omega - \omega_k} - \frac{\langle 0 | p_\beta | k \rangle \langle k | p_\alpha | 0 \rangle}{\omega + \omega_k} \right), \quad (152)$$

describes the time evolution of the  $\beta$ -cavity mode momentum when perturbing the  $\alpha$ -cavity mode

$$\langle\langle p_\alpha \rangle\rangle^{(1)}(t) = \int d\omega e^{-i\omega t + \eta t} \langle\langle p_\alpha, p_\beta \rangle\rangle_{\omega+i\eta} \frac{\tilde{j}_\beta(\omega)}{2\omega_\beta}. \quad (153)$$

As discussed in the other sections, the transformation in Eq. (33) links the response functions for the physical observables in the velocity and length form. For the creation and annihilation operators of the electric photon states, we then need to employ the transformation in Eq. (37).

We can also describe the time evolution of matter degrees of freedom when the system is perturbed through Eq. (147). The response function

$$\langle\langle d_j ; p_\alpha \rangle\rangle_\omega = \sum_{k>0} \left( \frac{\langle 0 | d_j | k \rangle \langle k | p_\alpha | 0 \rangle}{\omega - \omega_k} - \frac{\langle 0 | p_\alpha | k \rangle \langle k | d_j | 0 \rangle}{\omega + \omega_k} \right) \quad (154)$$

is analogous to Eq. (141) as it describes the time evolution of the dipole moment when the photon degrees of freedom are perturbed by  $j_\alpha(t)$

$$\langle\langle \mathbf{d} \rangle\rangle^{(1)}(t) = \int d\omega e^{-i\omega t + \eta t} \langle\langle \mathbf{d}, p_\alpha \rangle\rangle_{\omega+i\eta} \frac{\tilde{j}_\alpha(\omega)}{2\omega_\alpha}. \quad (155)$$

The response functions in Eqs. (135), (140), and (154) are examples of response functions which describe the cross-talk between photon and matter degrees of freedom. In fact, in the limit of  $\lambda = 0$ , the eigenstates of the system would be given by the direct product between bare molecular states and photons states. As a consequence, Eqs. (135), (140), (141), and (154) would be identically zero. This means that a perturbation acting on the molecular Hilbert space cannot induce any time evolution in the (decoupled) cavity-radiation space, and vice versa.

### 5.3.3. Static perturbations and energy derivatives

This section provides several examples of static perturbations on the polaritonic system and their connection to the energy derivatives.

*a. External electric and magnetic fields.* A static external electric field is described by the scalar potential  $\phi_e$  that can be expanded in a Taylor series around the origin

$$\phi_e(\mathbf{r}) = \phi(0) - r_i E_i^{(0)} - \frac{1}{2} r_i (\partial_i E_j)(0) r_j + \dots \quad (156)$$

where we employed Einstein's summation convention. If we retain only the lowest expansion term, the interaction operator in the Hamiltonian is the familiar electric dipole term

$$H_{int} = -\mathbf{d} \cdot \mathbf{E}_e(0). \quad (157)$$

Note that the transformation in Eq. (33) commutes with this operator, which implies it is the same in both the length and the velocity representation. The static electric dipole polarizability  $\alpha_0$  then reads

$$-\alpha_0 = \frac{d^2 E}{d^2 \mathbf{E}_e} \Big|_{\mathbf{E}_e=0} = 2 \sum_{k>0} \frac{\langle 0 | \mathbf{d} | k \rangle \langle k | \mathbf{d} | 0 \rangle}{E_0 - E_k} = \langle \langle \mathbf{d}; \mathbf{d} \rangle \rangle_{\omega=0}. \quad (158)$$

An analogous interaction term is introduced when the system is immersed in a static uniform external magnetic field, which can be described by the following vector potential<sup>206</sup>

$$\mathbf{A}_e = \frac{1}{2} \mathbf{B}_e \times \mathbf{r}.$$

In the length form, the interaction Hamiltonian reads

$$H_{int} = -\mathbf{m} \cdot \mathbf{B}_e - \frac{1}{2} \mathbf{B}_e^T \chi \mathbf{B}_e \quad (159)$$

where

$$\mathbf{m} = \sum_i \frac{1}{2c} \mathbf{l}_i = \sum_i \frac{1}{2c} \mathbf{r}_i \times \mathbf{p}_i \quad (160)$$

$$\chi_{\alpha\beta} = \sum_i \frac{1}{4c^2} (r_{i\alpha} r_{i\beta} - \delta_{\alpha\beta} r_i^2) \quad (161)$$

and since we are employing the length form, these quantities refer only to the matter subsystem. The static molecular magnetizability  $\xi_0$  is computed as the second derivative of the energy with respect to the magnetic field

$$\xi_0 = -\frac{d^2 E}{d^2 \mathbf{B}_e} \Big|_{\mathbf{B}_e=0} = -\langle \langle \mathbf{m}; \mathbf{m} \rangle \rangle_{\omega=0} - \langle 0 | \chi | 0 \rangle. \quad (162)$$

The first term in Eq. (162) is called paramagnetic contribution, while the second term is called diamagnetic contribution and usually dominates for closed-shell molecules. Magnetizabilities have been extensively studied in the framework of molecular response theory,<sup>219–225</sup> but the effect of photon-

dressing, to the best of our knowledge, is yet to be explored. The evaluation of magnetic properties for approximate wave functions is affected by an origin dependence on the choice of the gauge origin of the external field. In molecular response theory, the origin independence can be recovered by using gauge invariant atomic orbitals (GIAO).<sup>87,226</sup>

*b. Spin interactions.* Nuclear magnetic resonance (NMR) and electronic paramagnetic resonance (EPR) provide important information on the molecular structure and find wide applications in chemistry. The electron spin is connected to magnetic moment of the electron

$$\mathbf{m}_i^s = -g_e \mu_B \mathbf{s}_i, \quad (163)$$

where  $g_e$  is the electronic  $g$  factor,  $\mu_B$  is the Bohr magneton and  $\mathbf{s}_i$  is the spin operator of electron  $i$ . In the same way, the nuclear spin is connected to the nuclear magnetic moment

$$\mathbf{M}_N^s = \gamma_N \mathbf{I}_N. \quad (164)$$

where  $\gamma_N$  is the magnetogyric ratio and  $\mathbf{I}_N$  is the spin operator of nucleus  $N$ . The spin degrees of freedom modify the Pauli-Fierz Hamiltonian in Eq. (30), introducing spin-spin, spin-orbit and spin-external field interaction terms. The cavity environment introduces a twofold modification on NMR and EPR spectra: it modifies the ground state wave function, which is now dressed by the photons, and introduces further terms in the Hamiltonian due to the interaction of the spins with the cavity field. The effects of these additional QED terms are still to be explored and require going beyond the dipole approximation.

We now focus on the NMR properties of closed-shell molecules and disregard the electronic spin contribution to the magnetic field. The total vector potential  $\mathbf{A}^{tot}(\mathbf{r}_i)$  has contributions from the cavity field, the external field, and the nuclear spins

$$\mathbf{A}^{tot}(\mathbf{r}) = \mathbf{A}(\mathbf{r}) + \frac{\mathbf{B}_e \times \mathbf{r}}{2} + \frac{1}{c^2} \sum_N \left( \frac{\mathbf{M}_N^s \times (\mathbf{r} - \mathbf{R}_N)}{|\mathbf{r} - \mathbf{R}_N|^3} \right), \quad (165)$$

and the total magnetic induction is

$$\mathbf{B}^{tot}(\mathbf{r}) = \nabla \times \mathbf{A}^{tot}(\mathbf{r}). \quad (166)$$

Therefore, the following interaction terms need to be included in the Hamiltonian in Eq. (30):

$$H_{int} = -\sum_i \mathbf{m}_i^s \cdot \mathbf{B}^{tot}(\mathbf{r}_i) - \sum_N \mathbf{M}_N^s \cdot \mathbf{B}^{tot}(\mathbf{R}_N) + \sum_{M>N} \frac{1}{2c^2} \frac{R_{MN}^2 (\mathbf{M}_M^s \cdot \mathbf{M}_N^s) - 3(\mathbf{M}_M^s \cdot \mathbf{R}_{MN})(\mathbf{R}_{MN} \cdot \mathbf{M}_N^s)}{R_{MN}^5}, \quad (167)$$

where the first term mediates the indirect coupling of nuclear spins, the second term is the nuclear Zeeman interaction, and the last term in Eq. (167) is the direct couplings between nuclear dipole magnetic moments. Moreover, using Eq. (165) in

the velocity Hamiltonian leads to additional interaction terms. The NMR properties are then connected to the following energy derivatives<sup>87</sup>

$$\mathbf{E}_N^{(1,1)} = \left. \frac{d^2 E(\mathbf{B}_e, M^s)}{d\mathbf{B}_e dM_N^s} \right|_{\mathbf{B}_e=0, M^s=0} \quad (168)$$

$$\mathbf{E}_{M,N}^{(0,2)} = \left. \frac{d^2 E(\mathbf{B}_e, M^s)}{dM_M^s dM_N^s} \right|_{\mathbf{B}_e=0, M^s=0}, \quad (169)$$

where  $\mathbf{E}_N^{(1,1)}$  is related to the nuclear shielding tensor  $\sigma_N$

$$\sigma_N = \mathbf{1} + \mathbf{E}_N^{(1,1)}, \quad (170)$$

which describes the electron shielding effects on nucleus  $N$ . At the same time,  $\mathbf{E}_{M,N}^{(0,2)}$  is connected to the direct  $\mathbf{D}_{M,N}$  and indirect (electron-mediated)  $\mathbf{K}_{M,N}$  spin-spin coupling tensors

$$\mathbf{E}_{M,N}^{(0,2)} = \mathbf{K}_{M,N} + \mathbf{D}_{M,N}. \quad (171)$$

As for magnetizabilities, the computation of NMR properties is affected by origin dependencies, which are usually eliminated using GIAO orbitals. The modifications of the ground state density induced by the QED environment change how the nuclei are shielded from the electrons, affecting the NMR properties. Moreover, the novel interaction terms between spins and the cavity magnetic field can possibly affect spin-spin coupling, resulting in modifications to the shape of NMR signals.

*c. QED environment perturbations.* A modification of the QED environment is reflected in the coupling strength and the frequency of the cavity modes. If we consider a single-mode and perturb the coupling strength

$$\lambda \rightarrow \lambda + \Delta\lambda, \quad (172)$$

the Hamiltonian reads

$$\begin{aligned} H^l &= \sum_{pq} h_{pq} E_{pq} + \frac{1}{2} \sum_{pqrs} g_{pqrs} e_{pqrs} + h_{nuc} \\ &+ \sqrt{\frac{\omega_\alpha}{2}} (\boldsymbol{\lambda} \cdot \mathbf{d})(b^\dagger + b) + \frac{1}{2} (\boldsymbol{\lambda} \cdot \mathbf{d})^2 \\ &+ \omega_\alpha \left\{ b^\dagger b + \frac{1}{2} \right\} \\ &+ \sqrt{\frac{\omega_\alpha}{2}} (\Delta\boldsymbol{\lambda} \cdot \mathbf{d})(b^\dagger + b) + (\boldsymbol{\lambda} \cdot \mathbf{d})(\Delta\boldsymbol{\lambda} \cdot \mathbf{d}) \\ &+ \frac{1}{2} (\Delta\boldsymbol{\lambda} \cdot \mathbf{d})^2 \end{aligned} \quad (173)$$

$$= H^l + V^{(1)} + V^{(2)}, \quad (174)$$

where  $H^l$  is the unperturbed dipole Hamiltonian in the length representation Eq. (31), and we have defined the first and

second-order perturbators as

$$V^{(1)} = \sqrt{\frac{\omega_\alpha}{2}} (\Delta\boldsymbol{\lambda} \cdot \mathbf{d})(b^\dagger + b) + (\boldsymbol{\lambda} \cdot \mathbf{d})(\Delta\boldsymbol{\lambda} \cdot \mathbf{d}) \quad (175)$$

$$V^{(2)} = \frac{1}{2} (\Delta\boldsymbol{\lambda} \cdot \mathbf{d})^2. \quad (176)$$

We therefore obtain expressions for the first and second energy derivatives

$$\left. \frac{dE}{d\Delta\lambda} \right|_{\Delta\lambda=0} = \langle 0 | \mathbf{d} \left( \sqrt{\frac{\omega_\alpha}{2}} (b^\dagger + b) + (\boldsymbol{\lambda} \cdot \mathbf{d}) \right) | 0 \rangle \quad (177)$$

$$\left. \frac{d^2 E}{d\Delta\lambda^2} \right|_{\Delta\lambda=0} = \langle 0 | \mathbf{d} \mathbf{d} | 0 \rangle + \frac{1}{2} \langle \langle \frac{dV^{(1)}}{d\Delta\lambda}; \frac{dV^{(1)}}{d\Delta\lambda} \rangle \rangle_{\omega=0}. \quad (178)$$

These derivatives measure how sensitive the system is to a change in the coupling strength. In particular, Eq. (178) can be interpreted as the static ground state polarizability with respect to the cavity field fluctuations. We note that because of the dipole self-energy in  $H^l$ , at very large coupling strength, these expressions can be approximated as

$$\left. \frac{dE}{d\Delta\lambda} \right|_{\Delta\lambda=0} \approx \boldsymbol{\lambda} \cdot \langle 0 | \mathbf{d} \mathbf{d} | 0 \rangle \quad (179)$$

$$\left. \frac{d^2 E}{d\Delta\lambda^2} \right|_{\Delta\lambda=0} \approx \frac{1}{2} \langle \langle (\boldsymbol{\lambda} \cdot \mathbf{d}) \mathbf{d}; (\boldsymbol{\lambda} \cdot \mathbf{d}) \mathbf{d} \rangle \rangle_{\omega=0} \quad (180)$$

$$= - \sum_{k>0} \frac{|\boldsymbol{\lambda} \cdot \langle 0 | \mathbf{d} \mathbf{d} | k \rangle|^2}{E_k - E_0} \quad (181)$$

As we increase  $\boldsymbol{\lambda}$ , from Eq. (179) the energy increases since  $\langle 0 | \mathbf{d} \mathbf{d} | 0 \rangle$  is positive definite, but the Hessian in Eq. (181) is negative. Therefore, the system is endowed with a stable ground state. Riso et al. showed that for infinitely large coupling strength, the polaritonic ground state energy will converge to the SC-QED-HF energy.<sup>64</sup> On the other hand, if the dipole self-energy is disregarded, the remaining terms are

$$\left. \frac{dE}{d\Delta\lambda} \right|_{\Delta\lambda=0} \approx \langle 0 | \mathbf{d} \sqrt{\frac{\omega_\alpha}{2}} (b^\dagger + b) | 0 \rangle \quad (182)$$

$$\left. \frac{d^2 E}{d\Delta\lambda^2} \right|_{\Delta\lambda=0} \approx \frac{\omega_\alpha}{4} \langle \langle \mathbf{d}(b^\dagger + b); \mathbf{d}(b^\dagger + b) \rangle \rangle_{\omega=0} \quad (183)$$

$$= - \frac{\omega_\alpha}{2} \sum_{k>1} \frac{|\langle 0 | \mathbf{d}(b^\dagger + b) | k \rangle|^2}{E_k - E_0}. \quad (184)$$

While the Hessian is still negative, there is no guarantee from Eq. (182) that the energy is increasing, and the ground state energy could decrease indefinitely. The dipole self-energy has been shown to be fundamental for the stability of the ground state.<sup>186</sup>

A modification of the cavity environment can effectively change the photon frequency

$$\omega_\alpha \rightarrow \omega_\alpha + \Delta\omega_\alpha. \quad (185)$$

From the expansion

$$\sqrt{\omega_\alpha + \Delta\omega_\alpha} \approx \sqrt{\omega_\alpha} + \frac{1}{2}\sqrt{\omega_\alpha} \frac{\Delta\omega_\alpha}{\omega_\alpha} - \frac{1}{8}\sqrt{\omega_\alpha} \left(\frac{\Delta\omega_\alpha}{\omega_\alpha}\right)^2 + \dots \quad (186)$$

for  $\Delta\omega_\alpha \ll \omega_\alpha$ , the perturbed Hamiltonian reads

$$\begin{aligned} H' &= H^I \\ &+ \frac{1}{2} \frac{\Delta\omega_\alpha}{\omega_\alpha} \sqrt{\frac{\omega_\alpha}{2}} (\boldsymbol{\lambda} \cdot \mathbf{d})(b^\dagger + b) + \Delta\omega_\alpha b^\dagger b \\ &- \frac{1}{8} \left(\frac{\Delta\omega_\alpha}{\omega_\alpha}\right)^2 \sqrt{\frac{\omega_\alpha}{2}} (\boldsymbol{\lambda} \cdot \mathbf{d})(b^\dagger + b) + \dots \end{aligned} \quad (187)$$

The first and second-order perturbation operators are therefore

$$V^{(1)} = \frac{1}{2} \frac{\Delta\omega_\alpha}{\omega_\alpha} \sqrt{\frac{\omega_\alpha}{2}} (\boldsymbol{\lambda} \cdot \mathbf{d})(b^\dagger + b) + \Delta\omega_\alpha b^\dagger b \quad (188)$$

$$V^{(2)} = -\frac{1}{8} \left(\frac{\Delta\omega_\alpha}{\omega_\alpha}\right)^2 \sqrt{\frac{\omega_\alpha}{2}} (\boldsymbol{\lambda} \cdot \mathbf{d})(b^\dagger + b). \quad (189)$$

The energy first and second energy derivatives read

$$\left. \frac{dE}{d\Delta\omega_\alpha} \right|_{\Delta\omega_\alpha=0} = \langle 0 | \frac{1}{2\omega_\alpha} \sqrt{\frac{\omega_\alpha}{2}} (\boldsymbol{\lambda} \cdot \mathbf{d})(b^\dagger + b) + b^\dagger b | 0 \rangle \quad (190)$$

$$\begin{aligned} \left. \frac{d^2E}{d\Delta\omega_\alpha^2} \right|_{\Delta\omega_\alpha=0} &= -\frac{1}{4} \left(\frac{1}{\omega_\alpha}\right)^2 \sqrt{\frac{\omega_\alpha}{2}} \langle 0 | (\boldsymbol{\lambda} \cdot \mathbf{d})(b^\dagger + b) | 0 \rangle \\ &+ \frac{1}{2} \left\langle \left\langle \frac{dV^{(1)}}{d\Delta\omega_\alpha}; \frac{dV^{(1)}}{d\Delta\omega_\alpha} \right\rangle \right\rangle_{\omega=0}. \end{aligned} \quad (191)$$

These derivatives measure how sensitive the system is to a change in the photon frequency.

In the following section, we develop response theory for approximate wave functions, focusing on QED-HF and QED-CC response theory.

## 6. AB INITIO APPROXIMATIONS

In this section, we derive the linear and quadratic response equations for the *ab initio* QED-HF and QED-CC methods.

### 6.1. QED-HF

The QED-HF is the generalization of the HF model to molecules in a QED environment.<sup>60,61</sup> The system is de-

scribed through the dipole Hamiltonian

$$\begin{aligned} H &= \sum_{pq} h_{pq} E_{pq} + \frac{1}{2} \sum_{pqrs} g_{pqrs} e_{pqrs} + h_{nuc} \\ &+ \sum_{\alpha} \sqrt{\frac{\omega_\alpha}{2}} (\boldsymbol{\lambda}_\alpha \cdot \mathbf{d})_{pq} E_{pq} (b_\alpha^\dagger + b_\alpha) \\ &+ \frac{1}{2} \sum_{pqrs} \sum_{\alpha} (\boldsymbol{\lambda}_\alpha \cdot \mathbf{d})_{pq} (\boldsymbol{\lambda}_\alpha \cdot \mathbf{d})_{rs} E_{pq} E_{rs} \\ &+ \sum_{\alpha} \omega_\alpha \left( b_\alpha^\dagger b_\alpha + \frac{1}{2} \right) \end{aligned} \quad (192)$$

where the dipole self-energy term can be included in the molecular Hamiltonian by a proper modification of the one and two-electron integrals

$$H_{mol} = \sum_{pq} h_{pq} E_{pq} + \frac{1}{2} \sum_{pqrs} g_{pqrs} e_{pqrs} \quad (194)$$

$$\begin{aligned} &+ \frac{1}{2} \sum_{pqrs} \sum_{\alpha} (\boldsymbol{\lambda}_\alpha \cdot \mathbf{d})_{pq} (\boldsymbol{\lambda}_\alpha \cdot \mathbf{d})_{rs} E_{pq} E_{rs} \\ &= \sum_{pq} \bar{h}_{pq} E_{pq} + \frac{1}{2} \sum_{pqrs} \bar{g}_{pqrs} e_{pqrs}, \end{aligned} \quad (195)$$

where we have defined

$$\bar{g}_{pqrs} = g_{pqrs} + \sum_{\alpha} (\boldsymbol{\lambda}_\alpha \cdot \mathbf{d})_{pq} (\boldsymbol{\lambda}_\alpha \cdot \mathbf{d})_{rs} \quad (196)$$

$$\bar{h}_{pq} = h_{pq} + \frac{1}{2} \sum_r \sum_{\alpha} (\boldsymbol{\lambda}_\alpha \cdot \mathbf{d})_{pr} (\boldsymbol{\lambda}_\alpha \cdot \mathbf{d})_{rq}. \quad (197)$$

The QED-HF wave function ansatz is a factorized state

$$|\mathbf{R}\rangle = |\text{HF}\rangle \otimes \sum_{\mathbf{n}} \prod_{\alpha} (b_\alpha^\dagger)^{n_\alpha} |0\rangle c_{\mathbf{n}}, \quad (198)$$

where  $|\text{HF}\rangle$  is a single Slater determinant,  $|0\rangle$  is the photon vacuum, and  $c_{\mathbf{n}}$  are expansion coefficients for the photon number states. The QED-HF state is obtained by minimization of the mean value of the Hamiltonian

$$E_{\text{QED-HF}} = \langle \mathbf{R} | H | \mathbf{R} \rangle \quad (199)$$

with respect to electronic and photonic parameters. Haugland et al.<sup>60,61</sup> showed that the photonic parameters for the ground-state QED-HF wave function define a coherent state through the following transformation

$$|\mathbf{R}\rangle = |\text{HF}\rangle \otimes U_{\text{QED-HF}} |0\rangle \equiv U_{\text{QED-HF}} |\text{HF}, 0\rangle \quad (200)$$

$$U_{\text{QED-HF}} = \prod_{\alpha} \exp\left(-\frac{\boldsymbol{\lambda}_\alpha \cdot \langle \mathbf{d} \rangle_{\text{QED-HF}}}{\sqrt{2\omega_\alpha}} (b_\alpha^\dagger - b_\alpha)\right). \quad (201)$$

By transforming the dipole Hamiltonian using Eq. (201) we get

$$\begin{aligned}
U_{\text{QED-HF}}^\dagger H U_{\text{QED-HF}} &= \sum_{pq} h_{pq} E_{pq} + \frac{1}{2} \sum_{pqrs} g_{pqrs} e_{pqrs} + h_{nuc} \\
&+ \sum_{\alpha} \sqrt{\frac{\omega_{\alpha}}{2}} (\boldsymbol{\lambda}_{\alpha} \cdot (\mathbf{d} - \langle \mathbf{d} \rangle_{\text{QED-HF}})) (b_{\alpha}^{\dagger} + b_{\alpha}) \\
&+ \frac{1}{2} \sum_{\alpha} (\boldsymbol{\lambda}_{\alpha} \cdot (\mathbf{d} - \langle \mathbf{d} \rangle_{\text{QED-HF}}))^2 \\
&+ \sum_{\alpha} \omega_{\alpha} b_{\alpha}^{\dagger} b_{\alpha}. \tag{202}
\end{aligned}$$

We note that the transformed Hamiltonian Eq. (202) is now origin invariant also for charged systems. Minimizing the photon-averaged coherent state transformed dipole Hamiltonian in Eq. (202), with respect to the orbital coefficients, we obtain the QED-Fock matrix

$$\begin{aligned}
F_{pq} &= F_{pq}^e \\
&+ \frac{1}{2} \sum_{\alpha} \left( \sum_a (\boldsymbol{\lambda}_{\alpha} \cdot \mathbf{d}_{pa}) (\boldsymbol{\lambda}_{\alpha} \cdot \mathbf{d}_{aq}) - \sum_i (\boldsymbol{\lambda}_{\alpha} \cdot \mathbf{d}_{pi}) (\boldsymbol{\lambda}_{\alpha} \cdot \mathbf{d}_{iq}) \right), \tag{203}
\end{aligned}$$

where  $F_{pq}^e$  is the standard electronic Fock matrix and the indices  $a$  and  $i$  refer respectively to virtual and occupied orbitals. The optimization condition that defines the QED-HF molecular orbitals is Brillouin's theorem,  $F_{ia} = 0$ , as in standard HF theory. However, the eigenvalues of the Fock matrix  $\mathbf{F}$ , usu-

ally interpreted as orbital energies, are now origin dependent for charged systems. Nevertheless, the total QED-HF energy is origin invariant since the occupied-virtual blocks  $F_{ia}$  are origin independent.

### 6.1.1. Time-dependent QED-HF

Once the optimized QED-HF reference state  $|R\rangle$  has been obtained, the time development due to an external perturbation  $V^t$  is parametrized as

$$\exp(-i\Lambda(t)) |R\rangle = \exp(-i\Lambda(t)) |HF\rangle \otimes U_{\text{QED-HF}} |0\rangle, \tag{204}$$

where  $\Lambda(t)$  is the Hermitian operator

$$\begin{aligned}
\Lambda(t) &= \frac{1}{\sqrt{2}} \sum_{ai} (\kappa_{ai} E_{ai} + \kappa_{ai}^* E_{ia}) + \sum_{\alpha} (\gamma_{\alpha} b_{\alpha}^{\dagger} + \gamma_{\alpha}^* b_{\alpha}) \\
&= \boldsymbol{\kappa}(t) + \sum_{\alpha} (\gamma_{\alpha} b_{\alpha}^{\dagger} + \gamma_{\alpha}^* b_{\alpha}). \tag{205}
\end{aligned}$$

The  $\kappa_{ai}$  parameters in Eq. (205) are orbital rotation parameters,  $\gamma_{\alpha}$  describe the evolution of the QED-HF coherent state, and we compactly defined the orbital rotation operator as

$$\boldsymbol{\kappa}(t) = \frac{1}{\sqrt{2}} \sum_{ai} (\kappa_{ai} E_{ai} + \kappa_{ai}^* E_{ia}). \tag{206}$$

Notice that electronic and photonic operators commute, implying that the exponential in Eq. (204) can be split into the product of an orbital rotation exponential and a time-dependent coherent state for the field

$$\exp(-i\Lambda(t)) |R\rangle = \exp(-i \sum_{\alpha} (\gamma_{\alpha} b_{\alpha}^{\dagger} + \gamma_{\alpha}^* b_{\alpha})) \exp(-i\boldsymbol{\kappa}(t)) |R\rangle \tag{207}$$

$$= \exp(-i\boldsymbol{\kappa}(t)) \exp(-i \sum_{\alpha} (\gamma_{\alpha} b_{\alpha}^{\dagger} + \gamma_{\alpha}^* b_{\alpha})) |R\rangle \tag{208}$$

Equivalently, we can parameterize the time dependence as

$$|\text{QED-HF}\rangle(t) = \exp\left(-\sum_{\alpha} \frac{\boldsymbol{\lambda}_{\alpha} \cdot \langle \mathbf{d} \rangle_{\text{QED-HF}}}{\sqrt{2\omega}} (b_{\alpha}^{\dagger} - b_{\alpha})\right) \exp(-i \sum_{\alpha} (\gamma_{\alpha} b_{\alpha}^{\dagger} + \gamma_{\alpha}^* b_{\alpha})) \exp(-i\boldsymbol{\kappa}(t)) |HF\rangle \otimes |0\rangle, \tag{209}$$

where we moved the coherent state transformation to the left. Since Eq. (209) and Eq. (208) differ by an unimportant phase factor, these parameterizations lead to the same time evolution. By using the Ehrenfest theorem and developing the equations in orders of the perturbation, we obtain the zero, first and second-order equations

$$\langle [\Omega^{(0)}, H] \rangle_R = 0 \tag{210}$$

$$i \langle R | \left[ \frac{\partial}{\partial t} \Lambda^{(1)}, \Omega^{(0)} \right] | R \rangle = \langle R | [\Lambda^{(1)}, [\Omega^{(0)}, H]] | R \rangle - i \langle R | [\Omega^{(0)}, V^t] | R \rangle - i \langle R | [\Omega^{(1)}, H] | R \rangle \tag{211}$$

$$\begin{aligned}
\langle R | \left[ \frac{\partial}{\partial t} \Lambda^{(2)}, \Omega^{(0)} \right] + \left[ \frac{\partial}{\partial t} \Lambda^{(1)}, \Omega^{(1)} \right] + i \langle R | \left[ \Lambda^{(1)}, \left[ \frac{\partial}{\partial t} \Lambda^{(1)}, \Omega^{(0)} \right] \right] | R \rangle &= \langle R | [V^t, \Omega^{(1)}] | R \rangle + \langle R | [H, \Omega^{(2)}] | R \rangle \\
+ i \langle R | [\Lambda^{(2)}, [H, \Omega^{(0)}]] | R \rangle + i \langle R | [\Lambda^{(1)}, [V^t, \Omega^{(0)}]] | R \rangle + i \langle R | [\Lambda^{(1)}, [H, \Omega^{(1)}]] | R \rangle &- \frac{1}{2} \langle R | [\Lambda^{(1)}, [\Lambda^{(1)}, [H, \Omega^{(0)}]]] | R \rangle, \tag{212}
\end{aligned}$$

where we also accounted for the possibility that  $\Omega$  depends on the external perturbation  $\Omega \equiv \Omega(V^t)$ . The apexes (0)-(2) refer to the expansion order and

$$\Lambda^{(1)}(t) = \frac{1}{\sqrt{2}} \sum_{ai} (\kappa_{ai}^{(1)} E_{ai} + \kappa_{ai}^{*(1)} E_{ia}) + \sum_{\alpha} (\gamma_{\alpha}^{(1)} b^{\dagger} + \gamma_{\alpha}^{*(1)} b) \quad (213)$$

$$\Lambda^{(2)}(t) = \frac{1}{\sqrt{2}} \sum_{ai} (\kappa_{ai}^{(2)} E_{ai} + \kappa_{ai}^{*(2)} E_{ia}) + \sum_{\alpha} (\gamma_{\alpha}^{(2)} b^{\dagger} + \gamma_{\alpha}^{*(2)} b). \quad (214)$$

As long as  $\Omega$  is a one-electron operator or a purely photonic 1/2 operator, the zero-order condition is satisfied due to the QED-HF optimization condition. The first-order equation is non-trivial, and its solution gives us the time evolution of the parameters to first-order in the perturbation. Following the derivation of the response equations in molecular response theory,<sup>84,227</sup> we make use of the operators

$$\Omega \in \left\{ b_{\alpha}, \frac{1}{\sqrt{2}} e^{-i\kappa} E_{ia} e^{i\kappa}, b_{\alpha}^{\dagger}, \frac{1}{\sqrt{2}} e^{-i\kappa} E_{ai} e^{i\kappa} \right\}. \quad (215)$$

Making this choice, we ensure the response equations are identical to the ones derived from the time-dependent variational principle.<sup>84,228,229</sup> It is convenient to move from the time domain to the frequency domain by performing a Fourier transformation of the parameters

$$\kappa_{ai}(t) = \int d\omega e^{-i\omega t} \kappa_{ai}^{\omega} + \int \int d\omega d\omega' e^{-i\omega t} e^{-i\omega' t} \kappa_{ai}^{\omega, \omega'} + \dots \quad (216)$$

$$\gamma(t) = \int d\omega e^{-i\omega t} \gamma_{\alpha}^{\omega} + \int \int d\omega d\omega' e^{-i\omega t} e^{-i\omega' t} \gamma_{\alpha}^{\omega, \omega'} + \dots \quad (217)$$

such that the operators

$$\Lambda^{\omega} = \frac{1}{\sqrt{2}} \sum_{ai} (\kappa_{ai}^{\omega} E_{ai} + [\kappa_{ai}^{-\omega}]^* E_{ia}) + \sum_{\alpha} (\gamma_{\alpha}^{\omega} b_{\alpha}^{\dagger} + [\gamma_{\alpha}^{-\omega}]^* b_{\alpha}) \quad (218)$$

$$\Lambda^{\omega, \omega'} = \frac{1}{\sqrt{2}} \sum_{ai} (\kappa_{ai}^{\omega, \omega'} E_{ai} + [\kappa_{ai}^{-\omega, -\omega'}]^* E_{ia}) + \sum_{\alpha} (\gamma_{\alpha}^{\omega, \omega'} b_{\alpha}^{\dagger} + [\gamma_{\alpha}^{-\omega, -\omega'}]^* b_{\alpha}) \quad (219)$$

are the Fourier components of Eqs. (213) and (214)

$$\Lambda^{(1)}(t) = \int d\omega e^{-i\omega t} \Lambda^{\omega} \quad (220)$$

$$\Lambda^{(2)}(t) = \int d\omega d\omega' e^{-i\omega t} e^{-i\omega' t} \Lambda^{\omega, \omega'}. \quad (221)$$

*a. Linear response equations.* From Eq. (211), performing a Fourier transform and by using Eq. (218) and Eq. (215), after some algebra, we obtain the standard matrix equation

$$\left[ \begin{pmatrix} \mathbf{A} & \mathbf{B} \\ \mathbf{B}^* & \mathbf{A}^* \end{pmatrix} - \omega \begin{pmatrix} 1 & 0 \\ 0 & -1 \end{pmatrix} \right] \begin{pmatrix} \mathbf{X} \\ \mathbf{Y} \end{pmatrix} = i \begin{pmatrix} \mathbf{g}_1 \\ \mathbf{g}_2 \end{pmatrix} \equiv i\mathbf{g}, \quad (222)$$

where the vectors  $\mathbf{X}$  and  $\mathbf{Y}$  collect the Fourier transformed parameters

$$\mathbf{X} = \begin{pmatrix} \gamma_{\alpha}^{\omega} \\ \kappa_{ai}^{\omega} \end{pmatrix} \quad \mathbf{Y} = \begin{pmatrix} [\gamma_{\alpha}^{-\omega}]^* \\ [\kappa_{ai}^{-\omega}]^* \end{pmatrix}. \quad (223)$$

The right hand side of Eq. (222) is the generalized gradient

$$\mathbf{g}_1 = \begin{pmatrix} \langle [b_{\alpha}, V^{\omega}] \rangle_{\mathbf{R}} \\ \frac{1}{\sqrt{2}} \langle [E_{ia}, V^{\omega}] \rangle_{\mathbf{R}} \end{pmatrix} \quad \mathbf{g}_2 = \begin{pmatrix} \langle [b_{\alpha}^{\dagger}, V^{\omega}] \rangle_{\mathbf{R}} \\ \frac{1}{\sqrt{2}} \langle [E_{ai}, V^{\omega}] \rangle_{\mathbf{R}} \end{pmatrix}. \quad (224)$$

The matrix

$$\mathbf{E}^{[2]} = \begin{pmatrix} \mathbf{A} & \mathbf{B} \\ \mathbf{B}^* & \mathbf{A}^* \end{pmatrix} \quad (225)$$

is the generalized Hessian matrix while

$$\mathbf{S}^{[2]} = \begin{pmatrix} 1 & 0 \\ 0 & -1 \end{pmatrix} \quad (226)$$

is the generalized metric matrix. Therefore, Eq. (222) is a generalization of the Casida equations of TDHF in molecular response theory.<sup>230,231</sup> Indeed, the explicit expressions of  $\mathbf{A}$  and  $\mathbf{B}$  are

$$\mathbf{A} = \begin{pmatrix} \omega_{\alpha} \delta_{\alpha\beta} & \sqrt{\omega_{\alpha}} (\boldsymbol{\lambda}_{\alpha} \cdot \mathbf{d}_{ib}) \\ \sqrt{\omega_{\alpha}} (\boldsymbol{\lambda}_{\alpha} \cdot \mathbf{d}_{bi}) & \mathbf{A}_{el} \end{pmatrix} = \begin{pmatrix} \langle [b_{\alpha}, [H, b_{\alpha}^{\dagger}]] \rangle_{\mathbf{R}} & \frac{1}{\sqrt{2}} \langle [b_{\alpha}, [H, E_{ai}]] \rangle_{\mathbf{R}} \\ \frac{1}{\sqrt{2}} \langle [b_{\alpha}^{\dagger}, [H, E_{ia}]] \rangle_{\mathbf{R}} & \frac{1}{2} \langle [E_{jb}, [H, E_{ai}]] \rangle_{\mathbf{R}} \end{pmatrix} \quad (227)$$

$$\mathbf{B} = \begin{pmatrix} 0 & -\sqrt{\omega_{\alpha}} (\boldsymbol{\lambda}_{\alpha} \cdot \mathbf{d}_{ib}) \\ -\sqrt{\omega_{\alpha}} (\boldsymbol{\lambda}_{\alpha} \cdot \mathbf{d}_{bi}) & \mathbf{B}_{el} \end{pmatrix} = \begin{pmatrix} \langle [b_{\alpha}, [H, b_{\alpha}]] \rangle_{\mathbf{R}} & \frac{1}{\sqrt{2}} \langle [b_{\alpha}, [H, E_{ia}]] \rangle_{\mathbf{R}} \\ \frac{1}{\sqrt{2}} \langle [b_{\alpha}^{\dagger}, [H, E_{ai}]] \rangle_{\mathbf{R}} & \frac{1}{2} \langle [E_{bj}, [H, E_{ai}]] \rangle_{\mathbf{R}} \end{pmatrix}. \quad (228)$$

The electronic blocks

$$(A_{el})_{ia,bj} = \frac{1}{2} \langle \mathbf{R} | [E_{ia}, [H, E_{bj}]] | \mathbf{R} \rangle = \delta_{ij} F_{ab} - \delta_{ab} F_{ij} + 2\bar{g}_{aibj} - \bar{g}_{abji} \quad (229)$$

$$(B_{el})_{ia,jb} = \frac{1}{2} \langle \mathbf{R} | [E_{ia}, [H, E_{jb}]] | \mathbf{R} \rangle = \bar{g}_{biaj} - 2\bar{g}_{aibj}, \quad (230)$$

have the same definition as the standard Casida matrices,  $\mathbf{A}$  and  $\mathbf{B}$ , in the TDHF theory. Nevertheless, we point out that these blocks differ from the bare TDHF matrices for two reasons. First, the QED-HF orbitals and orbital energies differ from the bare molecular ones. Second, the two-electron integrals now contain the dipole self-energy contributions, as shown in Eq. (196). This contribution can be explicitly separated<sup>95</sup> following Eqs. (196) and (197)

$$\mathbf{A}_{el} = \mathbf{A}_{el}^{\text{HF}} + \mathbf{\Delta} \quad (231)$$

$$\mathbf{B}_{el} = \mathbf{B}_{el}^{\text{HF}} + \mathbf{\Delta}' \quad (232)$$

where the  $\mathbf{\Delta}$  and  $\mathbf{\Delta}'$  matrices now include the dipole self-energy contribution to the Hamiltonian, while  $\mathbf{A}_{el}^{\text{HF}}$  and  $\mathbf{B}_{el}^{\text{HF}}$

only include the standard electronic integrals. The TD-QED-HF matrices have additional dimensions due to the cavity modes. The coupling between the molecular and the photonic parameters is given by the projection of the transition dipole moments onto the coupling strength vector  $\boldsymbol{\lambda}$  in the off-diagonal terms of Eqs. (229) and (230). Moreover, the  $\mathbf{A}$  matrix has a non-zero photonic block that contains the frequencies  $\omega_\alpha$  of the cavity modes. As expected, in Eq. (227) there is no direct interaction between the photon modes, which are coupled indirectly through matter degrees of freedom. We see that these equations are an extension of the familiar TDHF response equations since in the zero coupling limit we recover TDHF solutions and the one photon lines of the empty cavity. We can then write the response function from the time evolution of an operator  $\Omega$

$$\begin{aligned} \langle \Omega \rangle(t) - \langle \Omega \rangle_{\mathbf{R}} &= \langle \Omega \rangle^{(1)}(t) + \dots = \\ &-i \int_{-\infty}^{\infty} e^{-i\omega t} \left( \sum_{ai} \frac{\kappa_{ai}^\omega}{\sqrt{2}} \langle [\Omega, E_{ai}] \rangle_{\mathbf{R}} + \sum_{ai} \frac{[\kappa_{ai}^{-\omega}]^*}{\sqrt{2}} \langle [\Omega, E_{ia}] \rangle_{\mathbf{R}} + \gamma^\omega \langle [\Omega, b^\dagger] \rangle_{\mathbf{R}} + [\gamma_\alpha^{-\omega}]^* \langle [\Omega, b] \rangle_{\mathbf{R}} \right) + \dots \end{aligned} \quad (233)$$

Inverting equation Eq. (222), we identify the linear response function

$$\begin{aligned} \langle \langle \Omega, V^\omega \rangle \rangle_\omega &= -i \left( \sum_{ai} \frac{\kappa_{ai}^\omega}{\sqrt{2}} \langle [\Omega, E_{ai}] \rangle_{\mathbf{R}} + \sum_{ai} \frac{[\kappa_{ai}^{-\omega}]^*}{\sqrt{2}} \langle [\Omega, E_{ia}] \rangle_{\mathbf{R}} + \gamma_\alpha^\omega \langle [\Omega, b^\dagger] \rangle_{\mathbf{R}} + [\gamma_\alpha^{-\omega}]^* \langle [\Omega, b] \rangle_{\mathbf{R}} \right) \\ &= i g_\Omega^\dagger \begin{pmatrix} \mathbf{X} \\ \mathbf{Y} \end{pmatrix} = -g_\Omega^\dagger \left[ \begin{pmatrix} \mathbf{A} & \mathbf{B} \\ \mathbf{B}^* & \mathbf{A}^* \end{pmatrix} - \omega \begin{pmatrix} 1 & 0 \\ 0 & -1 \end{pmatrix} \right]^{-1} \mathbf{g}, \end{aligned} \quad (234)$$

where  $\mathbf{g}_\Omega$  has the same structure as  $\mathbf{g}$  with the operator  $\Omega$  replacing the perturbation  $V^\omega$  in Eq. (224). We note that the response function fulfils the symmetry relation in Eq. (83). From the generalized eigenvalue equation

$$\left[ \begin{pmatrix} \mathbf{A} & \mathbf{B} \\ \mathbf{B}^* & \mathbf{A}^* \end{pmatrix} - \omega \begin{pmatrix} 1 & 0 \\ 0 & -1 \end{pmatrix} \right] \begin{pmatrix} \mathbf{X} \\ \mathbf{Y} \end{pmatrix} = \begin{pmatrix} 0 \\ 0 \end{pmatrix}, \quad (235)$$

we obtain the eigenvectors  $(\mathbf{x}_i, \mathbf{y}_i)^T$  and the spectral decomposition

$$\left[ \begin{pmatrix} \mathbf{A} & \mathbf{B} \\ \mathbf{B}^* & \mathbf{A}^* \end{pmatrix} - \omega \begin{pmatrix} 1 & 0 \\ 0 & -1 \end{pmatrix} \right]^{-1} = \sum_{i>0} \left( \frac{1}{\omega_j - \omega} \begin{pmatrix} \mathbf{x}_i \\ \mathbf{y}_i \end{pmatrix} \otimes \begin{pmatrix} \mathbf{x}_i^\dagger & \mathbf{y}_i^\dagger \end{pmatrix} - \frac{1}{\omega_j + \omega} \begin{pmatrix} \mathbf{y}_i^* \\ \mathbf{x}_i^* \end{pmatrix} \otimes \begin{pmatrix} (\mathbf{y}_i^*)^\dagger & (\mathbf{x}_i^*)^\dagger \end{pmatrix} \right).$$

We identify the excitation energies of the system as the eigenvalues of Eq. (235). The transition moments are obtained from

the residues of the response function, identified as

$$\langle 0 | \Omega | k \rangle = \begin{pmatrix} \mathbf{x}_k^\dagger & \mathbf{y}_k^\dagger \end{pmatrix} \cdot \begin{pmatrix} \langle [b_\alpha^\dagger, \Omega] \rangle_{\mathbf{R}} \\ \frac{1}{\sqrt{2}} \langle [E_{ai}, \Omega] \rangle_{\mathbf{R}} \\ \langle [b_\alpha, \Omega] \rangle_{\mathbf{R}} \\ \frac{1}{\sqrt{2}} \langle [E_{ia}, \Omega] \rangle_{\mathbf{R}} \end{pmatrix}. \quad (236)$$



Although the eigenvalue problem in Eq. (235) is non Hermitian, it is possible to show that if the computed reference state is close to the ground state, Eq. (235) has solutions with real and positive eigenvalues.<sup>84</sup> We note that in Eq. (222), setting  $\omega = 0$ , we obtain the static coupled-perturbed QED-HF equations.

Several approximations can be proposed for these response equations. A hierarchy of approximations has been discussed by Yang et al.<sup>95</sup> for their TDDFT-Pauli-Fierz (TDDFT-PF) model, which defined a eigenvalue problem analogous to Eq. (222). They define the Tamm-Dancoff approximation (TDA) by neglecting  $\mathbf{B}_{el}$ . However, contrary to standard electronic TDA, this is *not* equivalent to a CI-singles approach. For this

reason, we suggest it is more natural to define the TDA approximation by neglecting the whole  $\mathbf{B}$  matrix, since this is equivalent to a CI problem with singly excited determinants with zero photons and the ground state determinant with one photon. Neglecting  $\mathbf{B}$  and the dipole self-energy contribution in  $\mathbf{\Delta}$ , they define the TDDFT-Jaynes-Cummings approximation, similar to a JC calculation with all the single excited determinants.

*b. Quadratic response equations* The quadratic response equations are obtained in a similar fashion as for the linear response.<sup>84,85,232</sup> By employing Eq. (212) and the set of operators (215), we obtain the second-order response equation

$$(\omega_1 + \omega_2) \langle \mathbf{R} | [\Lambda^{\omega_1, \omega_2}, \boldsymbol{\xi}] | \mathbf{R} \rangle - \langle \mathbf{R} | [\Lambda^{\omega_1, \omega_2}, [\boldsymbol{\xi}, H]] | \mathbf{R} \rangle = \frac{1}{2} \hat{P}(\omega_1, \omega_2) \left( \frac{i}{2} \langle \mathbf{R} | [\Lambda^{\omega_1}, [\Lambda^{\omega_2}, [\boldsymbol{\xi}, H]]] | \mathbf{R} \rangle + \langle \mathbf{R} | [\Lambda^{\omega_1}, [\boldsymbol{\xi}, V^{\omega_2}]] | \mathbf{R} \rangle \right), \quad (237)$$

where  $\hat{P}(\omega_1, \omega_2)$  sums the permutations of  $\omega_1$  and  $\omega_2$  and we used the compact notation

$$\boldsymbol{\xi} = \begin{pmatrix} b_\alpha \\ \frac{1}{\sqrt{2}} E_{ia} \\ b_\alpha^\dagger \\ \frac{1}{\sqrt{2}} E_{ai} \end{pmatrix}. \quad (238)$$

To compute the quadratic response function  $\langle\langle A; B, C \rangle\rangle_{\omega_1, \omega_2}$ , together with the  $\mathbf{E}^{[2]}$  and  $\mathbf{S}^{[2]}$  matrices defined in Eqs. (225) and (226) for the linear response, we need the additional matrices

$$E_{ijk}^{[3]} = \frac{1}{2} \langle \mathbf{R} | [\xi_i^\dagger, [\xi_j^\dagger, [H, \xi_k]]] | \mathbf{R} \rangle \quad (239)$$

$$X_{ij}^{[2]} = \langle \mathbf{R} | [\xi_i^\dagger, [X, \xi_j]] | \mathbf{R} \rangle, \quad (240)$$

where  $X = A, B$  or  $C$ . The second-order variation of a time-independent observable  $A$  is

$$\begin{aligned} \langle A \rangle^{(2)}(t) &= i \langle [\Lambda^{(2)}, A] \rangle_{\mathbf{R}} - \frac{1}{2} \langle [\Lambda^{(1)}, [\Lambda^{(1)}, A]] \rangle_{\mathbf{R}} \\ &= \int \int d\omega_1 d\omega_2 \frac{1}{2} \hat{P}(\omega_1, \omega_2) \left( i \langle [\Lambda^{\omega_1, \omega_2}, A] \rangle_{\mathbf{R}} - \frac{1}{2} \langle [\Lambda^{\omega_2}, [\Lambda^{\omega_1}, A]] \rangle_{\mathbf{R}} \right) e^{-i(\omega_1 + \omega_2)t}, \end{aligned} \quad (241)$$

where we made the expression explicitly symmetric in the frequencies. From Eq. (241), we can identify the quadratic response function, which has poles where the frequencies or their sum match an excitation energy<sup>233</sup>

$$\langle\langle A; B, C \rangle\rangle_{\omega_1, \omega_2} = \hat{P}(\omega_1, \omega_2) \left( i \langle [\Lambda^{\omega_1, \omega_2}, A] \rangle_{\mathbf{R}} - \frac{1}{2} \langle [\Lambda^{\omega_2}, [\Lambda^{\omega_1}, A]] \rangle_{\mathbf{R}} \right). \quad (242)$$

For the residues and the response function, we then need the following vectors:

$$\begin{aligned} [\mathbf{N}^a(\omega_1 + \omega_2)]^\dagger &= \mathbf{g}_A^\dagger [\mathbf{E}^{[2]} - (\omega_1 + \omega_2) \mathbf{S}^{[2]}]^{-1} \\ \mathbf{N}^b(\omega_1) &= [\mathbf{E}^{[2]} - \omega_1 \mathbf{S}^{[2]}]^{-1} \mathbf{g}_B \\ \mathbf{N}^c(\omega_2) &= [\mathbf{E}^{[2]} - \omega_2 \mathbf{S}^{[2]}]^{-1} \mathbf{g}_C. \end{aligned}$$

As for the linear response equations, these vectors and matri-

ces have additional dimensions due to the photonic parameters.

### 6.1.2. On the definition of the photonic character of excited states

From the QED-Casida equations, it is possible to define a relative electronic/photonic contribution to the polaritonic

excitation.<sup>95,99</sup> Given a normalized eigenvector of Eq. (235), we define the "photonic character"  $\chi_n$  as the sum over the cavity modes  $\alpha$  of the squares of the photonic response parameters  $\gamma_\alpha$ <sup>95,99</sup>

$$\chi_n = \sum_{\alpha} |\gamma_{\alpha}|^2. \quad (243)$$

The electronic character of the excitation  $\rho_n$  is defined as the sum of the orbital rotation  $\kappa_{ai}$ , such that  $\chi_n + \rho_n = 1$

$$\rho_n = \sum_{ai} |k_{ai}|^2 = 1 - \chi. \quad (244)$$

However, such a definition of the excitation character is not straightforwardly connected to photon number nor to electronic excitations in a molecular sense. In fact, for the QED-HF equations, we used the dipole Hamiltonian in the length form. As a consequence of this choice, as pointed out at the end of section (4.2), the photon creation and annihilation operators cannot be simply identified with  $b^\dagger$  and  $b$ . These operators refer instead to the *displacement field* and therefore include matter contributions from the polarization in Eq. (38). Moreover, as the coupling strength increases, the ground state might gain significant contributions from photon states. The "photon character" of the excitation becomes, therefore, a slippery concept that requires careful examination also of the ground state. A clarification of this photon character ambiguity could be obtained by implementing the quadratic response equations, from which we obtain the expectation values of observables for excited states. Accordingly, we may compute the following expectation values

$$\langle n | b_{\alpha}^{\dagger} b_{\alpha} | n \rangle \quad (245)$$

$$\langle n | (b_{\alpha}^{\dagger} + \frac{1}{\sqrt{2\omega_{\alpha}}} \lambda_{\alpha} \cdot \mathbf{d}) (b_{\alpha} + \frac{1}{\sqrt{2\omega_{\alpha}}} \lambda_{\alpha} \cdot \mathbf{d}) | n \rangle. \quad (246)$$

In the length representation, Eq. (245) refers to the mean occupation number of the displacement field number states, while Eq. (246) to the mean electric field number states. We can then compare these calculations to the QED-HF ground state expectation values

$$\langle \mathbf{R} | b_{\alpha}^{\dagger} b_{\alpha} | \mathbf{R} \rangle = \frac{1}{2\omega_{\alpha}} (\lambda_{\alpha} \cdot \langle \mathbf{d} \rangle_{\text{QED-HF}})^2 \quad (247)$$

$$\langle \mathbf{R} | (b_{\alpha}^{\dagger} + \frac{1}{\sqrt{2\omega_{\alpha}}} \lambda_{\alpha} \cdot \mathbf{d}) (b_{\alpha} + \frac{1}{\sqrt{2\omega_{\alpha}}} \lambda_{\alpha} \cdot \mathbf{d}) | \mathbf{R} \rangle = 0 \quad (248)$$

to obtain an estimate of the cavity-field contribution to the excitations.

Employing these less straightforward but more precise definitions might clarify some results presented in the literature. When using the definition in Eq. (243), Yang et al.<sup>95</sup> found that the photon contribution of the lower polariton increases with the coupling strength, while the opposite is found for the upper polariton.<sup>95</sup> At the same time, the intensity of the lower (upper) polariton increases (decreases) with the coupling strength, which seems in contradiction with the zero oscillator strength associated with the photon states. It is argued that this apparent discrepancy results from the intrusion of higher-energy electronic states, which strengthen the intensity of the lower polariton, overcompensating for the increased photon character of the excitation.<sup>95</sup> Nevertheless, in this representation,  $b^\dagger$  involves both the photons and the matter polarization, which suggests that this interpretation might be revised.

We also note that since QED-HF introduces a coherent state transformation, it would be interesting to investigate the following expectation values

$$\langle n | b_{\alpha}^{\dagger} b_{\alpha} | n \rangle \quad (249)$$

$$\langle n | (b_{\alpha}^{\dagger} - \frac{1}{\sqrt{2\omega_{\alpha}}} \lambda_{\alpha} \cdot \langle \mathbf{d} \rangle_{\text{QED-HF}}) (b_{\alpha} - \frac{1}{\sqrt{2\omega_{\alpha}}} \lambda_{\alpha} \cdot \langle \mathbf{d} \rangle_{\text{QED-HF}}) | n \rangle \quad (250)$$

$$\langle n | (b_{\alpha}^{\dagger} + \frac{1}{\sqrt{2\omega_{\alpha}}} \lambda_{\alpha} \cdot (\mathbf{d} - \langle \mathbf{d} \rangle_{\text{QED-HF}})) (b_{\alpha} + \frac{1}{\sqrt{2\omega_{\alpha}}} \lambda_{\alpha} \cdot (\mathbf{d} - \langle \mathbf{d} \rangle_{\text{QED-HF}})) | n \rangle, \quad (251)$$

where Eq. (249) refers to the occupation of the displacement field coherent states, Eq. (250) refers to the displacement field number states, and Eq. (251) refers to the occupation of the electric field number states.

### 6.1.3. Equivalent transition moments in TD-QED-HF

Following the same procedure as for standard HF response theory,<sup>84,227</sup> we can show that Eqs. (102), (110), and (113), derived for exact wave functions, also hold in the QED-HF

response framework. In Tab. (I) we report the TD-QED-HF transition moments for the lower polariton of an ethylene molecule using different basis sets. We report the oscillator strengths in the length  $f_L$  and velocity  $f_V$  forms

$$f_L^{0n} = \frac{2}{3} \omega_n \sum_{i=x,y,z} |\langle 0 | d_i | n \rangle|^2 \quad (252)$$

$$f_V^{0n} = \frac{2}{3\omega_n} \sum_{i=x,y,z} |\langle 0 | p_i | n \rangle|^2, \quad (253)$$

and the transition photon displacement coordinate and momentum

$$\langle 0|p_\alpha|n\rangle = i\sqrt{\frac{\omega_\alpha}{2}} \langle 0|(b_\alpha^\dagger - b_\alpha)|n\rangle \quad (254)$$

$$\langle 0|q_\alpha|n\rangle = \frac{1}{\sqrt{2\omega_\alpha}} \langle 0|(b_\alpha^\dagger + b_\alpha)|n\rangle. \quad (255)$$

We numerically demonstrate the validity of Eqs. (102), (110), and (113). Notice that since Eq. (102) is fulfilled only in the complete basis set limit, Eqs. (252) and (253) will converge only for large basis sets, as seen from the table. At the same time, Eq. (113) holds independently of the basis set size and the photon space truncation. Notice that although the equivalence expressed by Eqs. (109) and (110) do not depend on the quality of the basis set, the computed values of the transition moments change with the basis, as expected from the connection between matter and photon moments expressed by (110). In particular, the use of diffuse functions strongly affects the computed results. Equivalence relations such as Eqs. (102) and (113) are well known in molecular response theory. How-

ever, they have not been explicitly investigated for QED systems. Furthermore, these relations do not hold for the Tamm-Dancoff approximation. The formal equivalence between the transition dipole and velocity momenta can be exploited in the computation of electronic circular dichroism (ECD) and optical rotation. From standard molecular response theory, the ECD spectrum is known to be proportional to the rotational strength

$$R_{n0} = \Im\{\langle 0|\boldsymbol{\mu}|n\rangle \cdot \langle n|\mathbf{m}|0\rangle\}. \quad (256)$$

The dipole formulation in Eq. (256) is origin dependent for a finite basis set, which can lead to unphysical results. If we are interested in the chirality effects promoted by a chiral cavity, such a formulation might be misleading. However, the equivalent velocity form

$$R_{n0} = \frac{1}{\omega_n} \Re\{\langle 0|\mathbf{p}|n\rangle \cdot \langle n|\mathbf{m}|0\rangle\} \quad (257)$$

is always origin independent, and Eqs. (256) and (257) are equivalent in the limit of a complete basis.

Basis set	$f_L$	$f_V$	$\langle 0 q_\alpha n\rangle$ [a.u.]	$i\langle 0 p_\alpha n\rangle$ [a.u.]	$\omega_n \langle 0 q_\alpha n\rangle$ [a.u.]	$\frac{\langle 0 \mathbf{d}\cdot\boldsymbol{\lambda}_\alpha n\rangle\omega_n\omega_\alpha}{\omega_n^2-\omega_\alpha^2}$ [a.u.]
sto-3g	0.00234	0.00096	1.36138	0.36641	0.36641	0.36641
6-31g	0.02540	0.01902	1.34118	0.35965	0.35965	0.35965
6-311g	0.04362	0.03158	1.32054	0.35349	0.35349	0.35349
6-311g*	0.04978	0.04891	1.30958	0.35036	0.35036	0.35036
6-311g**	0.05454	0.05192	1.30320	0.34852	0.34852	0.34852
6-311+g**	0.20610	0.19318	1.03720	0.27413	0.27413	0.27413
6-311++g**	0.20631	0.19327	1.03677	0.27401	0.27401	0.27401
cc-pVDZ	0.04267	0.04121	1.31895	0.35309	0.35309	0.35309
aug-cc-pVDZ	0.21694	0.21309	0.99843	0.26353	0.26353	0.26353
aug-cc-pV5Z	0.22561	0.22564	0.96941	0.25559	0.25559	0.25559

TABLE I. Oscillator strength in dipole  $f_L$  and velocity  $f_V$  form and transition photon displacement coordinate  $\langle 0|q_\alpha|n\rangle$  and momentum  $i\langle 0|p_\alpha|n\rangle$  for the lower polariton of an ethylene molecule, for different basis sets at TD-QED-HF level. The cavity frequency is set to 0.2695 a.u., and the coupling strength to 0.01 a.u. with field polarization along the transition dipole moment of the first non-dark excitation of ethylene. Eq. (102) holds only in the complete basis limit, and convergence between the velocity and length form of the oscillator strength strongly depends on the quality of the basis set. On the other hand, Eqs. (109) and (110) hold independently of the truncation of the electronic or photonic space.

#### 6.1.4. QED-HF static response equations

For static perturbations, the response equations for the optimized QED-HF state  $|\mathbf{R}\rangle$  can be derived using the same parametrization shown in Eq. (204), which now is time-independent

$$|\text{QED-HF}\rangle = \exp(i\Lambda) |\mathbf{R}\rangle. \quad (258)$$

Here  $\Lambda$  has the same form showed in Eq. (205) and may be written compactly as

$$\Lambda = \boldsymbol{\xi}^\dagger \cdot \boldsymbol{\Theta}, \quad (259)$$

where  $\Theta$  collects both photon and electron parameters and  $\xi$  the respective operators:

$$\Theta = \begin{pmatrix} \gamma_\alpha \\ \kappa_{ai} \\ \gamma_\alpha^* \\ \kappa_{ai}^* \end{pmatrix}; \quad \xi = \begin{pmatrix} b_\alpha \\ \frac{1}{\sqrt{2}}E_{ia} \\ b_\alpha^\dagger \\ \frac{1}{\sqrt{2}}E_{ai} \end{pmatrix}.$$

Following the perturbation expansion of the energy in Sec. (5), the first-order energy derivative is

$$E_{\text{QED-HF}}^{(1)} = \langle \mathbf{R} | H^{(1)} | \mathbf{R} \rangle, \quad (260)$$

which expresses the Hellmann-Feynman theorem for the QED-HF state. In Eq. (260),  $H^{(1)}$  refers to the first-order interactions. The second-order energy derivative is

$$E_{\text{QED-HF}}^{(2)} = \langle \mathbf{R} | H^{(2)} | \mathbf{R} \rangle + \langle \mathbf{R} | [\Lambda^{(1)}, H^{(1)}] | \mathbf{R} \rangle, \quad (261)$$

where  $H^{(2)}$  is the second-order interaction and  $\Lambda^{(1)}$  is the first-order correction to the parameterization. Since QED-HF state is a variational theory,<sup>60</sup> the optimization conditions are equivalent to those in standard HF<sup>87</sup>

$$\langle \mathbf{R} | [\xi, H^{(0)}] | \mathbf{R} \rangle = 0 \quad (262)$$

$$\sum_j \langle \mathbf{R} | [\xi_i^\dagger, [H^{(0)}, \xi_j]] | \mathbf{R} \rangle \Theta_j^{(1)} = i \langle \mathbf{R} | [\xi_i, H^{(1)}] | \mathbf{R} \rangle, \quad (263)$$

where Eq. (262) corresponds to the QED-HF Brillouin's theorem,<sup>60</sup> and Eq. (263) to the first-order static response equations. The left-hand side of Eq. (263) includes the generalized Hessian matrix, whose blocks are given in Eq. (227)-Eq. (228), and the first-order parameters  $\Theta^{(1)}$ . The right-hand side contains the first-order Hamiltonian, which includes the first-order interaction terms. We note that Eq. (263) is equivalent to the time-dependent response equation (222) with  $\omega = 0$ .

## 6.2. QED-CC

The reference wave function used in QED-CC is QED-HF, where we employ the coherent-state transformed Hamiltonian in Eq. (202).<sup>60</sup> The QED-CC state is defined as

$$|\text{QED-CC}\rangle = \exp(T) |\text{HF}, 0\rangle, \quad (264)$$

where  $T$  is the cluster operator

$$T = T_e + T_p + T_{int}. \quad (265)$$

The electronic cluster  $T_e$  is the standard electronic excitation operator<sup>185</sup>

$$T_e = \sum_\mu t_\mu \tau_\mu \quad (266)$$

$$\tau_\mu |\text{HF}\rangle = |\mu\rangle, \quad (267)$$

where  $|\mu\rangle$  is an excited HF determinant. The cluster operator  $T_p$  includes pure photonic excitations

$$T_p = \sum_{\mathbf{n}} \Gamma_{\mathbf{n}} = \sum_{\mathbf{n}} \gamma_{\mathbf{n}} \prod_{\alpha} (b_\alpha^\dagger)^{n_\alpha}, \quad (268)$$

where  $\mathbf{n}$  is a vector of integers  $n_\alpha$  referring to the  $\alpha$ -mode. Finally, the interaction operator  $T_{int}$  includes simultaneous excitations of matter and cavity modes

$$T_{int} = \sum_{\mathbf{n}} (S_1^n + S_2^n + \dots + S_{N_e}^n), \quad (269)$$

where for instance

$$S_1^n = \sum_{ai} s_{ai}^n E_{ai} \prod_{\alpha} (b_\alpha^\dagger)^{n_\alpha} \quad (270)$$

$$S_2^n = \frac{1}{2} \sum_{aibj} s_{aibj}^n E_{ai} E_{bj} \prod_{\alpha} (b_\alpha^\dagger)^{n_\alpha}. \quad (271)$$

The Schrödinger equation is solved by projection onto the space  $S$  spanned by the electronic determinants and the number states<sup>60</sup>

$$S = \text{Span}\{ |\text{HF}, 0\rangle, |\mu, 0\rangle, |\text{HF}, \mathbf{n}\rangle, |\mu, \mathbf{n}\rangle \}. \quad (272)$$

In Eq. (272), the state  $|\mu, \mathbf{n}\rangle$  is a simultaneous excitation to the  $\mu$  electronic excited determinant and the  $\mathbf{n}$  photon state

$$|\mu, \mathbf{n}\rangle = |\mu\rangle \otimes |\mathbf{n}\rangle = \tau_\mu \prod_{\alpha} \frac{(b_\alpha^\dagger)^{n_\alpha}}{\sqrt{n_\alpha!}} |\text{HF}, 0\rangle. \quad (273)$$

The ground state QED-CC equations are therefore

$$\langle \mu, \mathbf{n} | e^{-T} H e^T | \text{HF}, 0 \rangle = 0 \quad (274)$$

$$\langle \text{HF}, 0 | H | \text{QED-CC} \rangle = E_{\text{QED-CC}}. \quad (275)$$

The QED-CC dual state is defined as in standard CC theory

$$\langle \Lambda | = \langle \text{HF}, 0 | + \sum \bar{t}_{\mu\mathbf{n}} \langle \mu, \mathbf{n} | e^{-T}, \quad (276)$$

where  $\bar{t}_{\mu\mathbf{n}}$  are the Lagrangian multipliers.<sup>60,185</sup> A collective index  $t_{\mu\mathbf{n}}$  can also be defined for the cluster operator such that we can write  $T$  more compactly as

$$T = \sum_{\mu, \mathbf{n}} t_{\mu\mathbf{n}} \tau_\mu \prod_{\alpha} (b_\alpha^\dagger)^{n_\alpha}, \quad (277)$$

where

$$t_{\mu 0} = t_\mu \quad (278)$$

$$t_{\mu\mathbf{n}} = s_\mu^n \quad (279)$$

$$t_{\text{HF}\mathbf{n}} = \gamma_{\mathbf{n}}. \quad (280)$$

As in standard CC theory, QED-CC is based on a hierarchy of approximations where the cluster operators and the projection space are truncated.<sup>60,185</sup> Since the space  $S$  is larger than in standard CC theory, as it also includes the photonic excita-

tions, the QED-CC Jacobian  $\mathbf{A}$  has additional dimensions

$$A_{\mu n, \nu m} = \langle \mu, \mathbf{n} | [e^{-T} H e^T, \tau_\nu \prod_\alpha (b_\alpha^\dagger)^{m_\alpha}] | \text{HF}, 0 \rangle. \quad (281)$$

In addition to the electronic block  $\mathbf{A}_{e,e}$  similar to electronic CC, there is also a photonic block  $\mathbf{A}_{p,p}$  and blocks involving the electronic-photonic parameters

$$\mathbf{A} = \begin{pmatrix} \mathbf{A}_{e,e} & \mathbf{A}_{e,ep} & \mathbf{A}_{e,p} \\ \mathbf{A}_{ep,e} & \mathbf{A}_{ep,ep} & \mathbf{A}_{ep,p} \\ \mathbf{A}_{p,e} & \mathbf{A}_{p,ep} & \mathbf{A}_{p,p} \end{pmatrix}. \quad (282)$$

From the Jacobian  $\mathbf{A}$  and the  $\eta$  vector

$$\eta_{\mu n} = \langle \text{HF}, 0 | e^{-T} H e^T | \mu, \mathbf{n} \rangle, \quad (283)$$

we obtain the Lagrangian multipliers and the equation of motion (EOM)-QED-CC formalism for properties and excited states.<sup>60</sup>

### 6.2.1. Time-dependent QED-CC

Following the response theory for electronic CC,<sup>234–236</sup> we parametrize the time-evolution of the QED-CC state by a

time-dependent cluster operator  $T(t)$

$$|\text{QED-CC}\rangle(t) = e^{T(t)} |\text{HF}, 0\rangle e^{i\varepsilon(t)}. \quad (284)$$

The time-dependent parameters are obtained by projection of the time dependent Schrödinger equation

$$i \frac{d}{dt} (e^{T(t)} |\text{HF}, 0\rangle e^{i\varepsilon(t)}) = (H + V^t) e^{T(t)} |\text{HF}, 0\rangle e^{i\varepsilon(t)} \quad (285)$$

onto the space  $S$ . We obtain the following response equations for the cluster parameters

$$\frac{d\varepsilon}{dt} = -\langle \text{HF}, 0 | (H + V^t) e^{T(t)} | \text{HF}, 0 \rangle \quad (286)$$

$$\frac{dt_\mu}{dt} = -i \langle \mu, 0 | e^{-T(t)} (H + V^t) e^{T(t)} | \text{HF}, 0 \rangle \quad (287)$$

$$\frac{d\gamma_n}{dt} = -i \langle \text{HF}, \mathbf{n} | e^{-T(t)} (H + V^t) e^{T(t)} | \text{HF}, 0 \rangle \quad (288)$$

$$\frac{ds_\mu^n}{dt} = -i \langle \mu, \mathbf{n} | e^{-T(t)} (H + V^t) e^{T(t)} | \text{HF}, 0 \rangle, \quad (289)$$

where Eqs. (286) and (287) are analogous to standard CC response theory,<sup>234,235</sup> while Eqs. (288) and (289) are additional equations for the photon and electron-photon parameters. We then perform a perturbative expansion of the amplitudes and a Fourier decomposition

$$\begin{aligned} t_{\mu n} &= t_{\mu n}^{(0)} + t_{\mu n}^{(1)} + t_{\mu n}^{(2)} + \dots \\ &= t_{\mu n}^{(0)} + \int d\omega_1 X_{\mu n}^{(1)}(\omega_1) e^{-i\omega_1 t} + \int d\omega_1 \int d\omega_2 X_{\mu n}^{(2)}(\omega_1, \omega_2) e^{-i\omega_1 t - i\omega_2 t} + \dots \end{aligned} \quad (290)$$

Focusing now on a single cavity mode, although the generalization to a multimode system is straightforward, we obtain the following set of equations

$$\langle \mu, \mathbf{n} | e^{-T^{(0)}} H e^{T^{(0)}} | \text{HF}, 0 \rangle = 0 \quad (291)$$

$$\sum_{\nu m} (\omega_1 \mathbf{I} - \mathbf{A})_{\mu n, \nu m} X_{\nu m}^{(1)} = \xi_{\mu n}^{(1)} \quad (292)$$

$$\sum_{\nu m} ((\omega_1 + \omega_2) \mathbf{I} - \mathbf{A})_{\mu n, \nu m} X_{\nu m}^{(2)} = \xi_{\mu n}^{(2)}, \quad (293)$$

where

$$\xi_{\mu n}^{(1)}(\omega_1) = \langle \bar{\mu}, \bar{\mathbf{n}} | V^{\omega_1} | \text{QED-CC} \rangle \quad (294)$$

$$\xi_{\mu n}^{(2)}(\omega_1, \omega_2) = \frac{1}{2} \hat{P}(\omega_1, \omega_2) \left( \langle \bar{\mu}, \bar{\mathbf{n}} | [V^{\omega_1}, T^{(1)}(\omega_2)] | \text{QED-CC} \rangle + \frac{1}{2} \langle \bar{\mu}, \bar{\mathbf{n}} | [[H, T^{(1)}(\omega_1)], T^{(1)}(\omega_2)] | \text{QED-CC} \rangle \right), \quad (295)$$

and we defined the QED-CC-transformed states

$$\langle \bar{\mu}, \bar{\mathbf{n}} | = \langle \mu, \mathbf{n} | e^{-T^{(0)}} \quad (296)$$

$$| \text{QED-CC} \rangle = e^{T^{(0)}} | \text{HF}, 0 \rangle. \quad (297)$$

The zero, first and second-order cluster operators read

$$T^{(0)} = \sum_{\mu n} t_{\mu n} \tau_{\mu n} \quad (298)$$

$$T^{(1)}(\omega_1) = \sum_{\mu n} X_{\mu n}^{(1)}(\omega_1) \tau_{\mu n} \quad (299)$$

$$T^{(2)}(\omega_1, \omega_2) = \sum_{\mu n} X_{\mu n}^{(2)}(\omega_1, \omega_2) \tau_{\mu n}, \quad (300)$$

and we note that the zero-order equation in Eq (291) is the ground state QED-CC optimization condition. In an analogous way, we can parametrize the time dependence of the dual QED-CC state

$$\langle \Lambda(t) | = \left( \langle \text{HF} | + \sum_{\mu n} \bar{t}_{\mu n}(t) \langle \mu, n | e^{-T(t)} \right) e^{-i\epsilon(t)}, \quad (301)$$

where we have the standard normalization condition of CC at all times<sup>185</sup>

$$\langle \Lambda(t) | \text{QED-CC}(t) \rangle = 1. \quad (302)$$

The equations for the Lagrange multipliers are obtained by projection onto  $S$

$$\frac{d\bar{t}_{\mu n}}{dt} = i \langle \Lambda(t) | [H + V_t, \tau_{\mu}(b^{\dagger})^n] | \text{QED-CC}(t) \rangle \quad (303)$$

and using the same expansion as Eq. (290) we can write

$$\begin{aligned} \bar{t}_{\mu n} &= \bar{t}_{\mu n}^{(0)} + \bar{t}_{\mu n}^{(1)} + \bar{t}_{\mu n}^{(2)} + \dots \\ &= \bar{t}_{\mu n}^{(0)} + \int d\omega_1 Y_{\mu n}^{(1)}(\omega_1) e^{-i\omega_1 t} + \int d\omega_1 \int d\omega_2 Y_{\mu n}^{(2)}(\omega_1, \omega_2) e^{-i\omega_1 t - i\omega_2 t} + \dots \end{aligned} \quad (304)$$

We then obtain the equations

$$\sum_{\nu n} \bar{t}_{\nu n}^{(0)} A_{\nu n, \mu m} = - \langle R | [H, \tau_{\mu}(b^{\dagger})^n] | \text{QED-CC} \rangle \quad (305)$$

$$\sum_{\nu n} Y_{\nu n}^{(1)}(\omega_1 \mathbf{I} + \mathbf{A})_{\nu n, \mu m} = -\eta_{\mu m}^{(1)} - \sum_{\gamma k} F_{\mu m, \gamma k} X_{\gamma k}^{(1)} \quad (306)$$

$$\sum_{\nu n} Y_{\nu n}^{(2)}((\omega_1 + \omega_2) \mathbf{I} + \mathbf{A})_{\nu n, \mu m} = -\eta_{\mu m}^{(2)} - \sum_{\gamma k} F_{\mu m, \gamma k} X_{\gamma k}^{(2)}. \quad (307)$$

The zero-order equation in Eq. (305) is the ground state multiplier equation, and the vectors  $\eta$  are defined as

$$\eta_{\mu n}^{(1)}(\omega_1) = \langle \Lambda | [V^{\omega_1}, \tau_{\mu}(b^{\dagger})^n] | \text{QED-CC} \rangle \quad (308)$$

$$\begin{aligned} \eta_{\mu n}^{(2)}(\omega_1, \omega_2) &= \frac{1}{2} \hat{P}(\omega_1, \omega_2) \left( \langle \Lambda | [[V^{\omega_1}, \tau_{\mu}(b^{\dagger})^n], T^{(1)}(\omega_2)] | \text{QED-CC} \rangle + \frac{1}{2} \langle \Lambda | [[[H, \tau_{\mu}(b^{\dagger})^n], T^{(1)}(\omega_1)], T^{(1)}(\omega_2)] | \text{QED-CC} \rangle \right. \\ &\quad \left. + \sum_{\nu m} Y_{\nu, n}^{(1)}(\omega_1) \langle \overline{\nu, m} | [[H, \tau_{\mu}(b^{\dagger})^n], T^{(1)}(\omega_2)] + [V^{\omega_2}, \tau_{\mu}(b^{\dagger})^n] | \text{QED-CC} \rangle \right), \end{aligned} \quad (309)$$

$$(310)$$

where the matrix  $F$  as

$$F_{\mu m, \nu k} = \langle \Lambda | [[H, \tau_{\mu}(b^{\dagger})^m], \tau_{\nu}(b^{\dagger})^k] | \text{QED-CC} \rangle. \quad (311)$$

As for QED-HF, the response matrices and vectors have additional dimensions connected to the electromagnetic degrees of freedom. The  $X_{\mu n}$  and  $Y_{\nu m}$  vectors include, together with the standard CC electronic excitation response parameters, the purely photonic and the simultaneous electronic-photonic response parameters of Eqs. (268) and (269). As for the Jacobian matrix  $\mathbf{A}$ ,

the  $F$  matrix has additional photon and electron-photon blocks

$$F = \begin{pmatrix} F_{e,e} & F_{e,ep} & F_{e,p} \\ F_{ep,e} & F_{ep,ep} & F_{ep,p} \\ F_{p,e} & F_{p,ep} & F_{p,p} \end{pmatrix}. \quad (312)$$

Moreover, the perturbation  $V^\omega$  can act on both the electronic and the photon degrees of freedom, as in Eq. (147).

The CC expectation value is defined as<sup>234</sup>

$$\langle A \rangle_{\text{QED-CC}}(t) = \frac{1}{2} (\langle A(t) | A | \text{QED-CC}(t) \rangle + \langle A(t) | A | \text{QED-CC}(t) \rangle^*). \quad (313)$$

From the perturbative expansion

$$\langle A \rangle_{\text{QED-CC}}(t) = \langle A \rangle_{\text{QED-CC}} + \int d\omega_1 \langle \langle A, V^{\omega_1} \rangle \rangle_{\omega_1+i\eta} e^{-i\omega_1 t + i\eta t} + \dots$$

we can identify the QED-CC response functions

$$\langle \langle A, V^{\omega_1} \rangle \rangle_{\omega_1} = \frac{1}{2} \left( \mathcal{F}_{\omega_1}^{A, V^{\omega_1}} + \left( \mathcal{F}_{-\omega_1}^{A, V^{-\omega_1}} \right)^* \right) \quad (314)$$

$$\langle \langle A, V^{\omega_1}, V^{\omega_2} \rangle \rangle_{\omega_1, \omega_2} = \frac{1}{2} \left( \mathcal{F}_{\omega_1, \omega_2}^{A, V^{\omega_1}, V^{\omega_2}} + \left( \mathcal{F}_{-\omega_1, -\omega_2}^{A, V^{-\omega_1}, V^{-\omega_2}} \right)^* \right) \quad (315)$$

where

$$\mathcal{F}_{\omega_1}^{A, V^{\omega_1}} = \sum_{\mu n} \left( Y_{\mu n}^{(1)}(\omega_1) \langle \overline{\mu}, n | A | \text{QED-CC} \rangle + X_{\mu n}^{(1)}(\omega_1) \langle \Lambda | [A, \tau_{\mu n}] | \text{QED-CC} \rangle \right) \quad (316)$$

$$\begin{aligned} \mathcal{F}_{\omega_1, \omega_2}^{A, V^{\omega_1}, V^{\omega_2}} &= 2 \sum_{\mu n} \left( Y_{\mu n}^{(2)}(\omega_1, \omega_2) \langle \overline{\mu}, n | A | \text{QED-CC} \rangle + X_{\mu n}^{(2)}(\omega_1, \omega_2) \langle \Lambda | [A, \tau_{\mu}(b^\dagger)^n] | \text{QED-CC} \rangle \right) \\ &+ \sum_{\mu n, \nu m} \left( X_{\mu n}^{(1)}(\omega_1) F_{\mu n, \nu m}^A X_{\nu m}^{(1)}(\omega_2) + \hat{P}(\omega_1, \omega_2) Y_{\mu n}^{(1)}(\omega_1) \langle \overline{\mu}, m | [A, \tau_{\nu}(b^\dagger)^n] | \text{QED-CC} \rangle X_{\nu n}^{(1)}(\omega_2) \right). \end{aligned} \quad (317)$$

Here we have used the notation

$$F_{\mu m, \nu k}^A = \langle \Lambda | [[A, \tau_{\mu}(b^\dagger)^m], \tau_{\nu}(b^\dagger)^k] | \text{QED-CC} \rangle. \quad (318)$$

As for QED-HF, the static response equations can be obtained by setting the frequency of the external to zero. The poles and the residues of the response functions can be obtained assuming that  $\mathbf{A}$  can be diagonalized

$$(S^{-1} \mathbf{A} S)_{mn} = \delta_{mn} \omega_n, \quad (319)$$

where  $\omega_n$  is the  $n$ -th (real) excitation energy. We further introduce the notation

$$\tilde{\tau}_n = \sum_{\mu, m} S_{\mu m, n} \tau_{\mu}(b^\dagger)^m \quad (320)$$

$$\tilde{\tau}_n^\dagger = \sum_{\mu, m} S_{n, \mu m}^{-1} \tau_{\mu}^\dagger b^m \quad (321)$$

to describe the diagonal representation in Eq. (319). From the poles of the linear response function, we identify the residues

$$\begin{aligned} \lim_{\omega \rightarrow \omega_k} (\omega - \omega_k) \langle \langle A; B \rangle \rangle_{\omega} &= \\ \frac{1}{2} \left( \Gamma_k^A \Theta_k^B + (\Gamma_k^B \Theta_k^A)^* \right) &\equiv \langle 0 | A | k \rangle \langle k | B | 0 \rangle \end{aligned} \quad (322)$$

$$\begin{aligned} \lim_{\omega \rightarrow -\omega_k} (\omega + \omega_k) \langle \langle A; B \rangle \rangle_{\omega} &= \\ -\frac{1}{2} \left( (\Gamma_k^A \Theta_k^B)^* + \Gamma_k^B \Theta_k^A \right) &\equiv -(\langle 0 | A | k \rangle \langle k | B | 0 \rangle)^* \end{aligned} \quad (323)$$

where

$$\Theta_k^A = \langle \text{QED-HF} | \tilde{\tau}_k^\dagger e^{-T^{(0)}} A | \text{QED-CC} \rangle \quad (324)$$

$$\Gamma_k^A = \langle \Lambda | [A, \tilde{\tau}_k] | \text{QED-CC} \rangle$$

$$-\sum_n \frac{\langle \text{QED-HF} | \tilde{\tau}_k^\dagger e^{-T^{(0)}} A | \text{QED-CC} \rangle F_{nk}}{\omega_n + \omega_k}. \quad (325)$$

From these equations, we can compute the polaritonic properties.<sup>234</sup> Since we employ the QED-HF coherent-state transformed Hamiltonian in Eq. (202), the operators and the perturbations in the response functions must be described in the same representation.

### 6.2.2. QED-CC electronic and photonic excitation character

Since QED-CC is a highly correlated method, defined for the QED-HF coherent-state transformed Hamiltonian in Eq. (202), the definition of the electronic or photonic character of the excitation is not trivial. In the EOM framework, Haugland et. al<sup>60</sup> defined the electronic weight  $w_{el}$  of the state by means

of projection operators

$$w_{el}^k = \sqrt{\frac{\langle \Lambda_k | P_{el} | R_k \rangle}{\langle \Lambda_k | P | R_k \rangle}} \quad (326)$$

where  $\Lambda_k$  and  $R_k$  are the  $k$ -th left and right state,  $P$  is the projection operator onto the space  $S$  of Eq. (272) and  $P_{el}$  is the projector onto the states of  $S$  with zero photons. In the response framework, a similar definition can be obtained by considering the electronic components of the  $X_{\mu n}$  and  $Y_{\mu n}$  vectors, for instance

$$w_{el} = \sqrt{\sqrt{\frac{\sum_{\mu} |X_{\mu 0}|^2}{\sum_{\mu n} |X_{\mu n}|^2}} \times \sqrt{\frac{\sum_{\mu} |Y_{\mu 0}|^2}{\sum_{\mu n} |Y_{\mu n}|^2}}}. \quad (327)$$

Notice, however, that such a definition does not consider the contribution of the simultaneous electron-photon excitations. A more consistent definition of the photonic character could be obtained by considering the mean values of the field number operators from the quadratic response function, and comparing them to the ground state values, as discussed for QED-HF

$$\langle \Lambda_k | b^\dagger b | R_k \rangle \quad (328)$$

$$\langle \Lambda_k | (b_\alpha^\dagger - \frac{1}{\sqrt{2\omega_\alpha}} \lambda_\alpha \cdot \langle \mathbf{d} \rangle_{HF}) (b_\alpha - \frac{1}{\sqrt{2\omega_\alpha}} \lambda_\alpha \cdot \langle \mathbf{d} \rangle_{HF}) | R_k \rangle \quad (329)$$

$$\langle \Lambda_k | (b_\alpha^\dagger + \frac{1}{\sqrt{2\omega_\alpha}} \lambda_\alpha \cdot (\mathbf{d} - \langle \mathbf{d} \rangle_{HF})) (b_\alpha + \frac{1}{\sqrt{2\omega_\alpha}} \lambda_\alpha \cdot (\mathbf{d} - \langle \mathbf{d} \rangle_{HF})) | R_k \rangle. \quad (330)$$

## 7. CONCLUDING REMARKS

In this paper, we proposed a systematic discussion of polaritonic response theory based on the well-established molecular response theory routinely employed in quantum chemistry. The fundamental definitions and features of the response functions are still valid, but the explicit treatment of the electromagnetic degrees of freedom allows for novel perspectives. Additional equivalence relations between matter and photonic observables are introduced, and novel ways to probe the system are discussed. Particular care is needed when using different mathematical representations of the operators, as this can lead to misinterpretations of the computed results. We also provided QED-HF and QED-CC response equations that resemble the standard electronic response theory, providing the reader with a general framework for *ab initio* QED response theory. While significant progress in the theoretical description of polaritonic systems has been made, we emphasize several challenges that future research will have to address. These include a description of light-matter interaction beyond the electric dipole approximation, the issue of disorder in optical devices, the role of collective effects on polaritonic properties

and chemical reactions, and chiral polaritonics.

## 8. ACKNOWLEDGMENTS

We acknowledge Tor S. Haugland for insightful discussions.

## 9. FUNDING INFORMATION

M.C., A.B., and H.K. acknowledge funding from the European Research Council (ERC) under the European Union's Horizon 2020 Research and Innovation Programme (grant agreement No. 101020016). R.R.R and H.K. acknowledge funding from the Research Council of Norway through FRINATEK Project No. 275506. E.R acknowledges funding from the European Research Council (ERC) under the European Union's Horizon Europe Research and Innovation Programme (Grant n. ERC-StG-2021-101040197 - QED-SPIN). We acknowledge computing resources through UNINETT Sigma2—the National Infrastructure for High Performance



Computing and Data Storage in Norway, through Project No. NN2962k.

## 10. CONFLICT OF INTEREST

The authors declare no conflict of interest for this paper.

- <sup>1</sup>Huang K. Lattice vibrations and optical waves in ionic crystals. *Nature*. 1951;167(4254):779-80.
- <sup>2</sup>Hopfield J. Theory of the contribution of excitons to the complex dielectric constant of crystals. *Physical Review*. 1958;112(5):1555.
- <sup>3</sup>Tolpygo K. Physical properties of a rock salt lattice made up of deformable ions. *Zh eksp teor fiz*. 1950;20(6):497.
- <sup>4</sup>Jaynes ET, Cummings FW. Comparison of quantum and semiclassical radiation theories with application to the beam maser. *Proceedings of the IEEE*. 1963;51(1):89-109.
- <sup>5</sup>Rempe G, Walther H, Klein N. Observation of quantum collapse and revival in a one-atom maser. *Physical review letters*. 1987;58(4):353.
- <sup>6</sup>Brune M, Schmidt-Kaler F, Maali A, Dreyer J, Hagley E, Raimond J, et al. Quantum Rabi oscillation: A direct test of field quantization in a cavity. *Physical review letters*. 1996;76(11):1800.
- <sup>7</sup>Long JP, Simpkins B. Coherent coupling between a molecular vibration and Fabry–Perot optical cavity to give hybridized states in the strong coupling limit. *ACS photonics*. 2015;2(1):130-6.
- <sup>8</sup>Gordon J, Kogelnik H. Equivalence relations among spherical mirror optical resonators. *Bell System Technical Journal*. 1964;43(6):2873-86.
- <sup>9</sup>Fox AG, Li T. Resonant modes in a maser interferometer. *Bell System Technical Journal*. 1961;40(2):453-88.
- <sup>10</sup>Kojima J, Nguyen QV. Laser pulse-stretching with multiple optical ring cavities. *Applied optics*. 2002;41(30):6360-70.
- <sup>11</sup>Schmidt MK, Esteban R, González-Tudela A, Giedke G, Aizpurua J. Quantum mechanical description of Raman scattering from molecules in plasmonic cavities. *ACS nano*. 2016;10(6):6291-8.
- <sup>12</sup>Santhosh K, Bitton O, Chuntanov L, Haran G. Vacuum Rabi splitting in a plasmonic cavity at the single quantum emitter limit. *Nature communications*. 2016;7(1):1-5.
- <sup>13</sup>Weisbuch C, Nishioka M, Ishikawa A, Arakawa Y. Observation of the coupled exciton-photon mode splitting in a semiconductor quantum microcavity. *Physical review letters*. 1992;69(23):3314.
- <sup>14</sup>Yakovlev V, Nazin V, Zhizhin G. The surface polariton splitting due to thin surface film LO vibrations. *Optics Communications*. 1975;15(2):293-5.
- <sup>15</sup>Lidzey DG, Bradley D, Skolnick M, Virgili T, Walker S, Whittaker D. Strong exciton–photon coupling in an organic semiconductor microcavity. *Nature*. 1998;395(6697):53-5.
- <sup>16</sup>Fujita T, Sato Y, Kuitani T, Ishihara T. Tunable polariton absorption of distributed feedback microcavities at room temperature. *Physical Review B*. 1998;57(19):12428.
- <sup>17</sup>Hutchison JA, Schwartz T, Genet C, Devaux E, Ebbesen TW. Modifying chemical landscapes by coupling to vacuum fields. *Angewandte Chemie International Edition*. 2012;51(7):1592-6.
- <sup>18</sup>Thomas A, George J, Shalabney A, Dryzhakov M, Varma SJ, Moran J, et al. Ground-state chemical reactivity under vibrational coupling to the vacuum electromagnetic field. *Angewandte Chemie*. 2016;128(38):11634-8.
- <sup>19</sup>Lather J, Bhatt P, Thomas A, Ebbesen TW, George J. Cavity catalysis by cooperative vibrational strong coupling of reactant and solvent molecules. *Angewandte Chemie*. 2019;131(31):10745-8.
- <sup>20</sup>Thomas A, Lethuillier-Karl L, Nagarajan K, Vergauwe RM, George J, Chervy T, et al. Tilting a ground-state reactivity landscape by vibrational strong coupling. *Science*. 2019;363(6427):615-9.
- <sup>21</sup>Canaguier-Durand A, Devaux E, George J, Pang Y, Hutchison JA, Schwartz T, et al. Thermodynamics of molecules strongly coupled to the vacuum field. *Angewandte Chemie International Edition*. 2013;52(40):10533-6.
- <sup>22</sup>Sau A, Nagarajan K, Patraha B, Lethuillier-Karl L, Vergauwe RM, Thomas A, et al. Modifying Woodward–Hoffmann stereoselectivity under vibrational strong coupling. *Angewandte Chemie International Edition*. 2021;60(11):5712-7.
- <sup>23</sup>Eizner E, Martínez-Martínez LA, Yuen-Zhou J, Kéna-Cohen S. Inverting singlet and triplet excited states using strong light-matter coupling. *Science advances*. 2019;5(12):eaax4482.
- <sup>24</sup>Takahashi S, Watanabe K, Matsumoto Y. Singlet fission of amorphous rubrene modulated by polariton formation. *The Journal of Chemical Physics*. 2019;151(7):074703.
- <sup>25</sup>Martínez-Martínez LA, Du M, Ribeiro RF, Kéna-Cohen S, Yuen-Zhou J. Polariton-assisted singlet fission in acene aggregates. *The Journal of Physical Chemistry Letters*. 2018;9(8):1951-7.
- <sup>26</sup>Stranius K, Hertzog M, Börjesson K. Selective manipulation of electronically excited states through strong light–matter interactions. *Nature Communications*. 2018;9(1):1-7.
- <sup>27</sup>Yu Y, Mallick S, Wang M, Börjesson K. Barrier-free reverse-intersystem crossing in organic molecules by strong light-matter coupling. *Nature communications*. 2021;12(1):1-8.
- <sup>28</sup>Ulusoy IS, Gomez JA, Vendrell O. Modifying the nonradiative decay dynamics through conical intersections via collective coupling to a cavity mode. *The Journal of Physical Chemistry A*. 2019;123(41):8832-44.
- <sup>29</sup>Joseph K, Kushida S, Smarsly E, Ihiwakrim D, Thomas A, Paravicini-Bagliani GL, et al. Supramolecular assembly of conjugated polymers under vibrational strong coupling. *Angewandte Chemie International Edition*. 2021;60(36):19665-70.
- <sup>30</sup>Hirai K, Ishikawa H, Chervy T, Hutchison JA, Uji-i H. Selective crystallization via vibrational strong coupling. *Chemical science*. 2021;12(36):11986-94.
- <sup>31</sup>García-Vidal FJ, Ciuti C, Ebbesen TW. Manipulating matter by strong coupling to vacuum fields. *Science*. 2021;373(6551):eabd0336.
- <sup>32</sup>Chervy T, Thomas A, Akiki E, Vergauwe RM, Shalabney A, George J, et al. Vibro-polaritonic IR emission in the strong coupling regime. *ACS Photonics*. 2018;5(1):217-24.
- <sup>33</sup>George J, Wang S, Chervy T, Canaguier-Durand A, Schaeffer G, Lehn JM, et al. Ultra-strong coupling of molecular materials: spectroscopy and dynamics. *Faraday discussions*. 2015;178:281-94.
- <sup>34</sup>Xue B, Wang D, Tu L, Sun D, Jing P, Chang Y, et al. Ultrastrong absorption meets ultraweak absorption: unraveling the energy-dissipative routes for dye-sensitized upconversion luminescence. *The Journal of Physical Chemistry Letters*. 2018;9(16):4625-31.
- <sup>35</sup>del Pino J, Feist J, García-Vidal F. Signatures of vibrational strong coupling in Raman scattering. *The Journal of Physical Chemistry C*. 2015;119(52):29132-7.
- <sup>36</sup>Baranov DG, Munkhbat B, Länk NO, Verre R, Käll M, Shegai T. Circular dichroism mode splitting and bounds to its enhancement with cavity-plasmon-polaritons. *Nanophotonics*. 2020;9(2):283-93.
- <sup>37</sup>Guo J, Song G, Huang Y, Liang K, Wu F, Jiao R, et al. Optical Chirality in a Strong Coupling System with Surface Plasmons Polaritons and Chiral Emitters. *ACS Photonics*. 2021;8(3):901-6.
- <sup>38</sup>Itoh T, Yamamoto YS. Reproduction of surface-enhanced resonant Raman scattering and fluorescence spectra of a strong coupling system composed of a single silver nanoparticle dimer and a few dye molecules. *The Journal of Chemical Physics*. 2018;149(24):244701.
- <sup>39</sup>Herrera F, Spano FC. Absorption and photoluminescence in organic cavity QED. *Physical Review A*. 2017;95(5):053867.
- <sup>40</sup>Wang S, Scholes GD, Hsu LY. Coherent-to-incoherent transition of molecular fluorescence controlled by surface plasmon polaritons. *The Journal of Physical Chemistry Letters*. 2020;11(15):5948-55.
- <sup>41</sup>Takele WM, Piatkowski L, Wackenhut F, Gawinkowski S, Meixner AJ, Waluk J. Scouting for strong light–matter coupling signatures in Raman spectra. *Physical Chemistry Chemical Physics*. 2021;23(31):16837-46.
- <sup>42</sup>Barachati F, Simon J, Getmanenko YA, Barlow S, Marder SR, Kéna-Cohen S. Tunable third-harmonic generation from polaritons in the ultrastrong coupling regime. *Acs Photonics*. 2018;5(1):119-25.
- <sup>43</sup>Mund J, Yakovlev DR, Semina MA, Bayer M. Optical harmonic generation on the exciton-polariton in ZnSe. *Physical Review B*. 2020;102(4):045203.
- <sup>44</sup>Ebadian H, Mohebbi M. Extending the high-order-harmonic spectrum using surface plasmon polaritons. *Physical Review A*. 2017;96(2):023415.
- <sup>45</sup>Wang K, Seidel M, Nagarajan K, Chervy T, Genet C, Ebbesen T. Large optical nonlinearity enhancement under electronic strong coupling. *Nature Communications*. 2021;12(1):1-9.

- <sup>46</sup>Wang S, Chervy T, George J, Hutchison JA, Genet C, Ebbesen TW. Quantum yield of polariton emission from hybrid light-matter states. *The Journal of physical chemistry letters*. 2014;5(8):1433-9.
- <sup>47</sup>Imperatore MV, Asbury JB, Giebink NC. Reproducibility of cavity-enhanced chemical reaction rates in the vibrational strong coupling regime. *The Journal of Chemical Physics*. 2021;154(19):191103.
- <sup>48</sup>Ruggenthaler M, Sidler D, Rubio A. Understanding polaritonic chemistry from ab initio quantum electrodynamics. *arXiv preprint arXiv:221104241*. 2022.
- <sup>49</sup>Fregoni J, Garcia-Vidal FJ, Feist J. Theoretical challenges in polaritonic chemistry. *ACS photonics*. 2022;9(4):1096-107.
- <sup>50</sup>Hirai K, Hutchison JA, Uji-i H. Recent progress in vibropolaritonic chemistry. *ChemPlusChem*. 2020;85(9):1981-8.
- <sup>51</sup>Feist J, Galego J, Garcia-Vidal FJ. Polaritonic chemistry with organic molecules. *ACS Photonics*. 2018;5(1):205-16.
- <sup>52</sup>Sidler D, Ruggenthaler M, Schäfer C, Ronca E, Rubio A. A perspective on ab initio modeling of polaritonic chemistry: The role of non-equilibrium effects and quantum collectivity. *The Journal of Chemical Physics*. 2022;156(23):230901.
- <sup>53</sup>Hertzog M, Wang M, Mony J, Börjesson K. Strong light-matter interactions: a new direction within chemistry. *Chemical Society Reviews*. 2019;48(3):937-61.
- <sup>54</sup>Nagarajan K, Thomas A, Ebbesen TW. Chemistry under vibrational strong coupling. *Journal of the American Chemical Society*. 2021;143(41):16877-89.
- <sup>55</sup>Schäfer C, Flick J, Ronca E, Narang P, Rubio A. Shining light on the microscopic resonant mechanism responsible for cavity-mediated chemical reactivity. *Nature Communications*. 2022;13(1):7817.
- <sup>56</sup>Ruggenthaler M, Flick J, Pellegrini C, Appel H, Tokatly IV, Rubio A. Quantum-electrodynamical density-functional theory: Bridging quantum optics and electronic-structure theory. *Physical Review A*. 2014;90(1):012508.
- <sup>57</sup>Buchholz F, Theophilou I, Nielsen SE, Ruggenthaler M, Rubio A. Reduced density-matrix approach to strong matter-photon interaction. *ACS photonics*. 2019;6(11):2694-711.
- <sup>58</sup>Mallory JD, DePrince III AE. Reduced-density-matrix-based ab initio cavity quantum electrodynamics. *Physical Review A*. 2022;106(5):053710.
- <sup>59</sup>Mordovina U, Bungey C, Appel H, Knowles PJ, Rubio A, Manby FR. Polaritonic coupled-cluster theory. *Physical Review Research*. 2020;2(2):023262.
- <sup>60</sup>Haugland TS, Ronca E, Kjørstad EF, Rubio A, Koch H. Coupled cluster theory for molecular polaritons: Changing ground and excited states. *Physical Review X*. 2020;10(4):041043.
- <sup>61</sup>Haugland TS, Schäfer C, Ronca E, Rubio A, Koch H. Intermolecular interactions in optical cavities: An ab initio QED study. *The Journal of Chemical Physics*. 2021;154(9):094113.
- <sup>62</sup>Mandal A, Montillo Vega S, Huo P. Polarized Fock states and the dynamical Casimir effect in molecular cavity quantum electrodynamics. *The Journal of Physical Chemistry Letters*. 2020;11(21):9215-23.
- <sup>63</sup>Pavosevic F, Flick J. Polaritonic unitary coupled cluster for quantum computations. *The Journal of Physical Chemistry Letters*. 2021;12(37):9100-7.
- <sup>64</sup>Riso RR, Haugland TS, Ronca E, Koch H. Molecular orbital theory in cavity QED environments. *Nature communications*. 2022;13(1):1-8.
- <sup>65</sup>Bauer MM, Dreuw A. Perturbation theoretical approaches to strong light-matter coupling in ground and excited electronic states for the description of molecular polaritons. *The Journal of Chemical Physics*. 2023.
- <sup>66</sup>Salmon W, Gustin C, Settineri A, Di Stefano O, Zueco D, Savasta S, et al. Gauge-independent emission spectra and quantum correlations in the ultrastrong coupling regime of open system cavity-QED. *Nanophotonics*. 2022;11(8):1573-90.
- <sup>67</sup>Dicke RH. Coherence in spontaneous radiation processes. *Physical review*. 1954;93(1):99.
- <sup>68</sup>Tavis M, Cummings FW. Exact solution for an N-molecule-radiation-field Hamiltonian. *Physical Review*. 1968;170(2):379.
- <sup>69</sup>Frisk Kockum A, Miranowicz A, De Liberato S, Savasta S, Nori F. Ultrastrong coupling between light and matter. *Nature Reviews Physics*. 2019;1(1):19-40.
- <sup>70</sup>Imamoğlu A. Cavity QED based on collective magnetic dipole coupling: spin ensembles as hybrid two-level systems. *Physical review letters*. 2009;102(8):083602.
- <sup>71</sup>Knight J, Aharonov Y, Hsieh G. Are super-radiant phase transitions possible? *Physical Review A*. 1978;17(4):1454.
- <sup>72</sup>Vukics A, Domokos P. Adequacy of the Dicke model in cavity QED: A counter-no-go statement. *Physical Review A*. 2012;86(5):053807.
- <sup>73</sup>Grynberg G, Aspect A, Fabre C. Introduction to quantum optics: from the semi-classical approach to quantized light. Cambridge university press; 2010.
- <sup>74</sup>F Ribeiro R, Dunkelberger AD, Xiang B, Xiong W, Simpkins BS, Owrutsky JC, et al. Theory for nonlinear spectroscopy of vibrational polaritons. *The Journal of physical chemistry letters*. 2018;9(13):3766-71.
- <sup>75</sup>Gonzalez-Ballester C, Feist J, Badía EG, Moreno E, Garcia-Vidal FJ. Uncoupled dark states can inherit polaritonic properties. *Physical review letters*. 2016;117(15):156402.
- <sup>76</sup>Galego J, Garcia-Vidal FJ, Feist J. Cavity-induced modifications of molecular structure in the strong-coupling regime. *Physical Review X*. 2015;5(4):041022.
- <sup>77</sup>Luk HL, Feist J, Toppari JJ, Groenhof G. Multiscale molecular dynamics simulations of polaritonic chemistry. *Journal of chemical theory and computation*. 2017;13(9):4324-35.
- <sup>78</sup>Galego J, Climent C, Garcia-Vidal FJ, Feist J. Cavity Casimir-Polder forces and their effects in ground-state chemical reactivity. *Physical Review X*. 2019;9(2):021057.
- <sup>79</sup>Li TE, Nitzan A, Subotnik JE. Cavity molecular dynamics simulations of vibrational polariton-enhanced molecular nonlinear absorption. *The Journal of Chemical Physics*. 2021;154(9):094124.
- <sup>80</sup>Li TE, Subotnik JE, Nitzan A. Cavity molecular dynamics simulations of liquid water under vibrational ultrastrong coupling. *Proceedings of the National Academy of Sciences*. 2020;117(31):18324-31.
- <sup>81</sup>Fregoni J, Corni S, Persico M, Granucci G. Photochemistry in the strong coupling regime: A trajectory surface hopping scheme. *Journal of Computational Chemistry*. 2020;41(23):2033-44.
- <sup>82</sup>Fregoni J, Granucci G, Coccia E, Persico M, Corni S. Manipulating azobenzene photoisomerization through strong light-molecule coupling. *Nature communications*. 2018;9(1):4688.
- <sup>83</sup>Todorov Y, Sirtori C. Intersubband polaritons in the electrical dipole gauge. *Physical Review B*. 2012;85(4):045304.
- <sup>84</sup>Olsen J, Jørgensen P. Linear and nonlinear response functions for an exact state and for an MCSCF state. *The Journal of chemical physics*. 1985;82(7):3235-64.
- <sup>85</sup>Norman P, Ruud K, Saue T. Principles and practices of molecular properties: Theory, modeling, and simulations. John Wiley & Sons; 2018.
- <sup>86</sup>Casida ME, Huix-Rotllant M. Progress in time-dependent density-functional theory. *Annual review of physical chemistry*. 2012;63:287-323.
- <sup>87</sup>Helgaker T, Jaszunski M, Ruud K. Ab Initio Methods for the Calculation of NMR Shielding and Indirect Spin-Spin Coupling Constants. *Chemical Reviews*. 1999;99:293-352.
- <sup>88</sup>Christiansen O, Jørgensen P, Hättig C. Response functions from Fourier component variational perturbation theory applied to a time-averaged quasienergy. *International Journal of Quantum Chemistry*. 1998;68(1):1-52.
- <sup>89</sup>Sasagane K, Aiga F, Itoh R. Higher-order response theory based on the quasienergy derivatives: The derivation of the frequency-dependent polarizabilities and hyperpolarizabilities. *The Journal of chemical physics*. 1993;99(5):3738-78.
- <sup>90</sup>Langhoff P, Epstein S, Karplus M. Aspects of time-dependent perturbation theory. *Reviews of Modern Physics*. 1972;44(3):602.
- <sup>91</sup>Cammi R, Mennucci B. Linear response theory for the polarizable continuum model. *The Journal of chemical physics*. 1999;110(20):9877-86.
- <sup>92</sup>Helgaker T, Coriani S, Jørgensen P, Kristensen K, Olsen J, Ruud K. Recent advances in wave function-based methods of molecular-property calculations. *Chemical reviews*. 2012;112(1):543-631.
- <sup>93</sup>Lazzeretti P. Assessment of aromaticity via molecular response properties. *Physical chemistry chemical physics*. 2004;6(2):217-23.
- <sup>94</sup>Flick J, Welakuh DM, Ruggenthaler M, Appel H, Rubio A. Light-matter response in nonrelativistic quantum electrodynamics. *ACS photonics*. 2019;6(11):2757-78.
- <sup>95</sup>Yang J, Ou Q, Pei Z, Wang H, Weng B, Shuai Z, et al. Quantum-electrodynamical time-dependent density functional theory within Gaussian atomic basis. *The Journal of Chemical Physics*. 2021;155(6):064107.

- <sup>96</sup>Welakuh DM, Narang P. Tunable Nonlinearity and Efficient Harmonic Generation from a Strongly Coupled Light–Matter System. *ACS Photonics*. 2023;10(2):383-93.
- <sup>97</sup>Welakuh DM, Flick J, Ruggenthaler M, Appel H, Rubio A. Frequency-Dependent Sternheimer Linear-Response Formalism for Strongly Coupled Light–Matter Systems. *Journal of Chemical Theory and Computation*. 2022.
- <sup>98</sup>Bonini J, Flick J. Ab initio linear-response approach to vibro-polaritons in the cavity Born–Oppenheimer approximation. *Journal of Chemical Theory and Computation*. 2022;18(5):2764-73.
- <sup>99</sup>Flick J, Narang P. Ab initio polaritonic potential-energy surfaces for excited-state nanophotonics and polaritonic chemistry. *The Journal of Chemical Physics*. 2020;153(9):094116.
- <sup>100</sup>Welakuh DM, Narang P. Transition from Lorentz to Fano Spectral Line Shapes in Nonrelativistic Quantum Electrodynamics. *ACS Photonics*. 2022;9(9):2946-55.
- <sup>101</sup>Fregoni J, Haugland TS, Pipolo S, Giovannini T, Koch H, Corni S. Strong coupling between localized surface plasmons and molecules by coupled cluster theory. *Nano Letters*. 2021;21(15):6664-70.
- <sup>102</sup>Jackson JD. *Classical electrodynamics*. Wiley New York; 1977.
- <sup>103</sup>Fabry C. Theorie et applications d’une nouvelle méthode de spectroscopie interférentielle. *Ann Chim Ser 7*. 1899;16:115-44.
- <sup>104</sup>Pfeifer H, Ratschbacher L, Gallego J, Saavedra C, Faßbender A, von Haaren A, et al. Achievements and perspectives of optical fiber Fabry–Perot cavities. *Applied Physics B*. 2022;128(2):29.
- <sup>105</sup>Muller A, Flagg EB, Lawall JR, Solomon GS. Ultrahigh-finesse, low-mode-volume Fabry–Perot microcavity. *Optics letters*. 2010;35(13):2293-5.
- <sup>106</sup>Steinmetz T, Colombe Y, Hunger D, Hänsch T, Balocchi A, Warburton R, et al. Stable fiber-based Fabry–Pérot cavity. *Applied Physics Letters*. 2006;89(11):111110.
- <sup>107</sup>Rakhmanov M, Savage Jr R, Reitze D, Tanner D. Dynamic resonance of light in Fabry–Perot cavities. *Physics Letters A*. 2002;305(5):239-44.
- <sup>108</sup>Schlawin F, Kennes DM, Sentef MA. Cavity quantum materials. *Applied Physics Reviews*. 2022;9(1):011312.
- <sup>109</sup>Schouwink P, Berlepsch H, Dähne L, Mahrt R. Dependence of Rabi-splitting on the spatial position of the optically active layer in organic microcavities in the strong coupling regime. *Chemical physics*. 2002;285(1):113-20.
- <sup>110</sup>Wang Y, Ren Y, Luo X, Li B, Chen Z, Liu Z, et al. Manipulating cavity photon dynamics by topologically curved space. *Light: Science & Applications*. 2022;11(1):308.
- <sup>111</sup>McKeever J, Boca A, Boozer AD, Buck JR, Kimble HJ. Experimental realization of a one-atom laser in the regime of strong coupling. *Nature*. 2003;425(6955):268-71.
- <sup>112</sup>Culver R, Lampis A, Megyeri B, Pahwa K, Mudarikwa L, Holynski M, et al. Collective strong coupling of cold potassium atoms in a ring cavity. *New Journal of Physics*. 2016;18(11):113043.
- <sup>113</sup>Herskind PF, Dantan A, Marler JP, Albert M, Drewsen M. Realization of collective strong coupling with ion Coulomb crystals in an optical cavity. *Nature Physics*. 2009;5(7):494-8.
- <sup>114</sup>Favero I, Karrai K. Optomechanics of deformable optical cavities. *Nature Photonics*. 2009;3(4):201-5.
- <sup>115</sup>Plum E, Zheludev NI. Chiral mirrors. *Applied Physics Letters*. 2015;106(22):221901.
- <sup>116</sup>Viviescas C, Hackenbroich G. Field quantization for open optical cavities. *Physical Review A*. 2003;67(1):013805.
- <sup>117</sup>Maier SA. Plasmonics: Metal nanostructures for subwavelength photonic devices. *IEEE Journal of selected topics in quantum electronics*. 2006;12(6):1214-20.
- <sup>118</sup>Lee B, Lee IM, Kim S, Oh DH, Hesselink L. Review on subwavelength confinement of light with plasmonics. *Journal of Modern Optics*. 2010;57(16):1479-97.
- <sup>119</sup>Benz A, Campione S, Liu S, Montano I, Klem J, Allerman A, et al. Strong coupling in the sub-wavelength limit using metamaterial nanocavities. *Nature communications*. 2013;4(1):2882.
- <sup>120</sup>Dintinger J, Klein S, Bustos F, Barnes WL, Ebbesen T. Strong coupling between surface plasmon-polaritons and organic molecules in subwavelength hole arrays. *Physical Review B*. 2005;71(3):035424.
- <sup>121</sup>Ballarini D, De Liberato S. Polaritonics: from microcavities to sub-wavelength confinement. *Nanophotonics*. 2019;8(4):641-54.
- <sup>122</sup>Todorov Y, Andrews A, Sagnes I, Colombelli R, Klang P, Strasser G, et al. Strong light-matter coupling in subwavelength metal-dielectric microcavities at terahertz frequencies. *Physical review letters*. 2009;102(18):186402.
- <sup>123</sup>Xiao X, Li X, Caldwell JD, Maier SA, Giannini V. Theoretical analysis of graphene plasmon cavities. *Applied Materials Today*. 2018;12:283-93.
- <sup>124</sup>Li M, Liu C, Ruan B, Zhang B, Gao E, Zhang Z, et al. Strong coupling of plasmonic waves in graphene for light confinement. *Journal of Luminescence*. 2022;252:119332.
- <sup>125</sup>Qing YM, Ren Y, Lei D, Ma HF, Cui TJ. Strong coupling in two-dimensional materials-based nanostructures: a review. *Journal of Optics*. 2022;24(2):024009.
- <sup>126</sup>Li K, Fitzgerald JM, Xiao X, Caldwell JD, Zhang C, Maier SA, et al. Graphene plasmon cavities made with silicon carbide. *ACS omega*. 2017;2(7):3640-6.
- <sup>127</sup>Gan X, Mak KF, Gao Y, You Y, Hatami F, Hone J, et al. Strong enhancement of light–matter interaction in graphene coupled to a photonic crystal nanocavity. *Nano letters*. 2012;12(11):5626-31.
- <sup>128</sup>Koppens FH, Chang DE, García de Abajo FJ. Graphene plasmonics: a platform for strong light–matter interactions. *Nano letters*. 2011;11(8):3370-7.
- <sup>129</sup>Maier SA. Effective mode volume of nanoscale plasmon cavities. *Optical and Quantum Electronics*. 2006;38:257-67.
- <sup>130</sup>Hugall JT, Singh A, van Hulst NF. Plasmonic cavity coupling. *ACS Photonics*. 2018;5(1):43-53.
- <sup>131</sup>Mondal M, Semenov A, Ochoa MA, Nitzan A. Strong Coupling in Infrared Plasmonic Cavities. *The Journal of Physical Chemistry Letters*. 2022;13(41):9673-8.
- <sup>132</sup>Liang K, Guo J, Huang Y, Yu L. Fine-tuning of polariton energies in a tailored plasmon cavity and J-aggregates hybrid system. *Nanoscale*. 2020;12(45):23069-76.
- <sup>133</sup>Zhang H, Liu YC, Wang C, Zhang N, Lu C. Hybrid photonic-plasmonic nano-cavity with ultra-high Q/V. *Optics Letters*. 2020;45(17):4794-7.
- <sup>134</sup>Zhang C, ElAfandy R, Han J. Distributed Bragg reflectors for GaN-based vertical-cavity surface-emitting lasers. *Applied Sciences*. 2019;9(8):1593.
- <sup>135</sup>Emsley MK, Dosunmu O, Unlu M. Silicon substrates with buried distributed Bragg reflectors for resonant cavity-enhanced optoelectronics. *IEEE Journal of Selected Topics in Quantum Electronics*. 2002;8(4):948-55.
- <sup>136</sup>Menghrajani KS, Barnes WL. Strong coupling beyond the light-line. *ACS photonics*. 2020;7(9):2448-59.
- <sup>137</sup>Tao R, Arita M, Kako S, Kamide K, Arakawa Y. Strong coupling in non-polar GaN/AlGaIn microcavities with air-gap/III-nitride distributed Bragg reflectors. *Applied Physics Letters*. 2015;107(10):101102.
- <sup>138</sup>Butté R, Feltin E, Dorsaz J, Christmann G, Carlin JF, Grandjean N, et al. Recent progress in the growth of highly reflective nitride-based distributed Bragg reflectors and their use in microcavities. *Japanese journal of applied physics*. 2005;44(10R):7207.
- <sup>139</sup>Hu ML, Yang ZJ, Du XJ, Ma L, He J. Strong couplings between magnetic quantum emitters and subwavelength all-dielectric resonators with whispering gallery modes. *Optics Express*. 2021;29(16):26028-38.
- <sup>140</sup>Farr WG, Goryachev M, Creedon DL, Tobar ME. Strong coupling between whispering gallery modes and chromium ions in ruby. *Physical Review B*. 2014;90(5):054409.
- <sup>141</sup>Gupta SD, Agarwal GS. Strong coupling cavity physics in microspheres with whispering gallery modes. *Optics communications*. 1995;115(5-6):597-605.
- <sup>142</sup>O’shea D, Junge C, Pöllinger M, Vogler A, Rauschenbeutel A. All-optical switching and strong coupling using tunable whispering-gallery-mode microresonators. *Applied Physics B*. 2011;105:129-48.
- <sup>143</sup>Matsko AB, Ilchenko VS. Optical resonators with whispering-gallery modes-part I: basics. *IEEE Journal of selected topics in quantum electronics*. 2006;12(1):3-14.
- <sup>144</sup>Strekalov DV, Marquardt C, Matsko AB, Schwefel HG, Leuchs G. Non-linear and quantum optics with whispering gallery resonators. *Journal of Optics*. 2016;18(12):123002.
- <sup>145</sup>Matsko A, Savchenkov A, Strekalov D, Ilchenko V, Maleki L. Review of applications of whispering-gallery mode resonators in photonics and nonlinear optics. *IPN Progress Report*. 2005;42(162):1-51.

- <sup>146</sup>Kaliteevski M, Brand S, Abram R, Kavokin A, Dang LS. Whispering gallery polaritons in cylindrical cavities. *Physical Review B*. 2007;75(23):233309.
- <sup>147</sup>Gautier J, Li M, Ebbesen TW, Genet C. Planar chirality and optical spin-orbit coupling for chiral Fabry-Pérot cavities. *ACS Photonics*. 2022;9(3):778-83.
- <sup>148</sup>Voronin K, Taradin AS, Gorkunov MV, Baranov DG. Single-handedness chiral optical cavities. *ACS Photonics*. 2022;9(8):2652-9.
- <sup>149</sup>Feis J, Beutel D, Köpfler J, Garcia-Santiago X, Rockstuhl C, Wegener M, et al. Helicity-preserving optical cavity modes for enhanced sensing of chiral molecules. *Physical review letters*. 2020;124(3):033201.
- <sup>150</sup>Beutel D, Scott P, Wegener M, Rockstuhl C, Fernandez-Corbaton I. Enhancing the optical rotation of chiral molecules using helicity preserving all-dielectric metasurfaces. *Applied Physics Letters*. 2021;118(22):221108.
- <sup>151</sup>Scott P, Garcia-Santiago X, Beutel D, Rockstuhl C, Wegener M, Fernandez-Corbaton I. On enhanced sensing of chiral molecules in optical cavities. *Applied Physics Reviews*. 2020;7(4):041413.
- <sup>152</sup>Yoo S, Park QH. Chiral light-matter interaction in optical resonators. *Physical review letters*. 2015;114(20):203003.
- <sup>153</sup>Liu M, Plum E, Li H, Duan S, Li S, Xu Q, et al. Switchable chiral mirrors. *Advanced Optical Materials*. 2020;8(15):2000247.
- <sup>154</sup>Sofikitis D, Bougas L, Katsoprinakis GE, Spiliotis AK, Loppinet B, Rakitzis TP. Evanescent-wave and ambient chiral sensing by signal-reversing cavity ringdown polarimetry. *Nature*. 2014;514(7520):76-9.
- <sup>155</sup>Hodgkinson I, hong Wu Q, Knight B, Lakhtakia A, Robbie K. Vacuum deposition of chiral sculptured thin films with high optical activity. *Applied Optics*. 2000;39(4):642-9.
- <sup>156</sup>Graf F, Feis J, Garcia-Santiago X, Wegener M, Rockstuhl C, Fernandez-Corbaton I. Achiral, helicity preserving, and resonant structures for enhanced sensing of chiral molecules. *ACS Photonics*. 2019;6(2):482-91.
- <sup>157</sup>Hentschel M, Schäferling M, Duan X, Giessen H, Liu N. Chiral plasmonics. *Science advances*. 2017;3(5):e1602735.
- <sup>158</sup>Zheng G, He J, Kumar V, Wang S, Pastoriza-Santos I, Pérez-Juste J, et al. Discrete metal nanoparticles with plasmonic chirality. *Chemical Society Reviews*. 2021;50(6):3738-54.
- <sup>159</sup>Wang J, Zheng J, Li KH, Wang J, Lin HQ, Shao L. Excitation of Chiral Cavity Plasmon Resonances in Film-Coupled Chiral Au Nanoparticles. *Advanced Optical Materials*. 2023:2202865.
- <sup>160</sup>Govorov AO, Fan Z. Theory of chiral plasmonic nanostructures comprising metal nanocrystals and chiral molecular media. *ChemPhysChem*. 2012;13(10):2551-60.
- <sup>161</sup>Lan X, Wang Q. Self-assembly of chiral plasmonic nanostructures. *Advanced Materials*. 2016;28(47):10499-507.
- <sup>162</sup>Cohen-Tannoudji C, Dupont-Roc J, Grynberg G. *Photons and Atoms-Introduction to Quantum Electrodynamics*. John Wiley & Sons; 1997.
- <sup>163</sup>Craig DP, Thirunamachandran T. *Molecular quantum electrodynamics: an introduction to radiation-molecule interactions*. Courier Corporation; 1998.
- <sup>164</sup>Landau LD, Bell J, Kearsley M, Pitaevskii L, Lifshitz E, Sykes J. *Electrodynamics of continuous media*. vol. 8. elsevier; 2013.
- <sup>165</sup>Griesemer M, Lieb EH, Loss M. Ground states in non-relativistic quantum electrodynamics. *Inventiones mathematicae*. 2001;145(3):557-95.
- <sup>166</sup>Hiroshima F. Self-adjointness of the Pauli-Fierz Hamiltonian for arbitrary values of coupling constants. In: *Annales Henri Poincaré*. vol. 3. Springer; 2002. p. 171-201.
- <sup>167</sup>Golénia S. Positive commutators, Fermi golden rule and the spectrum of zero temperature Pauli-Fierz Hamiltonians. *Journal of Functional Analysis*. 2009;256(8):2587-620.
- <sup>168</sup>Dereziński J, Jakšić V. Spectral theory of Pauli-Fierz operators. *Journal of Functional analysis*. 2001;180(2):243-327.
- <sup>169</sup>Bach V, Fröhlich J, Sigal IM. Mathematical theory of nonrelativistic matter and radiation. *Letters in Mathematical Physics*. 1995;34(3):183-201.
- <sup>170</sup>Bach V, Fröhlich J, Sigal IM, Hepp K, Hunziker W. *Spectral analysis for systems of atoms and molecules coupled to the quantized radiation field*. Springer. 1999;207:249-90.
- <sup>171</sup>Flick J, Appel H, Ruggenthaler M, Rubio A. Cavity Born-Oppenheimer approximation for correlated electron-nuclear-photon systems. *Journal of chemical theory and computation*. 2017;13(4):1616-25.
- <sup>172</sup>Flick J, Rivera N, Narang P. Strong light-matter coupling in quantum chemistry and quantum photonics. *Nanophotonics*. 2018;7(9):1479-501.
- <sup>173</sup>Flick J, Ruggenthaler M, Appel H, Rubio A. Atoms and molecules in cavities, from weak to strong coupling in quantum-electrodynamics (QED) chemistry. *Proceedings of the National Academy of Sciences*. 2017;114(12):3026-34.
- <sup>174</sup>Kowalewski M, Bennett K, Mukamel S. Cavity femtochemistry: Manipulating nonadiabatic dynamics at avoided crossings. *The journal of physical chemistry letters*. 2016;7(11):2050-4.
- <sup>175</sup>Ribeiro RF, Martínez-Martínez LA, Du M, Campos-Gonzalez-Angulo J, Yuen-Zhou J. Polariton chemistry: controlling molecular dynamics with optical cavities. *Chemical science*. 2018;9(30):6325-39.
- <sup>176</sup>Bennett K, Kowalewski M, Mukamel S. Novel photochemistry of molecular polaritons in optical cavities. *Faraday discussions*. 2016;194:259-82.
- <sup>177</sup>Vendrell O. Collective Jahn-Teller interactions through light-matter coupling in a cavity. *Physical review letters*. 2018;121(25):253001.
- <sup>178</sup>Schäfer C, Ruggenthaler M, Rubio A. Ab initio nonrelativistic quantum electrodynamics: Bridging quantum chemistry and quantum optics from weak to strong coupling. *Physical Review A*. 2018;98(4):043801.
- <sup>179</sup>Fábrí C, Halász GJ, Cederbaum LS, Vibók Á. Born-Oppenheimer approximation in optical cavities: from success to breakdown. *Chemical science*. 2021;12(4):1251-8.
- <sup>180</sup>Power E, Thirunamachandran T. Quantum electrodynamics in a cavity. *Physical Review A*. 1982;25(5):2473.
- <sup>181</sup>Schuler M, De Bernardis D, Läuchli A, Rabl P. The vacua of dipolar cavity quantum electrodynamics. *SciPost Physics*. 2020;9(5):066.
- <sup>182</sup>De Bernardis D, Jaako T, Rabl P. Cavity quantum electrodynamics in the nonperturbative regime. *Physical Review A*. 2018;97(4):043820.
- <sup>183</sup>Barut A, Dowling J. Quantum electrodynamics based on self-energy: Spontaneous emission in cavities. *Physical Review A*. 1987;36(2):649.
- <sup>184</sup>Rokaj V, Ruggenthaler M, Eich FG, Rubio A. Free electron gas in cavity quantum electrodynamics. *Physical Review Research*. 2022;4(1):013012.
- <sup>185</sup>Helgaker T, Jørgensen P, Olsen J. *Molecular electronic-structure theory*. John Wiley & Sons; 2014.
- <sup>186</sup>Schäfer C, Ruggenthaler M, Rokaj V, Rubio A. Relevance of the quadratic diamagnetic and self-polarization terms in cavity quantum electrodynamics. *ACS photonics*. 2020;7(4):975-90.
- <sup>187</sup>Tokatly IV. Time-dependent density functional theory for many-electron systems interacting with cavity photons. *Physical review letters*. 2013;110(23):233001.
- <sup>188</sup>Rokaj V, Welakuh DM, Ruggenthaler M, Rubio A. Light-matter interaction in the long-wavelength limit: no ground-state without dipole self-energy. *Journal of Physics B: Atomic, Molecular and Optical Physics*. 2018;51(3):034005.
- <sup>189</sup>Riso RR, Grazioli L, Ronca E, Giovannini T, Koch H. Strong coupling in chiral cavities: nonperturbative framework for enantiomer discrimination. *arXiv preprint arXiv:220901987*. 2022.
- <sup>190</sup>Schäfer C, Baranov DG. Chiral Polaritonics: Analytical Solutions, Intuition, and Use. *The Journal of Physical Chemistry Letters*. 2023;14(15):3777-84.
- <sup>191</sup>Mauro L, Fregoni J, Feist J, Avriker R. Chiral discrimination in helicity-preserving Fabry-Pérot cavities. *Phys Rev A*. 2023 Feb;107:L021501.
- <sup>192</sup>List NH, Kauczor J, Saue T, Jensen HJA, Norman P. Beyond the electric-dipole approximation: A formulation and implementation of molecular response theory for the description of absorption of electromagnetic field radiation. *The Journal of chemical physics*. 2015;142(24):244111.
- <sup>193</sup>Bernadotte S, Atkins AJ, Jacob CR. Origin-independent calculation of quadrupole intensities in X-ray spectroscopy. *The Journal of chemical physics*. 2012;137(20):204106.
- <sup>194</sup>List NH, Melin TRL, van Horn M, Saue T. Beyond the electric-dipole approximation in simulations of x-ray absorption spectroscopy: Lessons from relativistic theory. *The Journal of Chemical Physics*. 2020;152(18):184110.
- <sup>195</sup>Lestrange PJ, Egidi F, Li X. The consequences of improperly describing oscillator strengths beyond the electric dipole approximation. *The Journal of Chemical Physics*. 2015;143(23):234103.
- <sup>196</sup>List NH, Saue T, Norman P. Rotationally averaged linear absorption spectra beyond the electric-dipole approximation. *Molecular Physics*. 2017;115(1-2):63-74.

- <sup>197</sup>Rokaj V, Penz M, Sentef MA, Ruggenthaler M, Rubio A. Quantum electrodynamic Bloch theory with homogeneous magnetic fields. *Physical review letters*. 2019;123(4):047202.
- <sup>198</sup>Rokaj V, Penz M, Sentef MA, Ruggenthaler M, Rubio A. Polaritonic Hofstadter butterfly and cavity control of the quantized Hall conductance. *Physical Review B*. 2022;105(20):205424.
- <sup>199</sup>Schäfer C, Buchholz F, Penz M, Ruggenthaler M, Rubio A. Making ab initio QED functional (s): Nonperturbative and photon-free effective frameworks for strong light–matter coupling. *Proceedings of the National Academy of Sciences*. 2021;118(41):e2110464118.
- <sup>200</sup>Schäfer C, Johansson G. Shortcut to self-consistent light-matter interaction and realistic spectra from first principles. *Physical Review Letters*. 2022;128(15):156402.
- <sup>201</sup>Schäfer C. Polaritonic chemistry from first principles via embedding radiation reaction. *The Journal of Physical Chemistry Letters*. 2022;13(30):6905-11.
- <sup>202</sup>Ehrenfest P. Bemerkung über die angenäherte Gültigkeit der klassischen Mechanik innerhalb der Quantenmechanik. *Zeitschrift für physik*. 1927;45(7):455-7.
- <sup>203</sup>Schrödinger E. Quantisierung als Eigenwertproblem. *Annalen der Physik*. 1926;386(18):109-39.
- <sup>204</sup>Hellmann J. Einführung in die Quantenchemie. Leipzig: Deuticke; 1937.
- <sup>205</sup>Feynman R. Forces in molecules. *Phys Rev*. 1939;56:340-3.
- <sup>206</sup>Barron LD. Molecular light scattering and optical activity. Cambridge University Press; 2009.
- <sup>207</sup>Houdré R, Stanley R, Ilegems M. Vacuum-field Rabi splitting in the presence of inhomogeneous broadening: Resolution of a homogeneous linewidth in an inhomogeneously broadened system. *Physical Review A*. 1996;53(4):2711.
- <sup>208</sup>Sidler D, Schäfer C, Ruggenthaler M, Rubio A. Polaritonic chemistry: Collective strong coupling implies strong local modification of chemical properties. *The journal of physical chemistry letters*. 2020;12(1):508-16.
- <sup>209</sup>Pavošević F, Rubio A. Wavefunction embedding for molecular polaritons. *The Journal of Chemical Physics*. 2022;157(9):094101.
- <sup>210</sup>Li TE, Nitzan A, Subotnik JE. Energy-efficient pathway for selectively exciting solute molecules to high vibrational states via solvent vibration-polariton pumping. *Nature Communications*. 2022;13(1):4203.
- <sup>211</sup>Wang DS, Yelin SF, Flick J. Defect polaritons from first principles. *ACS nano*. 2021;15(9):15142-52.
- <sup>212</sup>Hübener H, De Giovannini U, Schäfer C, Andberger J, Ruggenthaler M, Faist J, et al. Engineering quantum materials with chiral optical cavities. *Nature materials*. 2021;20(4):438-42.
- <sup>213</sup>Li M, Nizar S, Saha S, Thomas A, Azzini S, Ebbesen TW, et al. Strong coupling of chiral Frenkel exciton for intense, bisignate circularly polarized luminescence. *Angewandte Chemie International Edition*. 2023;62(6):e202212724.
- <sup>214</sup>Sun S, Gu B, Mukamel S. Polariton ring currents and circular dichroism of Mg-porphyrin in a chiral cavity. *Chemical science*. 2022;13(4):1037-48.
- <sup>215</sup>Allenmark S. Induced circular dichroism by chiral molecular interaction. *Chirality: The Pharmacological, Biological, and Chemical Consequences of Molecular Asymmetry*. 2003;15(5):409-22.
- <sup>216</sup>Saeva F, Wysocki J. Induced circular dichroism in cholesteric liquid crystals. *Journal of the American Chemical Society*. 1971;93(22):5928-9.
- <sup>217</sup>Gawroński J, Grajewski J. The significance of induced circular dichroism. *Organic letters*. 2003;5(18):3301-3.
- <sup>218</sup>Craig DP, Power EA, Thirunamachandran T. The dynamic terms in induced circular dichroism. *Proceedings of the Royal Society of London A Mathematical and Physical Sciences*. 1976;348(1652):19-38.
- <sup>219</sup>Bak KL, Jørgensen P, Jensen HJA, Olsen J, Helgaker T. First-order nonadiabatic coupling matrix elements from multiconfigurational self-consistent-field response theory. *The Journal of chemical physics*. 1992;97(10):7573-84.
- <sup>220</sup>Ruud K, Helgaker T, Bak KL, Jørgensen P, Jensen HJA. Hartree-Fock limit magnetizabilities from London orbitals. *The Journal of chemical physics*. 1993;99(5):3847-59.
- <sup>221</sup>Ruud K, Helgaker T, Jørgensen P, Bak KL. Theoretical calculations of the magnetizability of some small fluorine-containing molecules using London atomic orbitals. *Chemical physics letters*. 1994;223(1-2):12-8.
- <sup>222</sup>Ruud K, Ågren H, Helgaker T, Dahle P, Koch H, Taylor PR. The Hartree-Fock magnetizability of C60. *Chemical physics letters*. 1998;285(3-4):205-9.
- <sup>223</sup>Åstrand PO, Mikkelsen KV, Ruud K, Helgaker T. Magnetizabilities and nuclear shielding constants of the fluoromethanes in the gas phase and solution. *The Journal of Physical Chemistry*. 1996;100(51):19771-82.
- <sup>224</sup>Gauss J, Ruud K, Kállay M. Gauge-origin independent calculation of magnetizabilities and rotational g tensors at the coupled-cluster level. *The Journal of chemical physics*. 2007;127(7):074101.
- <sup>225</sup>Lutnæs OB, Teale AM, Helgaker T, Tozer DJ, Ruud K, Gauss J. Benchmarking density-functional-theory calculations of rotational g tensors and magnetizabilities using accurate coupled-cluster calculations. *The Journal of chemical physics*. 2009;131(14):144104.
- <sup>226</sup>London F. Théorie quantique des courants interatomiques dans les combinaisons aromatiques. *J Phys Radium*. 1937;8(10):397-409.
- <sup>227</sup>Dalgaard E. Time-dependent multiconfigurational Hartree-Fock theory. *The Journal of Chemical Physics*. 1980;72(2):816-23.
- <sup>228</sup>McLachlan A, Ball M. Time-dependent hartree-fock theory for molecules. *Reviews of Modern Physics*. 1964;36(3):844.
- <sup>229</sup>Di Ventra M, Pantelides ST. Hellmann-Feynman theorem and the definition of forces in quantum time-dependent and transport problems. *Physical Review B*. 2000;61(23):16207.
- <sup>230</sup>Casida ME. Time-dependent density-functional theory for molecules and molecular solids. *Journal of Molecular Structure: THEOCHEM*. 2009;914(1-3):3-18.
- <sup>231</sup>Casida ME. Time-dependent density functional response theory for molecules. In: *Recent Advances In Density Functional Methods: (Part I)*. World Scientific; 1995. p. 155-92.
- <sup>232</sup>Kjergaard T, Jørgensen P, Olsen J, Coriani S, Helgaker T. Hartree-Fock and Kohn-Sham time-dependent response theory in a second-quantization atomic-orbital formalism suitable for linear scaling. *The Journal of chemical physics*. 2008;129(5):054106.
- <sup>233</sup>Dalgaard E. Quadratic response functions within the time-dependent Hartree-Fock approximation. *Physical Review A*. 1982;26(1):42.
- <sup>234</sup>Pedersen TB, Koch H. Coupled cluster response functions revisited. *The Journal of chemical physics*. 1997;106(19):8059-72.
- <sup>235</sup>Koch H, Jørgensen P. Coupled cluster response functions. *The Journal of chemical physics*. 1990;93(5):3333-44.
- <sup>236</sup>Stanton JF, Bartlett RJ. The equation of motion coupled-cluster method. A systematic biorthogonal approach to molecular excitation energies, transition probabilities, and excited state properties. *The Journal of chemical physics*. 1993;98(9):7029-39.